Systematics and Biodiversity **2** (4): 375–417
doi:10.1017/S1477200004001574 Printed in the United Kingdom
Issued 18 April 2005

Phylogenetic systematics and historical biogeography of the Neotropical electric fish *Gymnotus* (Teleostei: Gymnotidae)

J. S. Albert[1,*], W. G. R. Crampton[1], D. H. Thorsen[2] & N. R. Lovejoy[3]
[1]Florida Museum of Natural History, University of Florida, Gainesville, FL 32611-7800, USA
[2]Department of Zoology, The Field Museum of Natural History, 1400 S. Lake Shore Drive, Chicago, IL 60605-2496, USA
[3]Department of Zoology, University of Manitoba, Winnipeg, R3T 2N2, Canada

submitted November 2003
accepted July 2004

Contents

Abstract Phylogenetic interrelationships of the Neotropical electric fish genus *Gymnotus* are documented from comparative study of phenotypic data. A data matrix was compiled of 113 phenotypic characters for 40 taxa, including 31 recognized *Gymnotus* species, six allopatric populations of *G. carapo*, two allopatric populations of *G. coropinae*, and three gymnotiform outgroups. MP analysis yielded 15 trees of equal length, the strict consensus of which is presented as a working hypothesis of *Gymnotus* interrelationships. Diagnoses are presented for 26 clades, including three species groups; the *G. cylindricus* group with two species restricted to Middle America, the *G. pantherinus* group with 12 species in South America, and the *G. carapo* group with 16 species in South America. The basal division of *Gymnotus* is between clades endemic to Middle and South America. Both the *G. pantherinus* and *G. carapo* groups include trans-Andean sister-taxon pairs, suggesting a minimum date for the origins of these groups in the late Middle Miocene (*c.* 12 Ma.). The geographically widespread species *G. carapo* is paraphyletic. Analysis of character state evolution shows characters of external morphology are more

*Corresponding author. Now at Department of Biology, University of Louisiana, Lafayette, LA 70504-42451, USA. Email: jxa4003@louisiana.edu

phylogenetically plastic and provide more phylogenetic information in recent branches than do characters of internal morphology, which themselves provide the more information in deeper branches. Nine regional species assemblages of *Gymnotus* are recognized, none of which is monophyletic. There are at least two independent origins of *Gymnotus* species in sediment rich, high conductivity, perennially hypoxic whitewater floodplains (*várzea*) derived from an ancestral condition of being restricted to low conductivity non-floodplain (*terra firme*) black and clearwater rivers and streams. These phylogenetic, biogeographic and ecological patterns suggest a lengthy and complex history involving numerous instances of speciation, extinction, migration and coexistence in sympatry. Evolution in *Gymnotus* has been a continent-wide phenomenon; i.e. Amazonian species richness is not a consequence of strictly Amazonian processes. These patterns are similar to those of other highly diverse groups of Neotropical fishes and do not resemble those of monophyletic, rapidly generated species flocks.

Key words biodiversity, character evolution, cladistics, classification, comparative morphology, diversification, historical ecology, Gymnotiformes, paraphyletic species, *várzea*

Introduction

Neotropical freshwaters are among the most diverse ecosystems on earth, containing an estimated 6000 species of fishes or approximately 11% of described vertebrates (Vari & Malabarba, 1998; Lundberg *et al*., 2000; Reis *et al*., 2003). The processes underlying the production and maintenance of this enormous diversity are poorly known. Recent studies of tropical diversification implicate the complex interactions of speciation, migration extinction and the coexistence in taxa in multispecies ecological assemblages (Henderson *et al*., 1998; Moritz *et al*., 2000; Plotkin *et al*., 2000; Hubbell, 2001; Volkov *et al*., 2003). The breadth of Neotropical freshwater diversity is also the consequence of a long history extending for tens of millions of years (Lundberg, 1993, 1997, 1998; Reis, 1998). The role of rapid speciation and the production of adaptive radiations has received much attention by systematists working in tropical freshwaters (e.g. Meyer *et al*., 1990; Seehausen, 2000; Sullivan *et al*., 2002; Verheyen *et al*., 2003; Seehausen, 2002; Balirwa *et al*., 2003). Yet the great majority of species in most tropical aquatic ecosystems are not the immediate products of explosive radiations. Less attention has been applied to groups whose extant diversity more fully represents the richness of processes underlying contemporary patterns of phenotypic and ecological diversity.

Species of the Neotropical electric fish genus *Gymnotus* are an attractive target for investigations into the origins and evolution of species-rich tropical taxa. *Gymnotus* is ecologically and phyletically diverse, with at least 32 species. *Gymnotus* species occur in all major river systems in the humid Neotropics (except the Maracaibo Basin) and inhabit a wide variety of lowland aquatic habitats. *Gymnotus* is a relatively ancient group, including at least four trans-Andean clades and putative members of the 'Old Southern Element' of Nuclear Middle American (*sensu* Bussing, 1976). These distributions indicate an origin of the genus before the late Middle Miocene uplift of the northwestern Andes (*c*. 12 Ma; Hoorn *et al*., 1995). *Gymnotus* is currently the subject of intensive investigations by several research teams such that the full nature of its alpha taxonomy, ecology and biogeography have only recently come to be appreciated (Campos-da-Paz, 1996; Campos-da-Paz & Costa 1996; Fernandes-Matioli & Almeida-Toledo *et al*., 1998, Fernandes-Matioli & Marchetto *et al*., 1998; Albert *et al*., 1999; Campos-da-Paz, 2000; Fernandes-Matioli *et al*., 2000, 2001; Albert & Crampton 2001; Fernandes-Matioli & Almeida-Toledo, 2001; Campos-da-Paz, 2002; Silva *et al*., 2003; Albert & Crampton, 2003; Crampton & Albert, 2003a, 2003b; Crampton *et al*., 2003; Fernandes *et al*., in press).

Gymnotus is the most geographically widespread of all gymnotiform genera, extending from the Rio Salado in the Pampas of Argentina (36°S) to the Rio San Nicolás of southeastern Chiapas, Mexico (18°N), and is present in the continental waters of all South and Middle American countries except Chile and Belize (Albert, 2001; Albert & Crampton, 2005). The locations of the type localities of *Gymnotus* species are depicted in Fig. 1 and Table 1, and biogeographic distributions are summarized in Table 2. *Gymnotus* is most diverse in the Amazon Basin where 18 species are known to reside including three undescribed forms (Crampton *et al*., 2005). There is no fossil record of *Gymnotus*; the only known fossil gymnotiforms are fragments from the Yecua Formation (Late Miocene) of Bolivia assigned to Sternopygidae or Sinusoidea (Gayet & Meunier 1991; Albert & Fink, unpubl. obs.).

Gymnotus is readily distinguished from other gymnotiform fishes in possessing a superior mouth with a prognathous lower jaw and ventrally curved rictus, a pair of dorsally oriented pipe-shaped anterior nares included within the gape, a lateral position of the eyes on the head, numerous long rami of the posterior lateral line extending obliquely on the caudal portion of the body, and a long body cavity, with a modal value of 31–51 precaudal vertebrae (Albert, 2001). Most *Gymnotus* species possess obliquely oriented bands of dark and light pigments along the length of the body, from which they derive the English common name 'banded knife-fish'. Adult body size in *Gymnotus* ranges almost an order of magnitude, from 80–160 mm in mature specimens of *G. coropinae* from the Amazon Basin, to one metre in *G. inaequilabiatus* from the Rio Paraná drainage. *Gymnotus* species are all aggressive nocturnal predators of fishes and other small aquatic animals, and most are also territorial (Black-Cleworth, 1970; pers. obs.). The males of at least two *Gymnotus* species form nests and guard larvae (Crampton & Hopkins, pers. obs.). The type species

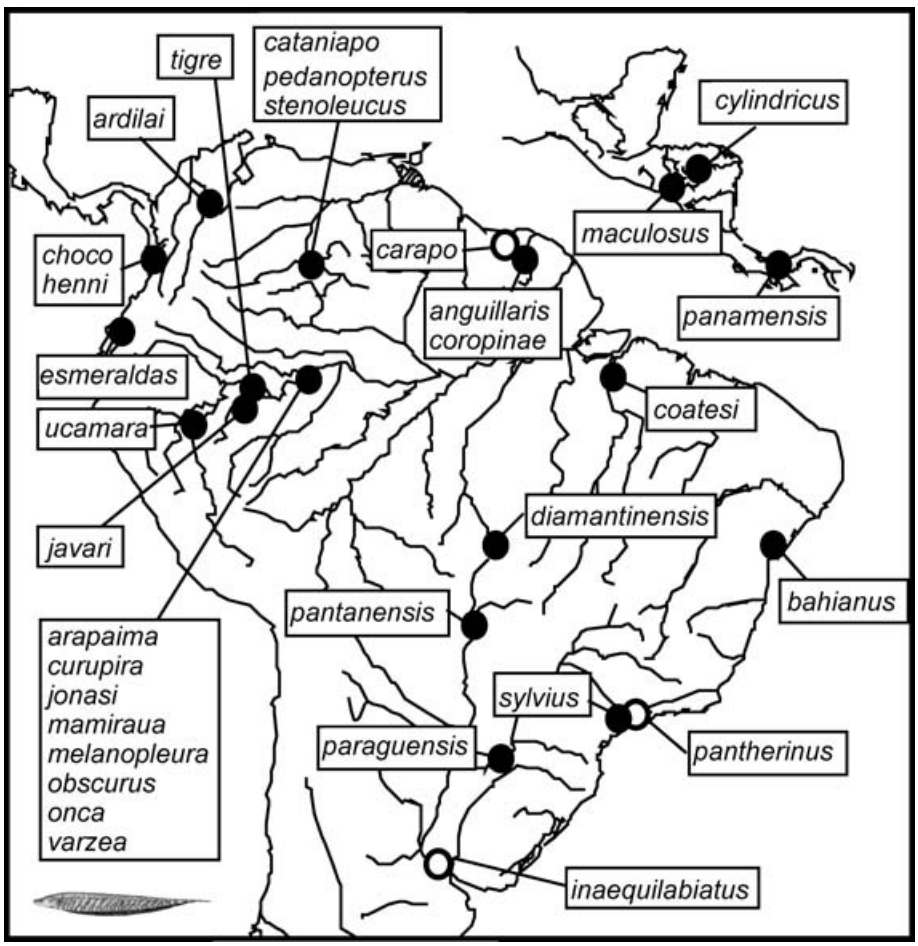

Figure 1 Type localities of 32 recognized species of *Gymnotus* listed in Table 1. Open circles represent approximate locations.

Gymnotus carapo (L.) is reported to mouth brood its eggs and larvae (Kirschbaum & Wieczorek, 2002). Most if not all *Gymnotus* species utilize aerial respiration in hypoxic conditions (Evans, 1929; Liem *et al*., 1984; Crampton, 1998b).

As in all gymnotiform electric fishes, *Gymnotus* generates an electric organ discharge (EOD) from an electric organ that is derived ontogenetically from hypaxial muscles along the entire ventral margin of the body and caudal appendage. The EOD of *Gymnotus* consists of a train of discrete pulses, each composed of one or several head positive and head negative phases, with each pulse extending for 0.8–2.0 ms duration, and separated by intervals of electric silence (Lissmann, 1958; Bennett, 1971). These electric signals provide a useful means to recognize and differentiate phenotypically similar sympatric species on the basis of spectral and temporal features (Hopkins & Heiligenberg, 1978; Heiligenberg, 1980; Westby, 1988; Hopkins *et al*., 1990; Hopkins, 1999). The stereotyped nature of the EOD, and the relative ease with which it can be monitored and quantified, have facilitated the use of electric fishes as model systems in vertebrate neuroethology (Heiligenberg & Bastian, 1986). These species-specific electric signals are a powerful means for separating visually cryptic species from among complex sympatric assemblages of electric fishes, and permit quantitative sampling and monitoring of behaviours in the wild and in the laboratory (Hopkins *et al*., 1990; Crampton, 1998a; Stopa & Hoshino, 1999; Stoddard *et al*., 1999; Schuster, 2000). *Gymnotus* in particular has been developed as a model for understanding the physiological basis of active electroreception (Lorenzo *et al*., 1988; Correa *et al*., 1998; Caputi, 1999; Aguilera *et al*., 2001; Ardanaz *et al*., 2001; Caputi *et al*., 2003).

In this study we present the result of a phylogenetic survey of morphological diversity of *Gymnotus* species from throughout the Neotropics. The data reported are 113 phenotypic characters of colour pattern, squamation, morphometrics, meristics, laterosensory system, osteology, myology, electric organ morphology, and electric organ discharge parameters coded for 31 *Gymnotus* species, two allopatric populations of *G. coropinae*, six allopatric populations of *G. carapo*, and three gymnotiform outgroups. The resulting phylogeny is used to interpret patterns of phenotypic evolution and biogeography, and to assess the relative roles of geography and habitat in the production and maintenance of species diversity.

History of the classification

There have been no previous formal analyses of relationships among species of *Gymnotus*. Three species groups have been recognized within the genus based on colour pattern, body

Group	Species	Author(s)	Year	HT (ST)	TL	Country	Drainage	Max. TL	Region
C	*carapo*	Linnaeus	1758	NRM 64,	262	Surinam	Surinam	418	GU
				NRM 8224	331	Surinam	Surinam		
				UUZM 56	293	Surinam	Surinam		
C	*inaequilabiatus*	Valenciennes	1847	MNHN 4615	NA	Argentina	La Plata	998	PA
B	*pantherinus*	Steindachner	1908	NMW 11275	NA	Brazil	Atlantic	242	SE
				NMW 76443-4	NA	Brazil	Atlantic		
B	*coatesi*	La Monte	1935	AMNH 12624	180	Brazil	Tocantins	180	EA
A	*cylindricus*	La Monte	1935	AMNH 1358	182	Guatemala	Atlantic	249	MA
B	*anguillaris*	Hoedeman	1962	ZMA 100338	228	Surinam	Surinam	302	GU
B	*coropinae*	Hoedeman	1962	ZMA 100185	47	Surinam	Surinam	160	GU
B	*cataniapo*	Mago-Leccia	1994	MBUCV-V-14736	253	Venezuela	Orinoco	316	GU
B	*pedanopterus*	Mago-Leccia	1994	MBUCV-V-14738	215	Venezuela	Orinoco	247	GU
B	*stenoleucus*	Mago-Leccia	1994	MBUCV-V-6218	141	Venezuela	Orinoco	142	GU
A	*maculosus*	Albert & Miller	1995	UMMZ 230830	191	Guatemala	Pacific	260	MA
C	*bahianus*	Campos-da-Paz & Costa	1996	MNRJ 12316	177	Brazil	São Francisco	275	NW
C	*sylvius*	Albert et al.	1999	LGP 0925.1	259	Brazil	Paraná	307	PA
C	*arapaima*	Albert & Crampton	2000	INPA 13505	192	Brazil	Amazon	460	WA
B	*jonasi*	Albert & Crampton	2000	INPA 13507	114	Brazil	Amazon	129	WA
C	*mamiraua*	Albert & Crampton	2000	INPA 13503	178	Brazil	Amazon	244	WA
B	*melanopleura*	Albert & Crampton	2000	INPA 9966	99	Brazil	Amazon	99	WA
B	*onca*	Albert & Crampton	2000	INPA 11512	116	Brazil	Amazon	116	WA
C	*diamantinensis*	Campos-da-Paz	2002	MZUSP 57505	125	Brazil	Tapajós	125	EA
C	*choco*	Albert & Crampton	2003	ICNMHN 6621	237	Colombia	Baudó	260	PS
C	*esmeraldas*	Albert & Crampton	2003	MCZ 58729	296	Ecuador	Esmeraldas	355	PS
C	*henni*	Albert & Crampton	2003	CAS 47290	308	Colombia	San Juan	314	PS
B	*javari*	Albert & Crampton	2003	UMMZ 224599	197	Perú	Javari	201	WA
B	*panamensis*	Albert & Crampton	2003	CAS 72209	236	Panamá	Caribbean	236	MA
C	*paraguensis*	Albert & Crampton	2003	UMMZ 206155	224	Paraguay	Paraguay	240	PA
C	*tigre*	Albert & Crampton	2003	UF 25552	411	Peru	Amazonas	411	WA
C	*ucamara*	Crampton et al.	2003	UF 126182	156	Peru	Ucayali	190	WA
C	*curupira*	Crampton & Albert	2005	MZUSP 60607	235	Brazil	Amazon	235	WA
C	*obscurus*	Crampton & Albert	2005	MZUSP 60604	215	Brazil	Amazon	215	WA
C	*varzea*	Crampton & Albert	2005	MZUSP 60601	173	Brazil	Amazon	237	WA
C	*pantanensis*	Fernandes et al.	In rev	MZUSP 67874	196	Brazil	Paraguay	264	PA
C	*ardilai*	Maldonado & Albert	In pre	IAvHP 3477	430	Colombia	Magdalena	430	NW

Table 1 Summary of taxonomic information for 32 valid species of *Gymnotus*. Species arranged chronologically by year of description. Abbreviations: CAR, *G. carapo* group CYL, *G. cylindricus* group; GRP, group; PAN, *G. pantherinus* group; TL, total length. Locality and length data for holotype (HT) or syntypes (ST).

proportions and the organization of the laterosensory canals (Albert & Miller, 1995; Albert, 2001; Albert & Crampton, 2003). The *G. cylindricus* group is represented by two species endemic to Nuclear Middle America. The *G. pantherinus* group is represented by 13 species with distributions from Panama to Paraguay. The *G. carapo* group is represented by 16 species with distributions from the Pacific slope of Colombia to the Pampas of Argentina.

Recent phylogenetic studies of Gymnotiformes support the hypothesis advanced by Ellis (1913) that *Gymnotus* and *Electrophorus* are one another's closest relatives, forming a taxon referred to as Gymnotidae (Triques, 1993; Gayet *et al*., 1994; Alves-Gomes *et al*., 1995; Albert & Campos-da-Paz, 1998; Albert, 2001). These studies disagree however on the position of Gymnotidae among other Gymnotiformes. By assuming the caudal fin of apteronotids as plesiomorphic, Triques (1993) and Gayet *et al*. (1994) regarded gymnotiforms with a 'pulse-type' electric organ discharge (i.e., Gymnotidae, Rhamphichthyidae and Hypopomidae) as monophyletic. Based largely on phylogenetic uncertainty surrounding the position of *Sternopygus* Alves-Gomes *et al*. (1995) regarded the position of Gymnotidae to be ambiguous. Based on a review of all available morphological and molecular data, Albert & Campos-da-Paz (1998) and Albert (2001) regarded Gymnotidae as the sister taxon to a clade composed of all other Gymnotiformes.

Materials and methods

Data acquisition

Morphological methods are described in detail in Northcutt *et al*. (2000), Albert (2001) and Albert & Crampton (2003).

GRP	Species	MA	PS	NW	GO	WA	EA	NE	SE	PA	HAB
CYL	*G. cylindricus*	X									TS
	G. maculosus	X									TS
PAN	*G. anguillaris*				X	Y	Y				TS, BF
	G. cataniapo				X						TS, BF
	G. coatesi					Y	X				TS
	G. coropinae				X	Y	Y				TS
	G. javari					X					TS, BF
	G. jonasi					X					WF
	G. melanopleura					X					WF
	G. onca					X					WF
	G. panamensis	X									TS
	G. pantanensis									X	TS, WF
	G. pantherinus								X		TS
	G. pedanopterus				X		Y				TS, BF
	G. stenoleucus				X		Y				TS, BF
CAR	*G. arapaima*					X					TS, BF, WF
	G. ardilai			X							TS
	G. bahianus							X			TS
	G. carapo				X	Y	Y	Y			TS, BF, WF
	G. choco		X								TS
	G. curupira					X					TS
	G. diamantinensis						X				TS
	G. esmeraldas		X								TS
	G. henni		X								TS
	G. inaequilabiatus								Y	X	WF
	G. mamiraua					X					WF
	G. obscurus					X					WF
	G. paraguensis									X	WF
	G. sylvius								X	Y	TS, WF
	G. tigre					X	Y				WF
	G. ucamara					X					WF
	G. varzea					X					WF
		3	3	1	6	15	8	2	3	4	

Table 2 Geographic and ecological distributions of 32 valid *Gymnotus* species, arranged alphabetically within species groups. Hydrogeographic regions from Fig. 23. X, region with type locality; Y, specimens from other region(s). Abbreviations: BF, blackwater or other nutrient-poor rivers with seasonal flood cycle; HAB, habitats; TS, *terra firme* systems or coastal streams and rivers including seasonally flooded lower reaches, low sediment, low conductivity; WF, whitewater floodplains (*várzea*), high sediment, high conductivity. Other abbreviations as in Table 1. Data from literature and unpublished observations.

In brief, morphometric data are taken as point-to-point linear distances from standard landmarks using digital calipers to the nearest 0.1 mm. Anal-fin ray and precaudal vertebrae data were taken from radiographs under a dissecting microscope. Morphometric and meristic data for 29 *Gymnotus* species are presented in Albert & Crampton (2003), for *G. ucamara* in Crampton *et al*. (2003), and for *G. coropinae* in Crampton & Albert (2003a). Morphometric data are reported as mean adult values. Body proportions reported include head length (HL), from posterior margin of bony operculum to tip of snout (dorsal midline of upper jaw); postorbital length (PO), from posterior margin of bony opercle to posterior margin of eye; preorbital length (PR), from anterior margin of eye to tip of snout; body depth (BD), vertical distance from origin of anal fin to dorsal body border (with lateral line held horizontally); pectoral-fin length (P1), from dorsal border of fin base where it contacts cleithrum to tip of longest ray; interorbital distance (IO), between dorsomedial margins of eyes; size of branchial opening (BO), from posterodorsal to anteroventral extent of branchial fold; pre-anal distance (PA), from anterior insertion of anal fin to posterior margin of anus.

Body size is represented by total length in millimeters (mm TL). Sex and sexual maturity can be assessed in *Gymnotus* only by dissection or histology (Albert & Crampton, 2003). Specimens in which the caudal appendage was obviously damaged and not, or only partially, regenerated were excluded from measurements of total length. Size at morphological maturity is ascertained for each species at an asymptotic value of HL% in TL. Specimens examined for morphometric and meristic data are reported in Albert & Crampton (2003), Crampton *et al*. (2003) and Crampton & Albert (2003a).

Descriptions of meristic features apply to both juvenile and adult specimens. Scale, lateral-line pore, and pectoral-fin ray counts were taken directly from ethanol-preserved and cleared-and-stained specimens under a dissecting microscope. Precaudal vertebrae and anal-fin ray counts were taken from radiographs or cleared-and-stained specimens under a dissecting microscope (Albert & Fink, 1996). Gymnotiform fishes maintain approximately the same number of fin ray and vertebral counts from juvenile to adult sizes, and scale counts change with size (Albert, 2001). Abbreviations used for meristic variables are: AFR, number of branched and unbranched anal-fin rays, rounded to the nearest multiple of five, and counted from radiographs only of specimens with little or no damage to the caudal appendage (10 repeated counts from a single radiograph differed by ± 5 due to presence of numerous faint posterior anal-fin rays); APS, number of anal-fin pterygiophore scales counted as the number of scale rows over the pterygiophores (counted from an origin vertically below the base of the first lateral line ramus); BND, number of oblique lateral pigment bands; CEP, caudal electroplate rows counted as the number of horizontally aligned rows of electroplates in the electric organ at a distance of one head length from the tip of the caudal appendage (with the scales above the electric organ removed and the specimen placed under a stereoscopic microscope against strong backlighting, not counted from specimens with a heavily damaged caudal appendage); PCV, number of precaudal vertebrae including the five elements of the Weberian Apparatus; P1R, number of branched and unbranched pectoral-fin rays; PLL, number of pored lateral-line scales in posterior lateral line posterior to neurocranium; PLR, number of pored lateral line scales to first ventral ramus; SAL, number of scales above lateral line at midbody; VLR, number of ventrally oriented lateral line rami. Protocols for counting band numbers and lateral-line rami are described in Albert *et al*. (1999). Counts of bilaterally paired series (APS, CEP, P1R, PLL, PLR, SAL, VLR) were taken on the left side when possible. PLL were not counted from specimens with a damaged caudal appendage.

Dissection methods and morphological nomenclature are described in Albert (2001). Bones were disarticulated to functional groups (e.g., neurocranium, suspensorium, pectoral girdle), or to individual elements, using microdissection tools under an Olympus SZ12 or SZ60 dissecting microscope. Outlines and standardized features (e.g., ridges, surface ornamentation) of each bone were traced from lateral and medial aspects with the aid of a camera lucida, and the line art scanned and edited using iGrafx Designer 8.0 on a PC. Laterosensory canals and pores were illustrated by integrating camera-lucida tracings of canal pores from ethanol-preserved specimens and canal bones from cleared-and-stained specimens (Albert *et al*., 1998). Laterosensory and electric organ nerves are visualized in cleared specimens stained with Sudan black B (Northcutt *et al*., 2000). Osteological data were taken from specimens cleared with KOH, trypsin and glycerin, and stained with alizarin red and alcian blue, following Taylor & Van Dyke (1985) with reagent concentrations and reaction times adjusted to specimen size and preservation quality. A list of the cleared and stained specimens examined is provided in Appendix 1. To determine the amount of osteological variation within a single population the skeletons of 10 specimens of *G. carapo* GO (UF 80734, 165–262 mm) were disarticulated to functional group and line drawings made in lateral view of the neurocranium, oral jaws, suspensorium, and pectoral girdle. The variation observed in these skeletal elements was used to guide decisions regarding hypotheses of characters and states when coding interspecific differences.

Terminal taxa used in the phylogenetic analysis consisted of 31 recognized *Gymnotus* species, two allopatric populations of *G. coropinae*, six allopatric populations of *G. carapo*, and three gymnotiform outgroup species, all from specimens captured in the hydrogeographic region of the type locality. Populations of the geographically widespread and variable taxon *G. carapo* were selected based on a previous review of the alpha taxonomy of *Gymnotus* (Albert & Crampton, 2003). The six allopatric populations of *G. carapo* recognized differ in certain aspects of colour patterns and the mean, modal or median values of morphometric and meristic traits: 1, *G. carapo* EA from the Eastern Amazon; 2, *G. carapo* NE from the Parnaíba and Itapicuru Basins of northeastern Brazil; 3, *G. carapo* RO from the Rio Branco Basin in the Brazilian state of Roraima; 4; *G. carapo* GO from the Guiana Shield and Orinoco Basin; 5, *G. carapo* MD from the Rio Madeira Basin of Brazil, Bolivia and Peru; and 6, *G. carapo* WA from the Western Amazon Basin of Brazil, Colombia, Ecuador and Peru.

The three gymnotiform outgroup species were selected on the basis of results from previous phylogenetic investigations (Albert & Campos-da-Paz, 1998; Albert, 2001). *Electrophorus electricus* is the immediate sister taxon to *Gymnotus* and the only other known species of the Gymnotidae. The sister-taxon to Gymnotidae is a clade constituting all other gymnotiform fishes, which is itself composed of two clades, the Rhamphichthyoidea and Sinusoidea. *Hypopomus artedi* and *Sternopygus macrurus* are phylogenetically basal members of the Rhamphichthyoidea and Sinusoidea, respectively, and also retain many plesiomorphic morphological features of these clades (Albert, 2001).

Institutional abbreviations follow Leviton *et al*. (1985), with the addition of: ICNMHN (Instituto de Ciencias Naturales Museo de Historia Natural, Bogotá), INPA (Instituto Nacional de Pesquisas da Amazônia, Manaus), MUSM (Museo de Historia Natural de la Universidad Nacional Mayor de San Marcos, Lima), NRM (Swedish Museum of Natural History, Stockholm), and UUZM (Uppsala University, Museum of Evolution, Zoology Section, Uppsala).

Habitat preferences of *Gymnotus* species are defined by water quality and habitat structure (Crampton, 1998a), and taxa assigned to the following three aquatic systems: (1) *terra firme* (non-floodplain) or coastal streams and rivers and their seasonally flooded lower reaches with low sediment load and low conductivity, (2) blackwater, clearwater or other nutrient-poor rivers with a seasonal flood cycle, and with a low sediment load and low conductivity, and (3) whitewater floodplains (*várzea)* with high sediment load and high conductivity. The use of MP to optimize the evolution of habitat preference is discussed by Albert (2001).

Phylogenetic methods

In selecting and coding characters we were guided by the philosophy that phylogenetic congruence among all observations is the most reliable method to assess homology (Patterson, 1982; Eernisse & Kluge, 1993). MacClade 4.03 (Maddison & Maddison, 2000) was used to construct and analyse a data matrix containing 113 characters of phenotypic data for 40 taxa. The following options were employed in maximum parsimony (MP) analyses using PAUP 4.0b10 (Swofford, 2003). Heuristic searches were used with the MULPARS option set to save all minimum length trees. Tree-bisection-reconnection (TBR) branch-swapping was performed with and without the steepest descent option and branches having maximum length zero were collapsed to yield polytomies. Three support indices (*sensu* Wilkinson *et al*., 2003) are reported for each internal node, including branch lengths as character state changes (steps) of unambiguous optimization, Bremer decay values (Bremer, 1994) calculated using TreeRot (Sorenson, 1999) to generate constraint files for PAUP, and Bootstrap consensus value calculated using PAUP with 100 replicates (only Bootstrap values over 70% are reported).

Because the criteria for ordering multistate characters are often ambiguous most multistate characters were analysed unordered, with the exception of four meristic characters (100, 101, 103 and 111) for which explicit transformation series are hypothesized. The use of phenotypic similarity alone to order multistate characters undermines the efficacy of the tree topology to establish the sequence of evolutionary transformations, and the freedom allowed to unordered multistate characters renders the results non-comparable with those of binary coding (Farris *et al*., 1970; Wilkinson, 1992; Albert, 2001).

Morphometric and meristic traits were examined as both continuous and discrete (coded) data using MacClade 4.03. Relative mean, median or modal adult trait values were coded into multiple alternative character states and the coding scheme was selected that exhibited maximum congruence with the distributions of other characters in the data matrix (Westneat, 1993; Weins, 2000). The alternative coding schemes differ in the number of states and range cutoffs. Tree statistics calculated from character states were optimized unambiguously on a strict consensus topology of all the data, interpreting character state changes on 'hard' polytomies (multiple speciation events). Congruence was assessed by values of the "rescaled consistency index", which is not influenced by symplesiomorphies or autapomorphies (Farris, 1989). Table 3 illustrates an example of alternative schemes for mean relative adult head length (HL% in TL). In this example five alternative coding schemes were designed employing two or three states and different range cutoffs. The preferred character coding (HL1) selected was that most congruent with the preponderance of data; i.e. exhibits the highest rescaled consistency index.

Clade diagnoses were generated with all characters optimized unambiguously on a strict consensus topology, and steps calculated for polytomies assuming hard-polytomy option (Maddison & Maddison, 2000). Diagnoses refer to conditions observed in mature specimens. Descriptions of some morphometric and pigmentation characters may apply to juveniles as well as adults in species paedomorphic for these characters. Osteological, morphometric and pigmentation characteristics apply to only morphologically (as opposed to reproductively) mature specimens unless otherwise stated.

Character	States	HL%	N	Steps	RC
HL1	0	8.4–9.4	8	10	0.12
	1	9.5–11.0	16		
	2	11.1–13.5	15		
HL2	0	8.4–9.4	14	14	0.08
	1	9.5–11.0	10		
	2	11.1–13.5	15		
HL3	0	8.4–11.0	24	5	0.11
	1	11.1–13.5	15		
HL4	0	8.4–10.0	14	5	0.09
	1	10.1–13.5	25		
HL5	0	8.4–9.4	8	8	0.06
	1	9.5–13.5	31		

Table 3 Alternative methods for coding continuous trait data into discrete states. The character is relative mean adult head length (HL%; data from Albert & Crampton, 2003). Coding alternatives employ different numbers of states (2 or 3) and different range cutoffs. N, number of taxa assigned that state. Tree statistics calculated from character state data in Table 4, as unambiguously optimized on the strict consensus topology of Fig. 21, and interpreting character state changes on 'hard' polytomies (multiple speciation events). Value of rescaled consistency index (RC) not influenced by examining characters ordered or unordered. Note character coding HL1 (character 17) is most congruent (shows highest RC) with the preponderance of data.

To determine the relative contributions of characters of internal and external morphology to the phylogenetic results, MP analyses were performed on three different datasets: (1) all 113 characters included, (2) characters of body proportions, pigmentation, squamation and fin ray counts excluded, and (3) characters of osteological, myological and neural traits excluded. This exercise determines the degree of support that characters of external and internal morphology give to the topology of the most parsimonious tree derived from the entire data set. "Clade rank" corresponds to the number of branching events in the most diverse subclade of a clade, on the assumption that overall rates of diversification (speciation and extinction) are proportional to the number of extant species in that clade (Norrell & Novacek, 1992; Albert *et al*., 1998; Paradis, 1998; Wagner & Sidor, 2000). The degree of phylogenetic plasticity ('evolvability' *sensu* de Visser *et al*., 2003; Rutherford, 2003) was assessed from alternative values of an index of character congruence, the rescaled consistency index (RC) of Farris (1989). The RC for all characters on a tree is the consistency index (CI) multiplied by the retention index (RI; Maddison & Maddison, 2000). RC ranges from 0 to 1, with higher RC values indicating that characters in the data set are more congruent with each other and the tree topology.

Conclusions of the analysis of character state rate heterogeneity were drawn from reconstructions across the whole phylogeny and, in the case of *G. carapo* from detailed population-level sampling, to minimize effects of isolated inaccuracies in ancestral character-state reconstruction (Omland, 1997, 1999).

Results

Descriptive morphology

Character coding

Figures 2–20 illustrate the morphology of the 113 characters used in constructing the data matrix of Table 4. Characters of pigmentation are listed first, followed by characters of body proportions, cranial osteology and myology, pectoral girdle, squamation, axial skeleton and electric organs. Morphometric values for character states represent mean adult values. Characters 1–5 coding different aspects of pigmentation are phylogenetically and logically independent. Character 1 codes diversity in the presence or absence of obliquely oriented pigment bands. Character 2 codes diversity in the appearance of the pigment band margins. Character 3 codes diversity in the density of chromatophores within pigment bands. Character 4 codes diversity in the appearance of pigment bands in the area of the body above the lateral line. Character 5 codes diversity in the width of the pigment bands. The derived states of these five characters exhibit distinct distributions among species of *Gymnotus* indicating they are distinct phenotypes and not pleiotropic consequences of a single phylogenetic change.

Pigmentation

1. Pigment bands. 0: absent. 1: obliquely oriented alternating dark and light pigment bands or band-pairs, sometimes broken into irregular strips of dark pigment patches or spots.
2. Pigment band (or pigment patch) margins. 0: no bands or patches. 1: bands (or patches) with irregular wavy margins. 2: bands with regular straight margins.
3. Pigment band density. 0: no bands. 1: dark bands become paired during growth, pale in middle, darker near bands margins in specimens more than 120 mm. 2: dark bands evenly pigmented in juveniles and adults.
4. Dark pigment bands above lateral line. 0: all continuous (unbroken) on anterior half of body. 1: most broken or absent in specimens more than 150 mm.
5. Pigment band (or band pair) width at midbody. 0: no bands. 1: dark bands 2–3 times broader than pale bands. 2: dark bands 4–5 times broader than pale bands. 3: dark bands narrower than pale bands.
6. Pigment band (or band pair) number. 0: few, median 0–16. 1: many, median 17–29.
7. Head colour pattern. 0: not blotched. 1: head with brown ground colour and irregularly shaped pale-yellow blotches located on chin, gular area, behind and under eyes, over opercle, and between eyes.
8. Ground colour of middorsum at midbody. 0: dark, bands indistinct from ground colour with low contrast margins over dorsal midline. 1: light, bands with high contrast margins over dorsal midline.
9. White cheek patch. 0: absent. 1: present below orbit.
10. Nape pale yellow band or patch. 0: absent. 1: present.
11. Anal fin posterior membrane. 0: pigmentation of posterior 10% of fin not different from anterior portion of fin. 1: posterior 10% of fin clear or translucent hyaline.
12. Anal fin color. 0: anterior half hyaline to brown. 1: anterior half black.
13. Anal fin posterior stripes. 0: absent from posterior region. 1: obliquely oriented hyaline and dark stripes at caudal end of anal fin.

Body proportions

14. Body size small. 0: grows to a maximum total length of more than 160 mm. 1: grows to less than 160 mm.
15. Body size large. 0: grows a maximum total length of less than 900 mm. 1: grows to more than 901 mm.
16. Body profile (BD). 0: deep, BD = 9.1–11.7% TL. 1: slender, BD = 6.1–9.0% TL.
17. Head length (HL). 0: short, HL 8.4–9.4% TL. 1: moderate, HL 9.5–11.0% TL. 2. long, mean HL 11.1–13.5% TL.
18. Head depth (HD). 0: very deep, HD = 66–75% HL. 1: moderate, HD = 60–65% HL. 2: shallow, HD 53–59% HL.
19. Head width (HW). 0: wide, HW = 68–70% HL. 1: moderate, HW = 57–65% HL. 2: narrow, HW 51–56% HL.
20. Snout length (PR). 0: short, PR = 28–33% HL. 1: moderate, PR = 34–36%. 2: long, PR = 37–40% HL.
21. Mouth width (MW). 0: narrow, MW = 27–35% HL. 1: moderate, MW = 36–44% HL. 2: wide, MW = 45–49% HL.
22. Interorbital distance (IO). 0: narrow, IO = 31–35% HL. 1: broad, IO = 36–40% HL. 2: very broad, IO: 41–50% HL.
23. Branchial opening (BO). 0: broad, BO = 33–44% HL. 1: narrow, BO = 25–32% HL.
24. Preanal distance (PA). 0: long, PA = 90–128% HL. 1: short, PA = 56–89% HL.
25. Pectoral fin length (P1). 0: large, P1= 45–54% HL. 1: small, P1 = 34–44% HL.
26. Anal-fin length (AF). 0: long, AF= 76–83%. 1: short, AF = 67–75%.
27. Body shape (BW/BD). 0: laterally compressed, BW = 58–73% BD. 1: cylindrical, BW = 74–90% BD.
28. Gape size in mature specimens. 0: small, not extending to posterior nares. 1: large, extending to posterior nares.
29. Mouth position. 0: terminal, jaws approximately equal, rictus horizontal. 1: superior, lower jaw strongly prognathous, rictus decurved.
30. Eye position. 0: Above horizontal of mouth. 1: At horizontal of mouth.

Cranial osteology and myology

31. Mesethmoid anterior margin. 0: convex, rounded, or straight. 1: concave with paired anterolateral processes (Figs 2–6).

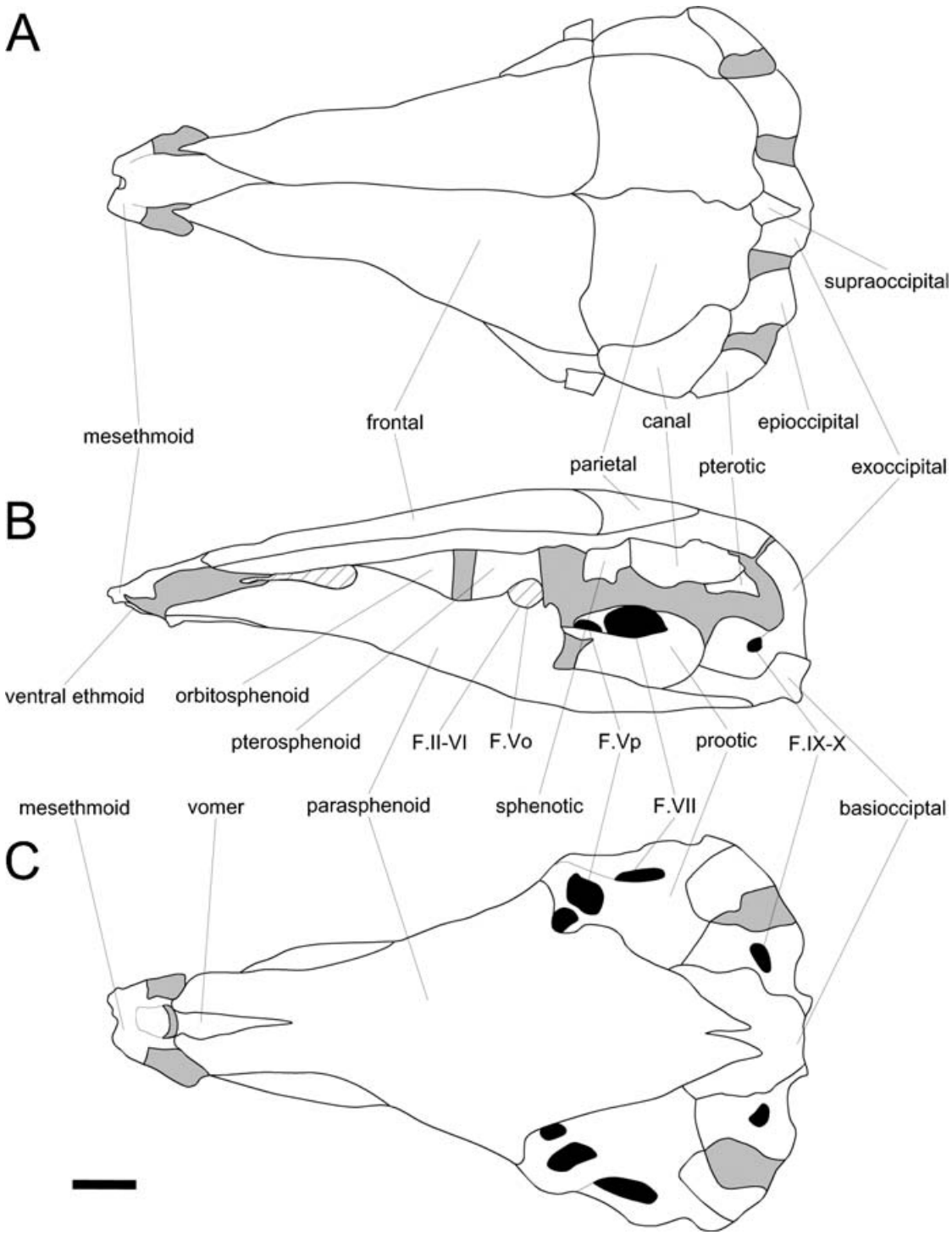

Figure 2 Neurocranium of juvenile *Electrophorus electricus* (UF 42193, 108 mm). (A) dorsal view, (B) lateral view, (C) ventral view. Cartilage indicated by uniform grey shading. Foramina indicated by uniform black shading. Hatching indicates open area dorsal to parasphenoid. Note this specimens is a juvenile with extensive area of cartilage in posterior part of neurocranium and no ossified lateral line canal bones. Abbreviations: F. II–VI, foramen of optic tract, oculomotor, trochlear and abducens nerves; F. V_{2-3}, foramen of some trigeminal and lateral line nerve rami; F. VII, foramen of facial nerve; F. IX–X, foramen of glossopharyngeal and vagus nerves. Note largely unossified areas in periotic region and lack of laterosensory canal bones fused to roof of neurocranium. Scale bar = 1 mm.

32. Mesethmoid neck. 0: narrow, approximately twice the width of the anterolateral mesethmoid process. 1: broad, 3–4 times width of lateral mesethmoid process (Figs 2–6).
33. Anterior narial pore. 0: flush on head surface. 1: pipe-shaped, partially or entirely included within gape.
34. Circumorbital series. 0: circumorbital ossifications forming an ovoid series, forming a right or slightly acute angle (60–90°) at the junction of the supraorbital and infraorbital canals (Figs 3A and 4A). 1: circumorbital ossifications forming a tear-drop shaped series, strongly

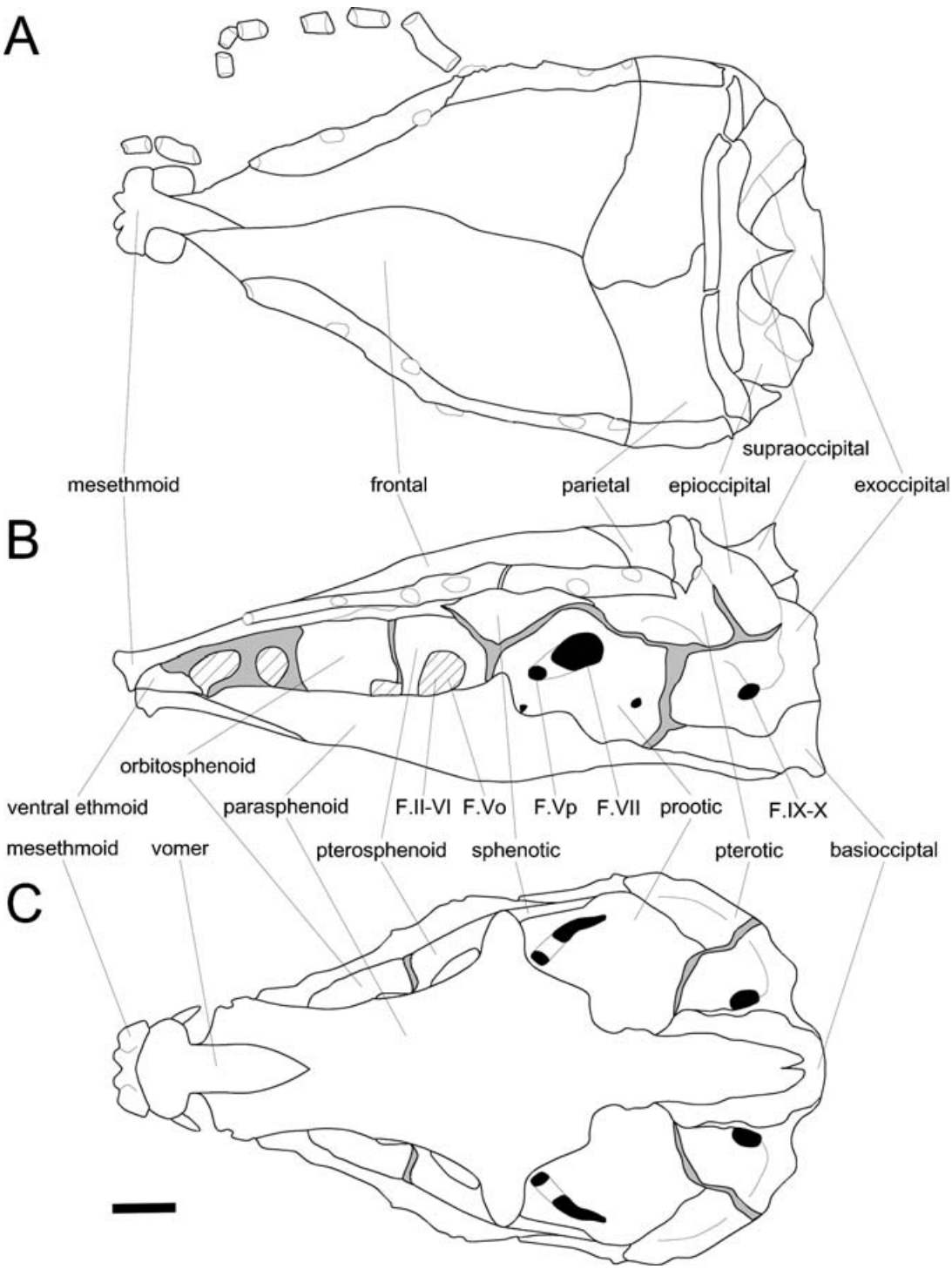

Figure 3 Neurocranium of *Gymnotus varzea* (MCP uncat. WGRC 10.030597). (A) dorsal view, (B) lateral view, (C) ventral view. Shading scheme and abbreviations as in Fig. 2. Numbers indicate foraminae of laterosensory canal bones where they connect to membranous portions of canal tubes. Infraorbital laterosensory series and nasal bones illustrated on right side only. Scale bar = 1 mm.

acute angle (40–60°) between supraorbital and infraorbital canals (Fig. 6A).

35. Maxilla-palatine position. 0: near tip of mesopterygoid. 1: posterior to anterior tip of mesopterygoid (Fig. 7).
36. Maxilla orientation. 0: long axis horizontal (Fig. 7). 1: long axis oblique, almost vertical (Fig. 8).
37. Maxilla shape. 0: sickle-shaped in lateral view with concave dorsal margin. 1: rod- or paddle-shaped in lateral with straight dorsal margin (Fig. 8). 2: triangular in lateral view, with concave dorsal margin (Fig. 7).
38. Maxilla length. 0: short, equal to width of about 4–6 teeth along dentary oral margin (Figs. 8A–B and 8D).

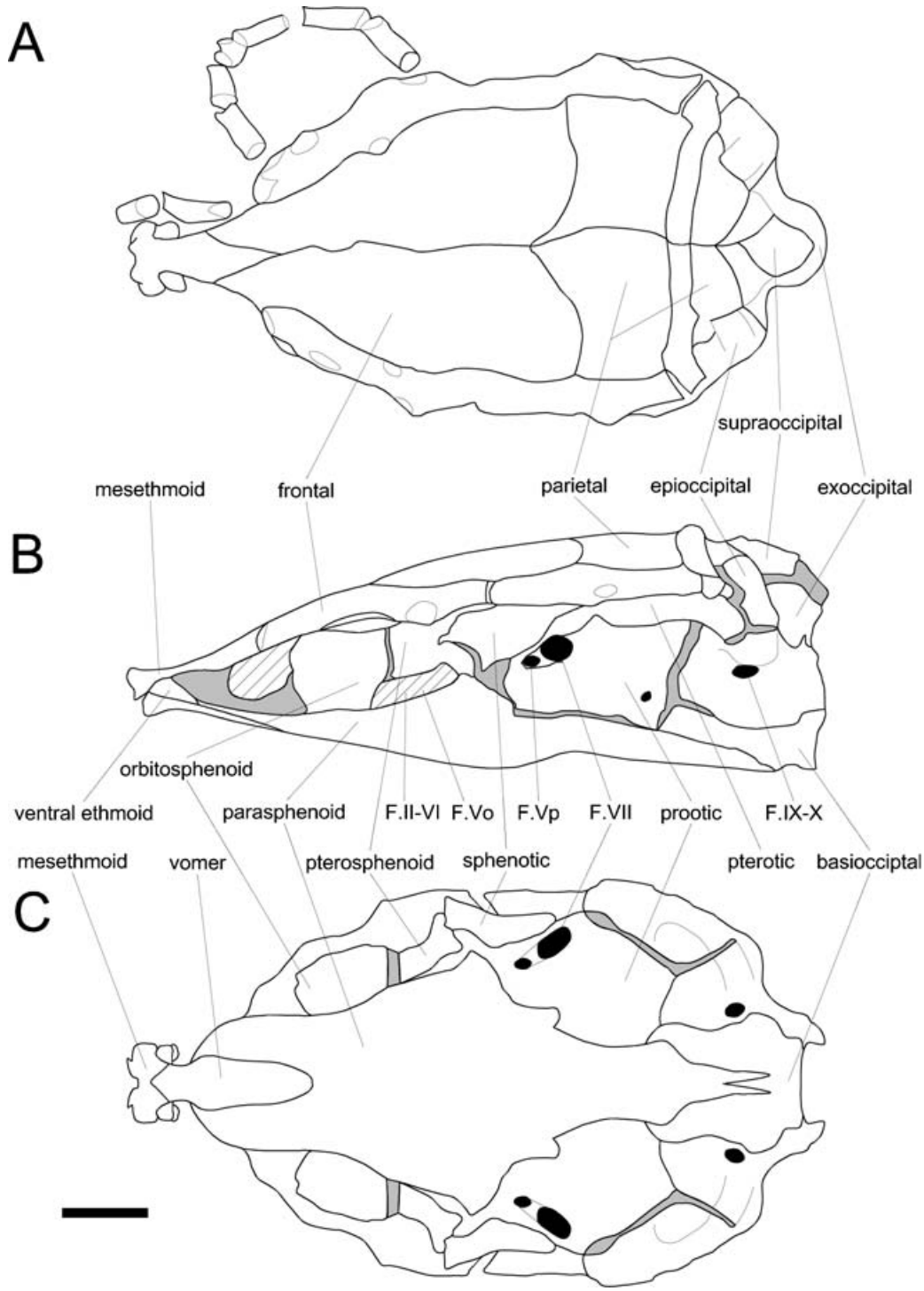

Figure 4 Neurocranium of *Gymnotus jonasi (*MCP uncat. WGRC 17.020698). (A) dorsal view, (B) lateral view, (C) ventral view. Shading scheme and abbreviations as in Fig. 2. Infraorbital laterosensory canal bones in A shown on right side only. Note rounded aspect of neurocranium in dorsal and ventral views. Scale bar = 1 mm.

1: moderate, equal to width of 7–9 teeth along dentary oral margin (Fig. 8C). 2: long, equal to width of about 10–12 teeth along dentary oral margin (Fig. 7).

39. Maxilla shape distally. 0: broad distally, paddle-shaped (Figs 8C–D). 1: narrow distally, rod-shaped (Figs 8A–B).
40. Premaxilla, number of teeth in outer row. 0: many, 11–16 (Figs 9A–C). 1: few, 3–10 (Fig. 9D).
41. Premaxilla shape. 0: median margin strongly curved (9A–C). 1: median margin straight (Fig. 9D).
42. Premaxillary tooth rows. 0: one row of mature teeth arranged along oral margin (Figs 9B and 9D). 1: two rows of mature teeth, second row sometimes present as a small patch of 2–3 teeth at anterior portion (Figs 9A and 9C).

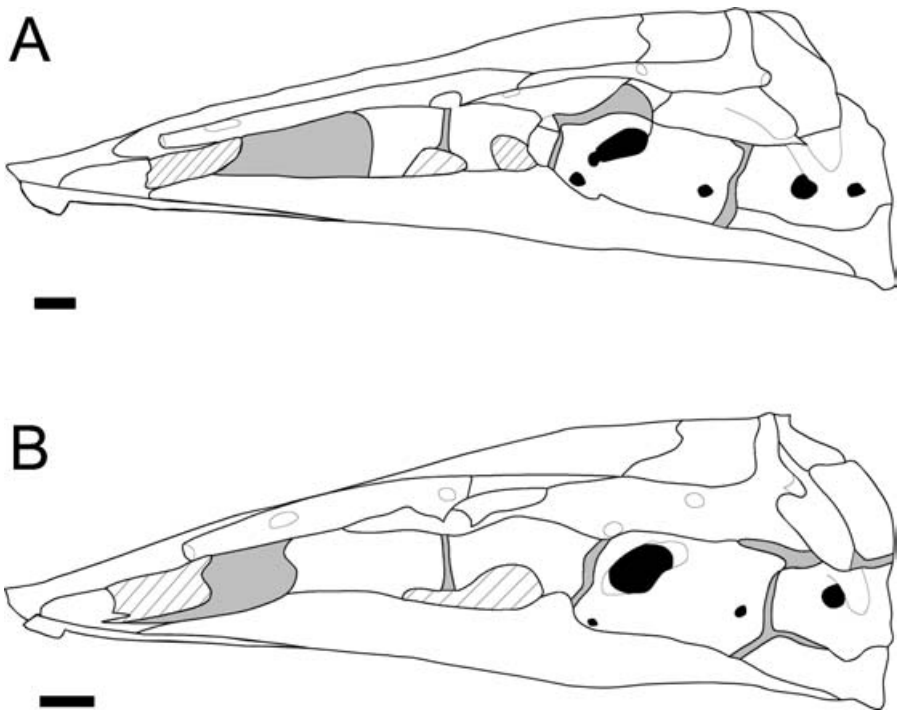

Figure 5 Lateral view of the neurocranium in mature specimens of similar absolute size representing the *Gymnotus carapo* and *G. pantherinus* groups. (A) *Gymnotus carapo* (UMMZ 190414, 260 mm), (B) *Gymnotus anguillaris* (UMMZ 190413, 289 mm). Shading scheme as in Fig. 2. Note the longer basioccipital in A. Scale bars = 1 mm.

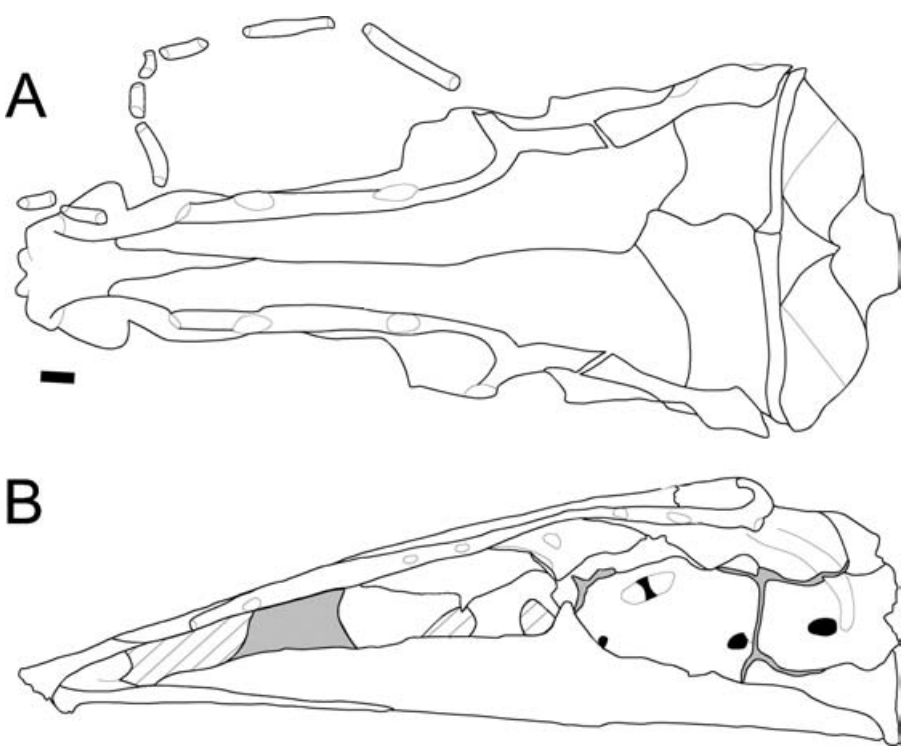

Figure 6 (A) Dorsal and (B) lateral views of the neurocranium of *Gymnotus arapaima* (MCP uncat. WGRC 01.040599, Brazil). Shading scheme as in Fig. 2. Numbers as in Fig. 3. Note region of neurocranium anterior to laterosensory foraminae 3 is longer than in congeners. Scale bar = 1 mm.

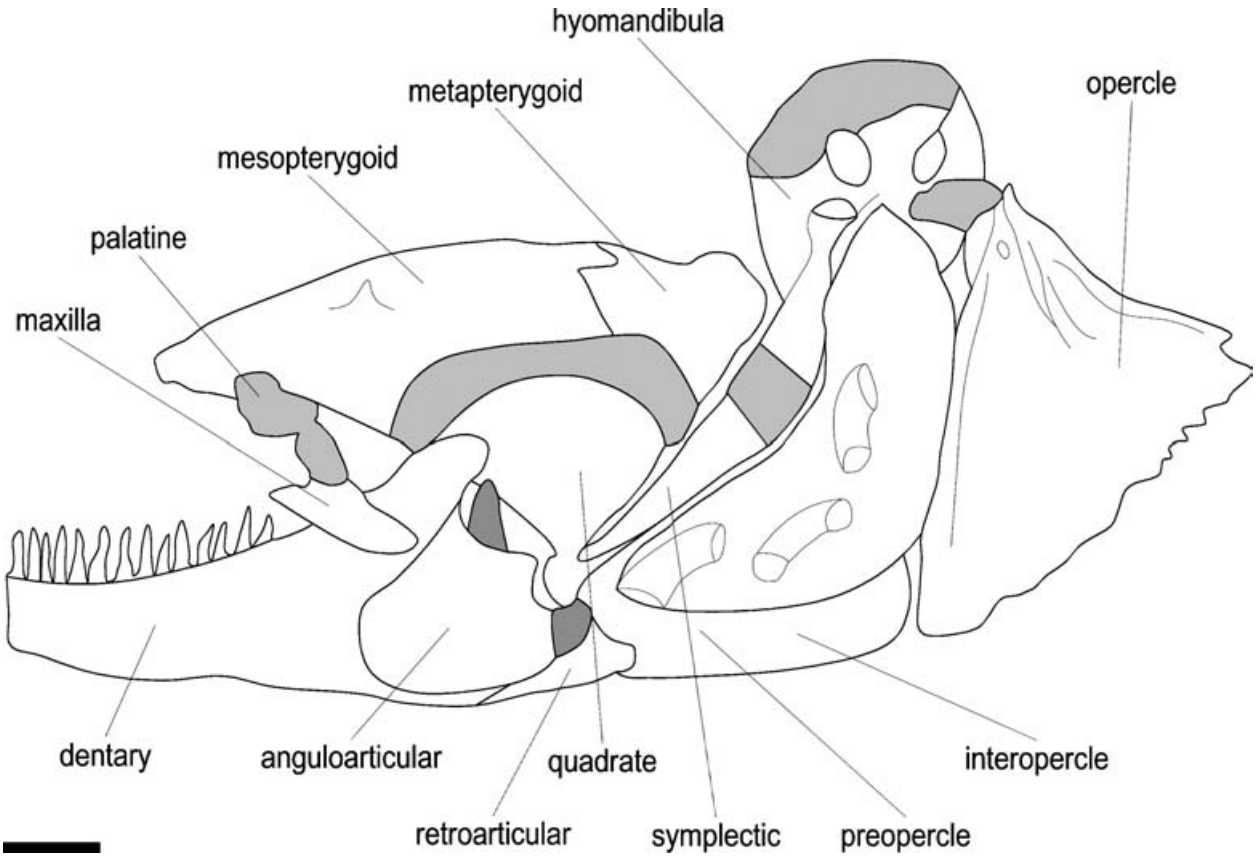

Figure 7 Lateral view of suspensorium of a juvenile *Electrophorus electricus* (UF 42193, 108 mm TL). Note character states of the maxilla (23-1, 24-0, 25-1, 26-2, 27-0), retroarticular (5-1, 54-1), mesopterygoid (47-0, 48-0), opercle (35-1, 36-0, 41-1, 44-0). Grey shading indicates cartilage. Scale bar = 1 mm.

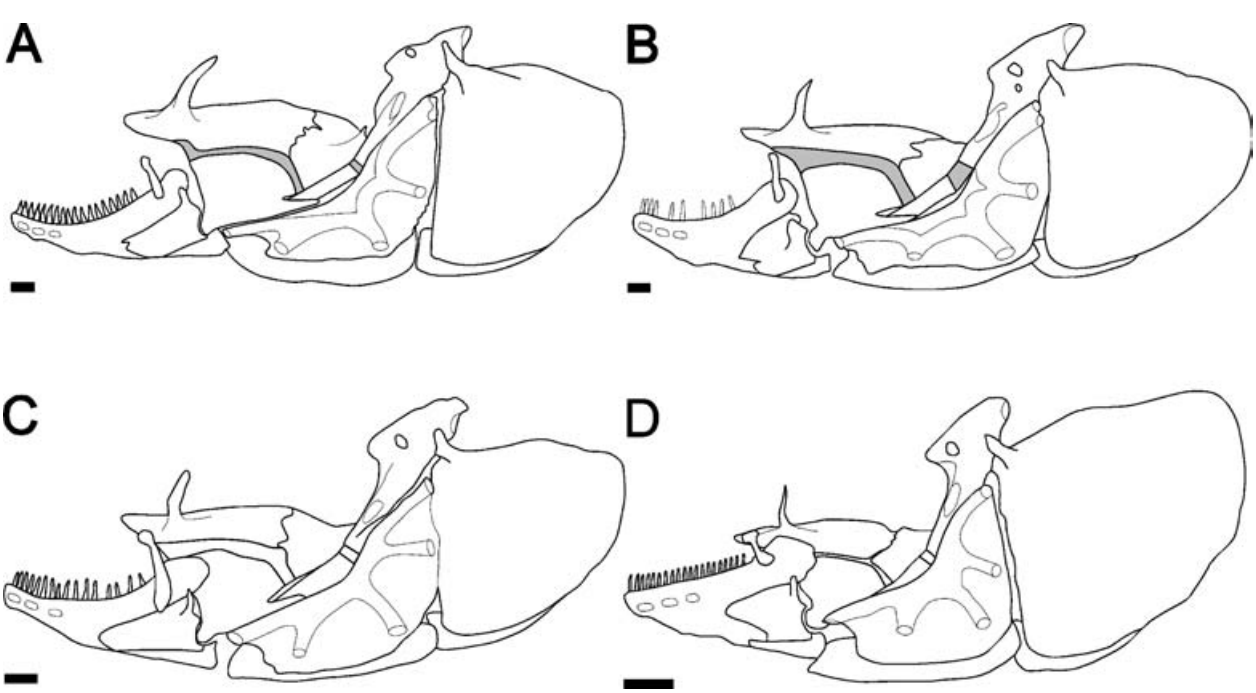

Figure 8 Lateral views of the suspensorium in four *Gymnotus* species. (A) *Gymnotus carapo* GU (UMMZ 190414), (B) *Gymnotus varzea* (MCP uncat. WGRC10.030597), (C) *Gymnotus anguillaris*, UMMZ 190413, (D) *Gymnotus jonasi* (MCP uncat. WGRC17.020698). Cartilage indicated by uniform grey shading. Scale bars = 1 mm.

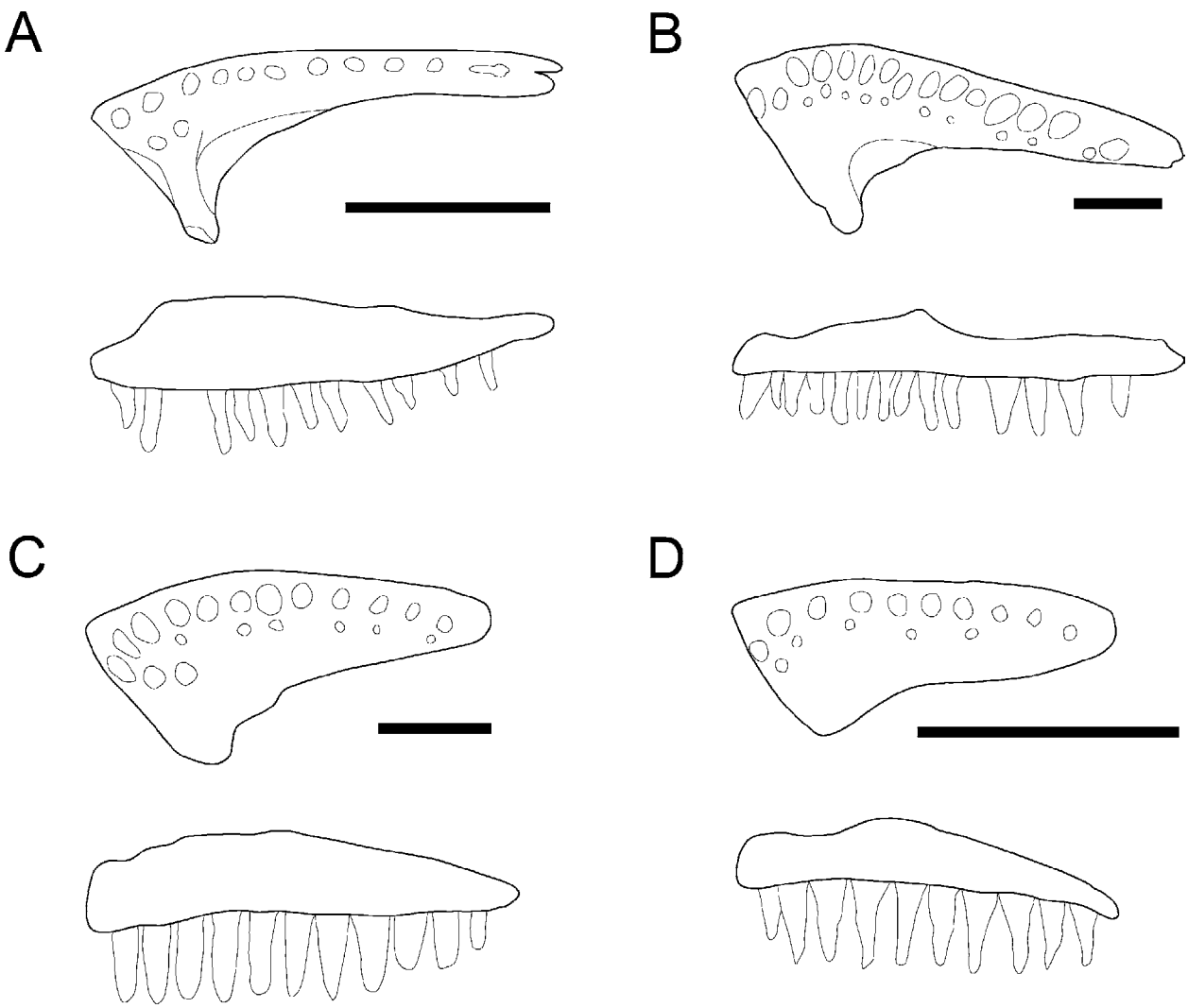

Figure 9 Ventral (top) and lateral (bottom) views of the premaxilla in four gymnotid species. (A) *Electrophorus electricus* (UF 42193), (B) *Gymnotus arapaima* (MCP uncat. WGRC 06.060899), (C) *Gymnotus anguillaris* (UMMZ 190413), (D) *Gymnotus jonasi* (MCP uncat. WGRC 17.020698). Note the derived shape and number of teeth associated with reduction of the premaxilla in D. Scale bar = 1 mm.

43. Dentary teeth needle-shaped. 0: all dentary teeth conical (or flattened), their cross-sectional area at base more than three times that near their distal tip (Figs 10A–B, 10). 1: 5–10 needle-shaped teeth along dentary margin, their cross-sectional area at base approximately equal to that near their distal tip (Figs 7, 10C–D).
44. Dentary teeth arrowhead-shaped. 0: all dentary teeth conical (or needle-shaped), circular in cross section. 1: 2–4 arrowhead-shaped teeth in anterior portion of dentary, their cross-sectional area at base compressed anteroposteriorly. 2: 4–7 arrowhead-shaped teeth in anterior portion of dentary. 3: 8–16 arrowhead-shaped teeth distributed along majority of dentary oral margin (Fig. 11).
45. Dentary teeth outer row. 0: mode 0–12 teeth. 1: mode 12–15 teeth. 2: 16–20 teeth.
46. Dentary tooth rows. 0: one row of mature teeth along oral margin. 1: mature teeth present in an inner row or patch of 2–3 teeth anteriorly.
47. Dentary posterior processes. 0: dorsoposterior process overlaps ventroposterior process (Fig. 10A). 1: Dorsoposterior and ventroposterior processes abut (Figs 10C–D).
48. Dentary ventroposterior process. 0: shorter than dorsoposterior process, its posterior tip in advance (Figs 10B–C). 1: as long or almost as long as dorsoposterior process (Fig. 10A and 10D).
49. Dentary dorsoposterior process. 0: tapered to distal tip of process (Figs 10A, 10B and 10D). 1: more broad distally than at base of process (Fig. 10C).
50. Dentary ventral margin. 0: with small lamella small, less than depth of ventroposterior process (Figs 8A–B and 8D). 1: with large lamella, greater than width of ventroposterior process (Fig. 8C).
51. Dentary anterior hook. 0: ventral margin of mental symphysis smooth (Figs 10A–B). 1: ventral margin of mental symphysis with paired ventroposterior oriented processes, appearing as a hook in lateral view (Figs 10C–D).
52. Opercle dorsal margin. 0: straight or convex (Figs 8A–D). 1: concave (Fig. 7).

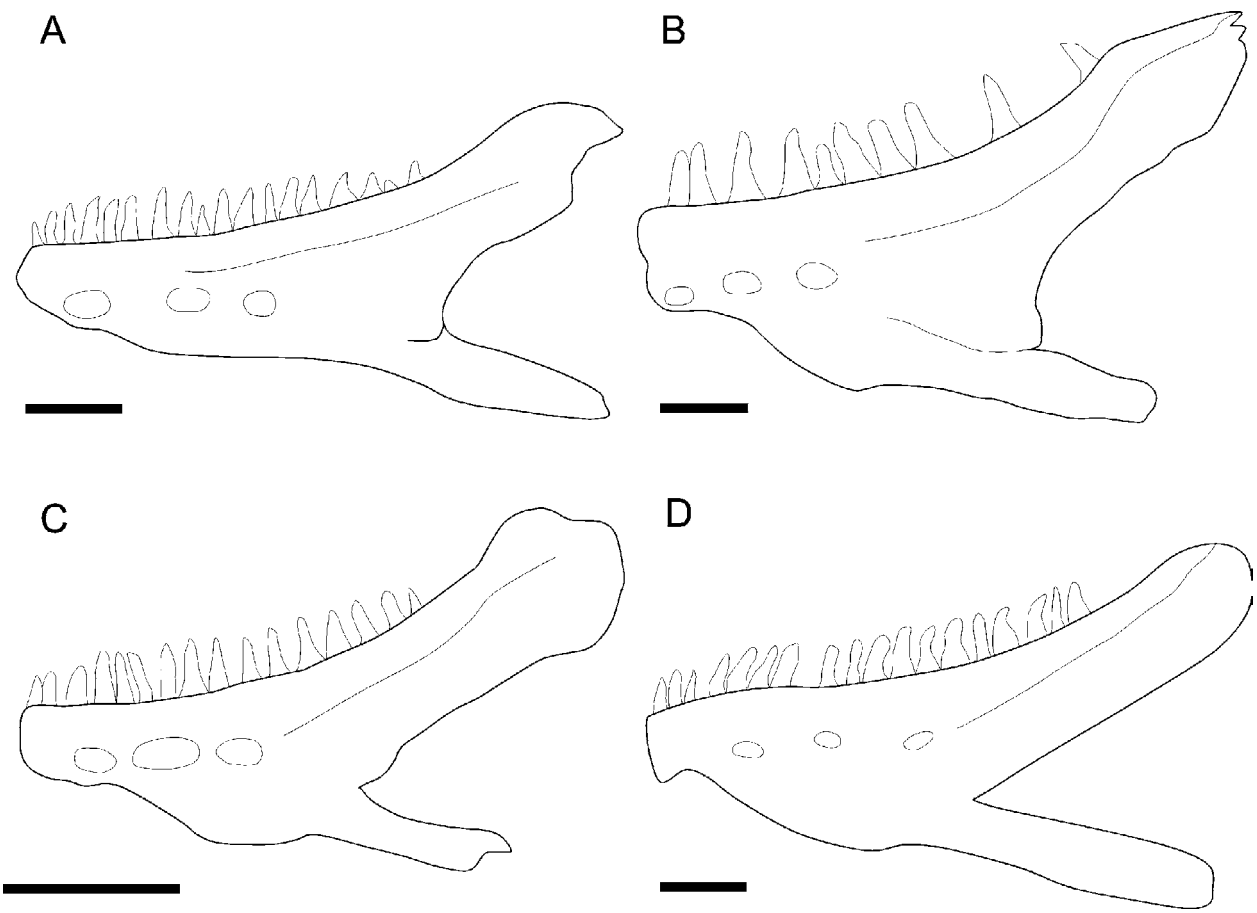

Figure 10 Lateral views of the dentary in four gymnotid species. (A) *Electrophorus electricus* (UF 42193, juvenile, 108 mm), (B) *Gymnotus arapaima* (MCP uncat. WGRC 06.060899), (C) *Gymnotus jonasi* (MCP uncat. WGRC 17.020698), (D) *Gymnotus anguillaris* (UMMZ 190413). Scale bars = 1 mm.

53. Opercle posterior margin. 0: smooth, entire (Figs 8A–D). 1: ridges produced to spines (Fig. 7).
54. Preopercle laterosensory pore. 0: single pore at dorsoposterior corner of preopercle (second pore of preopercular-mandibular lateral line; Fig. 12B). 1: two pores at dorsoposterior corner of preopercle (Fig. 12A).
55. Preopercle anterior notch. 0: ventral and dorsal margins of preopercle forming an acute angle (Albert & Miller, 1995, fig. 6). 1: anterior margin of preopercle concave (Figs 12A–B).
56. Preopercle median shelf margin. 0: entire. 1: serrate.
57. Preopercle median shelf. 0: small, less than half width of symplectic (Fig. 12B). 1: large, more than half width of symplectic (Fig. 12A).
58. Mesopterygoid ascending process size. 0: robust (Figs 13B–C). 1: gracile (Fig. 13D).
59. Mesopterygoid ascending process length. 0: short, its base subequal to its length (Fig. 13A). 1: long, its length more than its base (Figs 13B–D).
60. Mesopterygoid ascending process shape. 0: straight, position of its distal tip dorsal to posterior margin of its base (Figs 13B and 13D). 1: curved posteriorly, position of its distal tip posterior to posterior margin of its base (Fig. 13C).
61. Mesopterygoid ascending process tip. 0: simple, with smooth margin (Figs 13C–D). 1: complex, with multiple small interdigitating processes (Fig. 13B).
62. Metapterygoid superior portion. 0: large, its anterior margin ossifies to a vertical with anterior margin of metapterygoid inferior portion (Figs 13A and 13C). 1: small, its anterior margin ossifies posterior to anterior margin of inferior portion (Figs 13B and 13D).
63. Interopercle ascending process. 0: present on anterior portion of interopercle dorsal margin. 1: absent, interopercle dorsal margin straight or slightly convex.
64. Subopercle dorsal margin. 0: concave. 1: convex.
65. Retroarticular ventroposterior margin. 0: short, angle of ventroposterior margin square (Figs 8A–D). 1: elongate, angle of ventroposterior margin acute (Fig. 7).
66. Angular ventrolateral lamellae. 0: absent or small, not extending laterally over retroarticular. 1: expanded, extending laterally over retroarticular (Figs 8A–D).
67. Anguloarticular ascending process. 0: long, extending beyond ventral margin of dentary (Figs 8A, C–D). 1: short, extending to ventral margin of dentary (Figs 8B).
68. Mandible shape. 0: short and compressed. 1: long and extended.

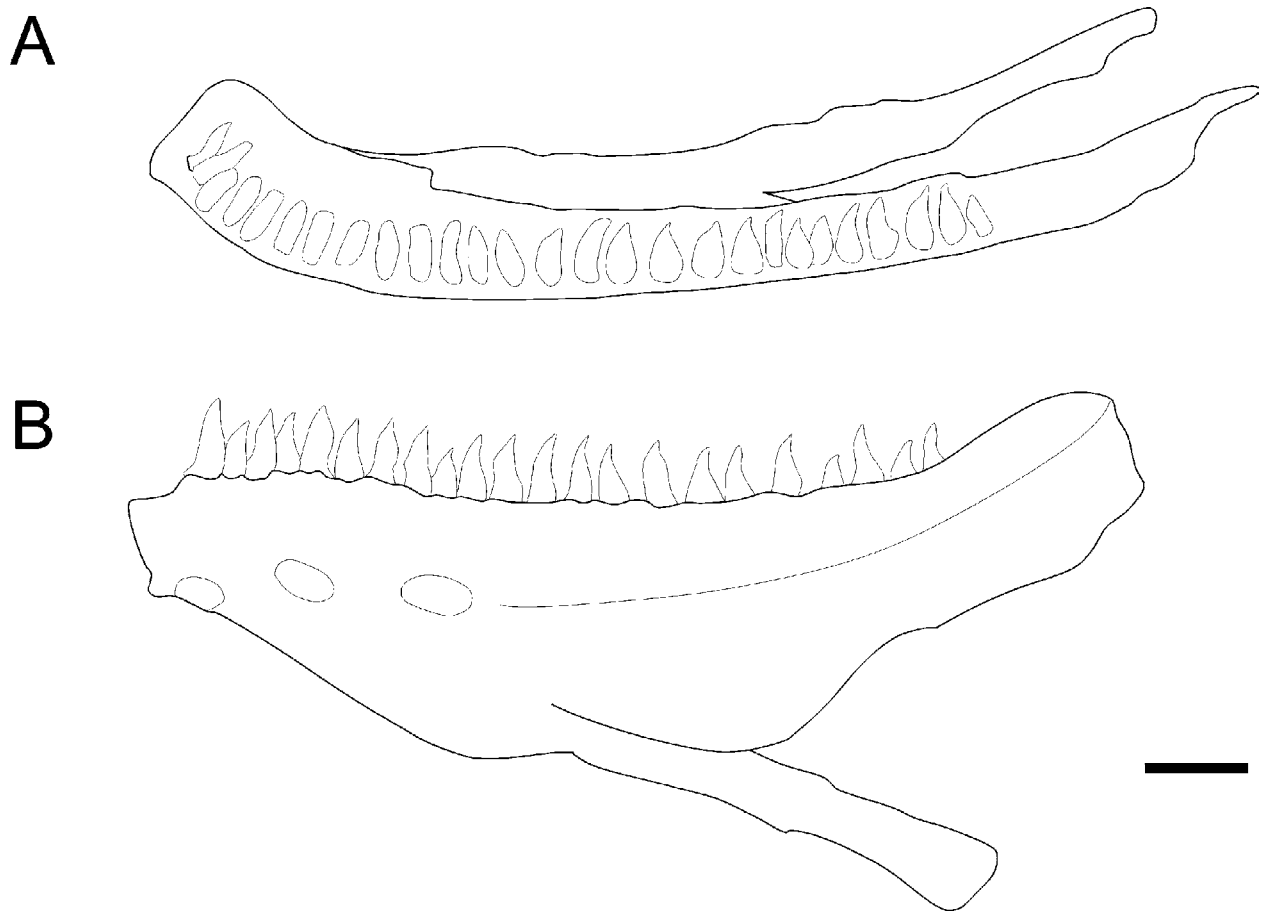

Figure 11 Dorsal (top) and lateral (bottom) views of the dentary in *Gymnotus arapaima* (MCP uncat. WGRC 06.060899). Note most teeth are arrowhead-shaped and flattened anteroposteriorly. Scale bar = 1 mm.

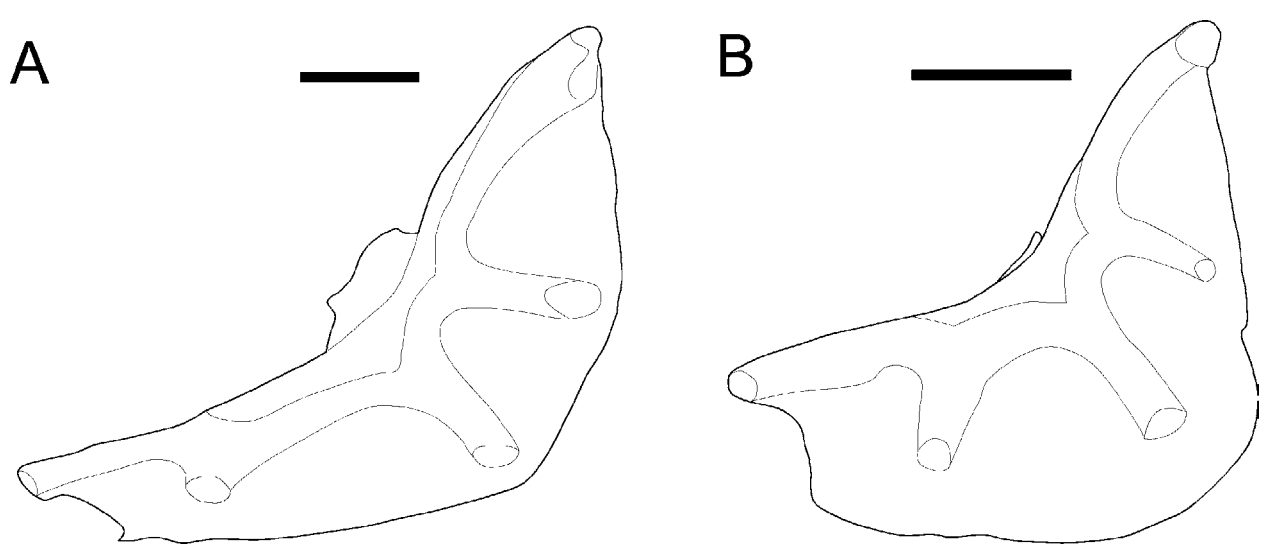

Figure 12 Lateral views of the preopercle in two *Gymnotus* species. (A) *Gymnotus carapo* GU (UMMZ 190414, Surinam), (B) *Gymnotus jonasi* (MCP uncat. WGRC 19.170597). Note two pores at dorsoposterior corner of preopercle in (A) and single pore in B. Also note large size of median shelf in (A) vs. small size in (B), and presence of an anterior notch both (A) and (B). Scale bars = 1 mm.

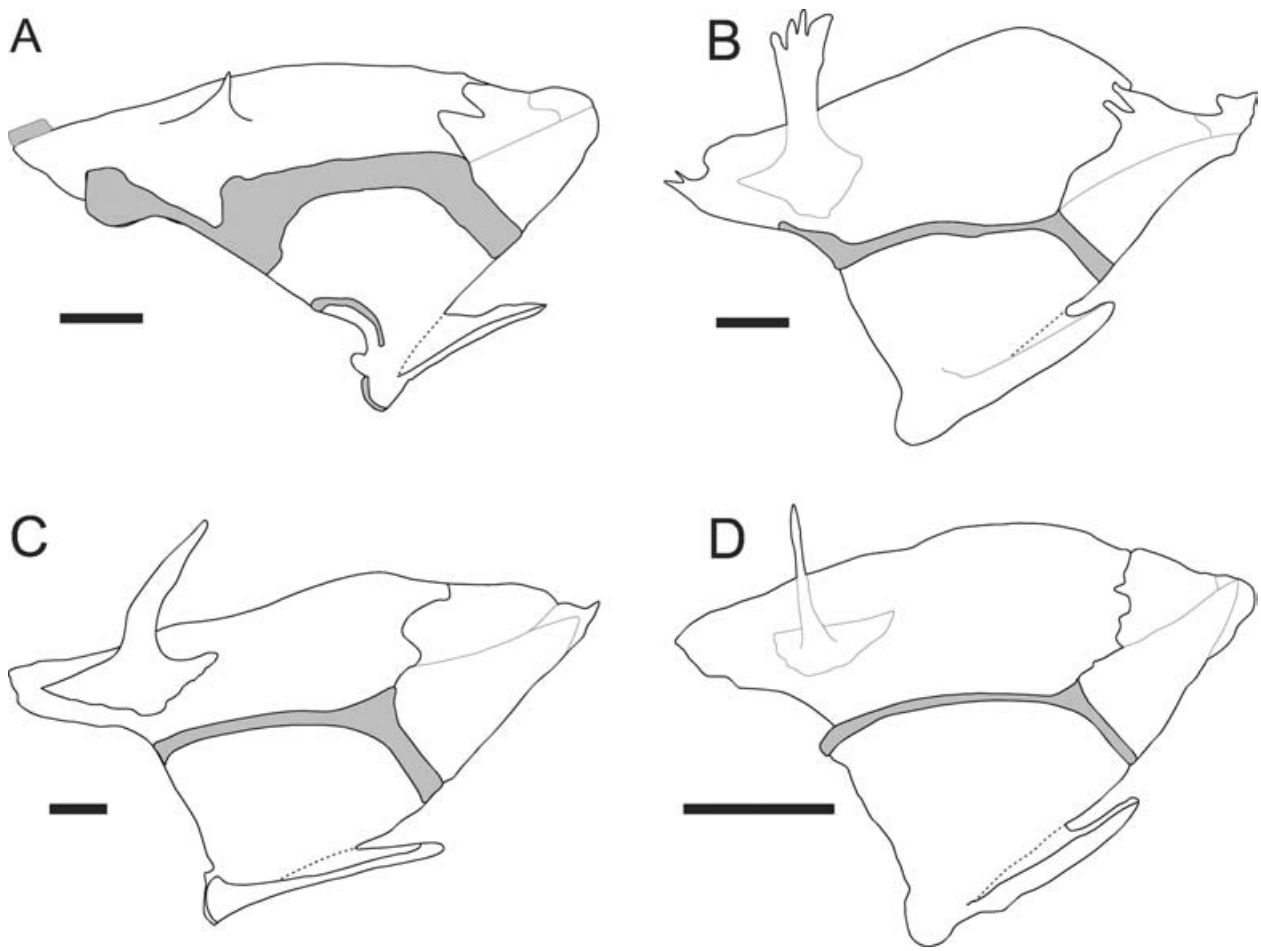

Figure 13 Lateral views of the mesopterygoid in four *Gymnotus* species. (A) *Electrophorus electricus* (UF 42193). (B) *Gymnotus mamiraua* (MCP uncat. WGRC 24.180699). (C) *Gymnotus arapaima* (MCP uncat. WGRC 06.060899). (D) *Gymnotus jonasi* (MCP uncat. WGRC 19.170597). Scale bars = 1 mm.

69. Hyomandibula trigeminal canals. 0: supraorbital and infraorbital lateral line nerves connected (Figs 14B, 14D). 1: supraorbital and infraorbital lateral line nerves divided (Figs 14A, 14C).
70. Hyomandibula posterior lateral line canal. 0: lateral fenestra remote from dorsoposterior margin of hyomandibula (Fig. 14A). 1: lateral fenestra at dorsoposterior margin of hyomandibula (Figs 14B–D).
71. Cranial fontanels. 0: paired frontal and parietal bones separated by fontanels along majority or entirely of their medial margins (Ellis, 1913, fig. 1; Mago-Leccia, 1978, fig. 12). 1: closed in adults, paired frontal and parietal bones in contact along their entire medial margins (Figs 2A, 3A, 4A, 6B).
72. Frontal laterosensory canal. 0: narrow, its anterior margin confluent with lateral margin of adjacent frontal bone (Figs 2A, 3A, 6B). 1: wide, its anterior margin not confluent with lateral margin of adjacent frontal bone (Fig. 4A).
73. Frontal postorbital process. 0: narrow, less than two times width of supraorbital canal at its junction with neurocranium (Figs 1A, 3A, 4A). 1: broad, more than two times width of supraorbital canal at its junction with neurocranium (Fig. 6A).
74. Frontal shape. 0: broad, its width at junction of supraorbital canal with neurocranium about 1/3 its length (Figs 2A, 3A, 4A). 1: narrow, its width at junction of supraorbital canal with neurocranium less than 1/4 its length (Fig. 6A).
75. Lateral ethmoid. 0: ossified. 1: unossified or absent.
76. Parasphenoid shape. 0: very narrow and elongate, its length 3.0–3.5 times its width (Fig. 2C; Albert & Fink, 1996, fig. 4C). 1: moderately narrow, its length 2.2–3.0 times its width. 2: broad, its length 2.0–2.2 times its width (Figs 3A, 4A).
77. Vomer. 0: short, extending less than half the distance to the lateral process of the parasphenoid (Figs 2B–C, 3B–C, 4B–C, 5B). 1: long, extending more than half the distance to the lateral process of the parasphenoid (Figs 5A, 6A).
78. Parasphenoid posterior processes. 0: robust, stout, convexity of posterior margin shallow, poorly incised (Figs 2C, 3C). 1: gracile, elongate, convexity of posterior margin deeply incised (Fig. 4C).

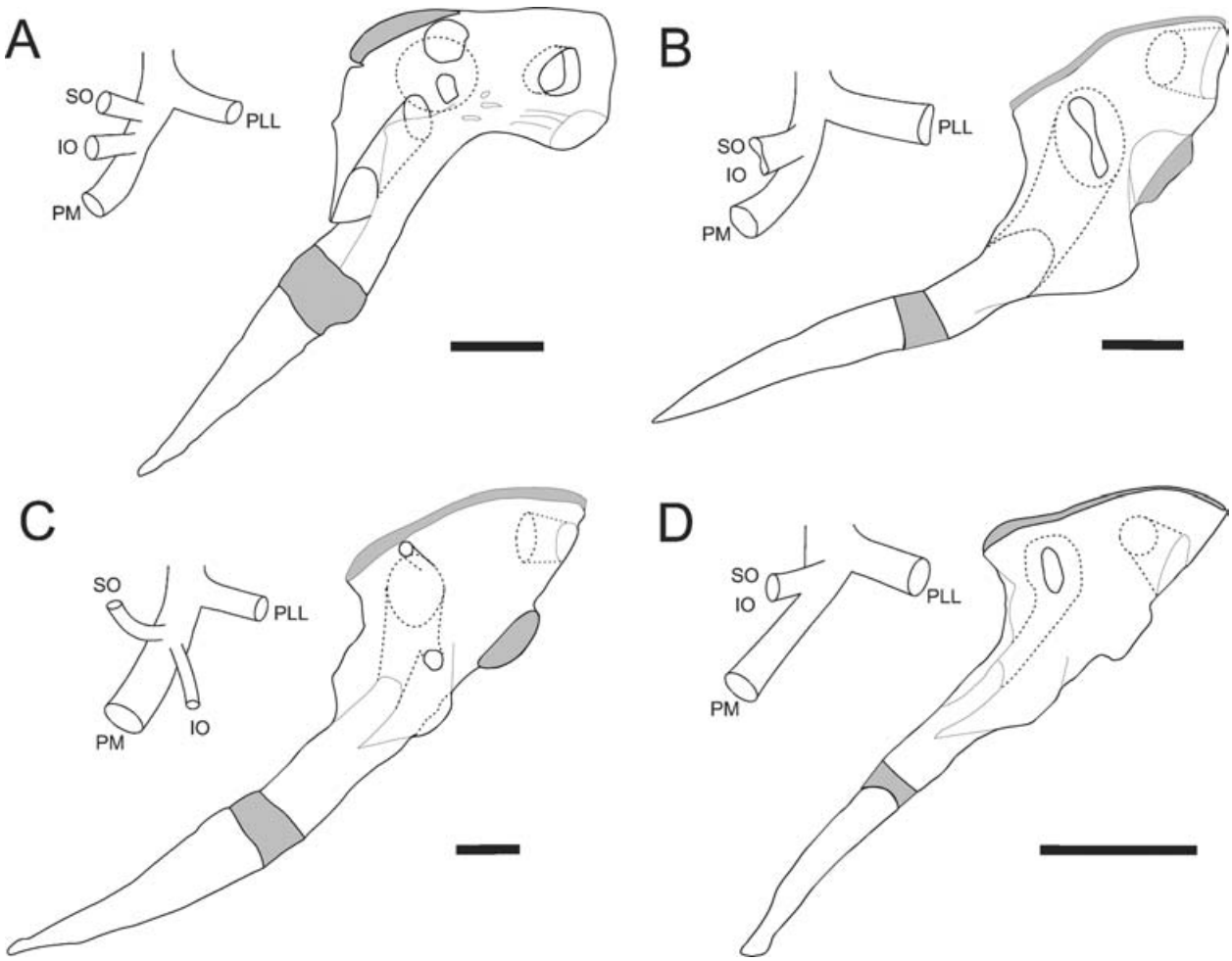

Figure 14 Lateral views of the hyomandibula in four *Gymnotus* species (right) and branching patterns of trigeminal/lateralis nerve complex (left). (A) *Electrophorus electricus* (UF 42193, juvenile, 108 mm TL). (B) *Gymnotus mamiraua* (MCP uncat. WGRC 24.180699). (C) *Gymnotus arapaima* (MCP uncat. WGRC 06.060899). (D) *Gymnotus jonasi* (MCP uncat. WGRC 19.170597). Scale bars = 1 mm.

79. Parietal shape. 0: square, its length subequal to its width (Fig. 2A; Albert & Fink, 1996, fig. 4A). 1: rectangular, its length less than its width (Figs 3A, 4A, 6B).
80. Pterosphenoid anteroventral portion. 0: robust, extends ventral to lateral margin of parasphenoid (Figs 2B, 3B). 1: reduced, extends dorsal to lateral margin of parasphenoid (Fig. 4B).
81. Prootic foramen. 0: separate foraminae for the profundus branch of the trigeminal nerve (Vp) and the other branches of the trigeminal (V_{2-3}) and facial (VII) nerves (Figs 2B, 3B). 1: a single foramen for the trigeminal and facial nerves (Figs 4B, 5B).
82. Adductor mandibula insertion. 0: only to maxilla. 1: to maxilla and to first infraorbital laterosensory canal bone. 2: undivided.
83. Adductor mandibula intermuscular bones. 0: absent. 1: ossified.
84. Basibranchials. 0: ossified. 1: unossified.
85. Gill rakers. 0: contacting gill bar. 1: not contacting gill bar.

Pectoral girdle

86. Pectoral-fin rays (P1R). 0: mode = 17–21. 1: mode = 14–16. 2: mode = 12–13.
87. Pectoral fin, medial radial cartilage(s). 0: large (Figs 15B–C, 16). 1: small or absent (Fig. 15D).
88. Mesocoracoid proximal portion. 0: thin (Fig. 16; Albert & Miller, 1995, fig. 5B). 1: broad.
89. Mesocoracoid distal portion. 0: ossified. 1: not ossified.
90. Postcleithrum. 0: robust. 1: thin, discoid or sickle-shaped.
91. Cleithrum shape. 0: broad, ventral margin curved (Figs 15A–B, 16). 1: narrow, ventral margin straight (Fig. 15C). 2: very narrow at anterior tip, ventral margin straight or convex (Fig. 15D).
92. Cleithrum length anterior limb. 0: short, about 1.5 times length of ascending limb (Albert & Miller, 1995, fig. 5). 1: long, 1.8–2.0 times length of ascending limb (Figs 15B–D, 16).
93. Cleithrum anterior notch. 0: anteroventral margin of cleithrum smooth or with a slender concavity, less than half

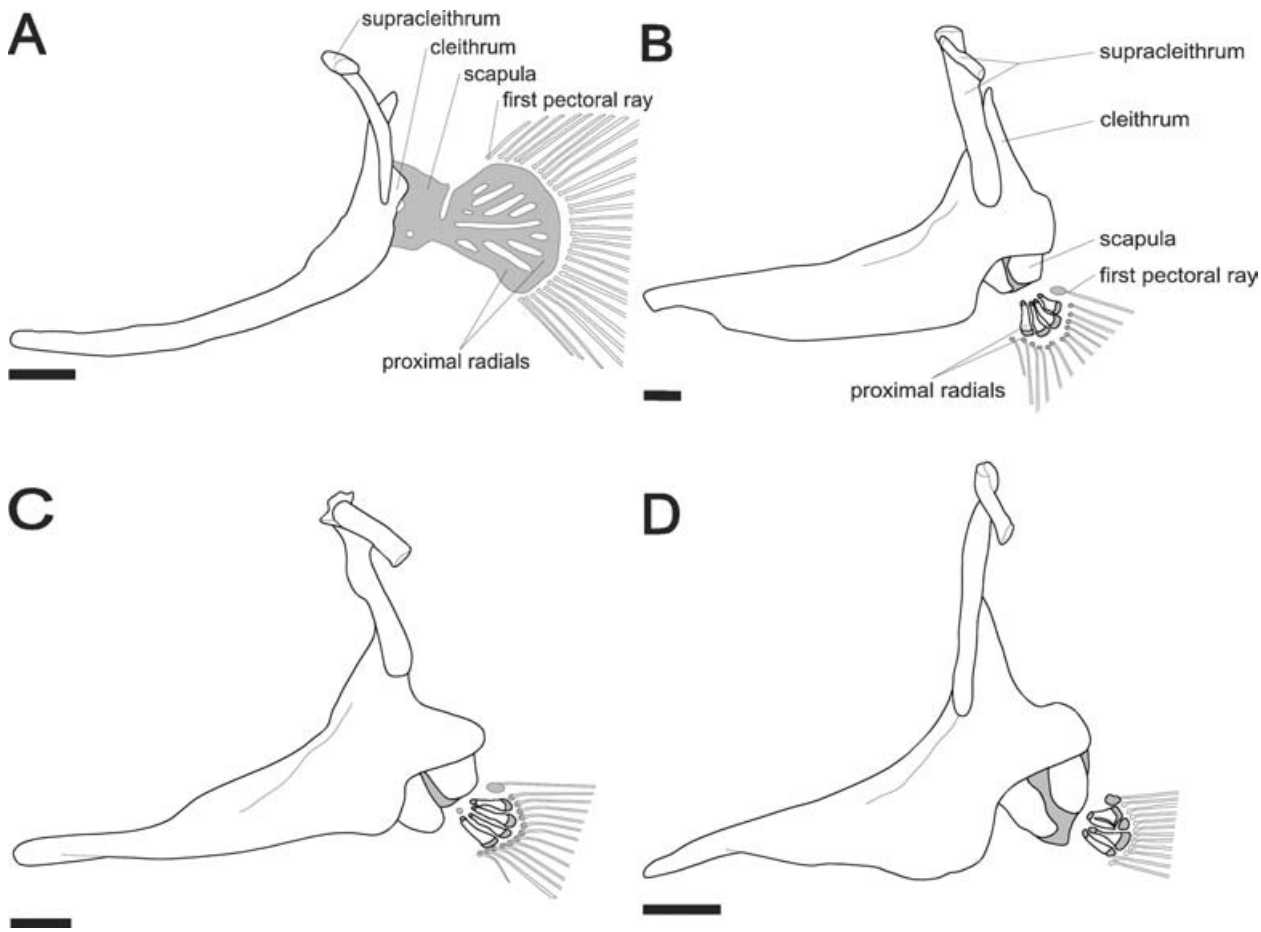

Figure 15 Lateral views of the pectoral girdle in four gymnotid species. (A) *Electrophorus electricus*, UF 42193. (78-0). (B) *Gymnotus carapo* GU (UMMZ 190414), (77-1, 78-1). (C) *Gymnotus anguillaris* (UMMZ 190413). (D) *Gymnotus jonasi* (MCP uncat. WGRC 17.020698). Cartilage indicated by uniform grey shading. Fin rays drawn incomplete. Scale bars = 1 mm.

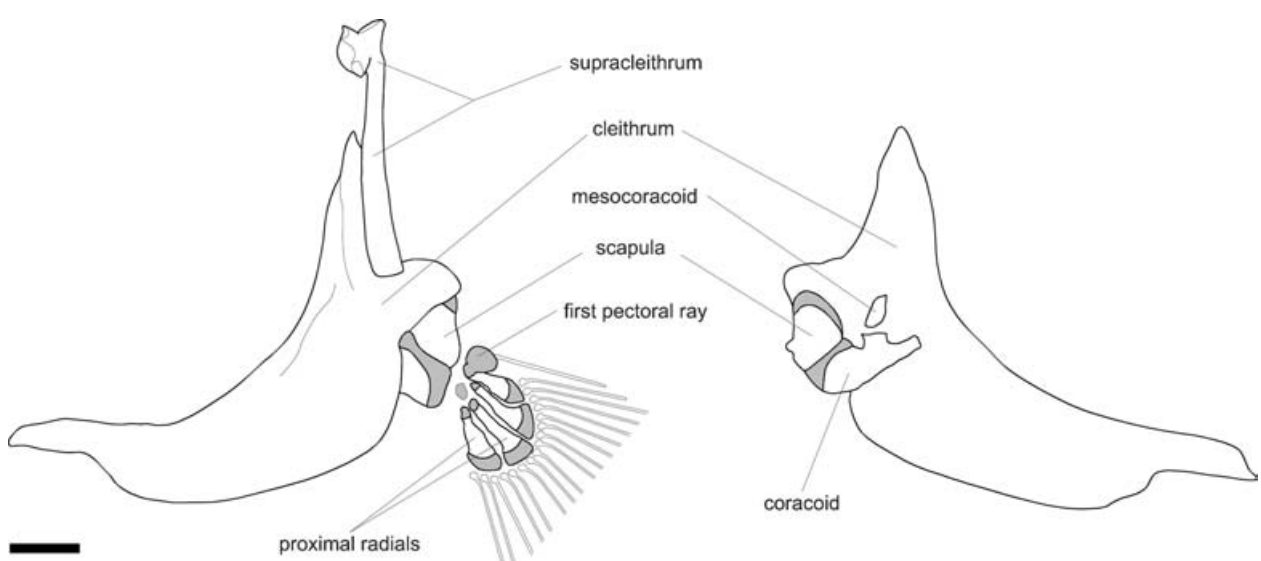

Figure 16 Pectoral girdle of *Gymnotus varzea* (MZUSP uncat., WGRC 10.030597. Left: lateral view. Right: medial view. Note the mesocoracoid is ossified and the proximal portion is thin. Note also the cleithrum is broad with a curved ventral margin, possesses a long anterior limb and an anterior notch. Scale bar = 1 mm.

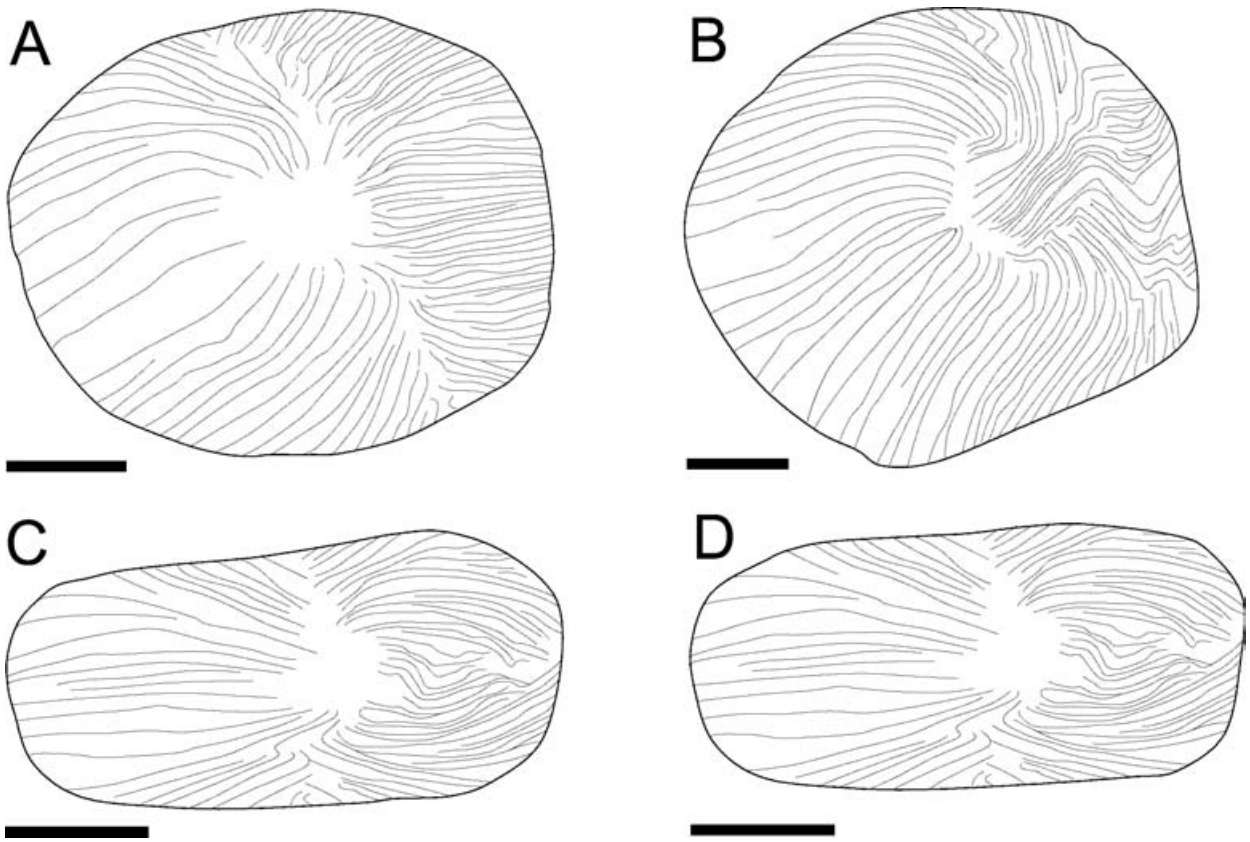

Figure 17 Scales at midbody one row above the lateral line in four *Gymnotus* species. (A) *G. arapaima*. (B) *G. carapo* RO. (C) *G. tigre*. (D) *G. henni*. Scale bars =1 mm. Anterior to left.

width of anterior cleithral process (Fig. 15A; Albert & Miller, 1995, fig. 5). 1: anteroventral margin of cleithrum with a deep convexity, more than half width of anterior cleithral process (Figs 15B, 16). 2: anteroventral margin of cleithrum deeply incised with semi-lunar concavity.

94. Cleithrum dorsoposterior facet. 0: groove for insertion of ligaments attaching to supracleithrum absent or shallow. 1: groove for insertion of ligaments attaching to supracleithrum deep and long.

Squamation

95. Body squamation. 0: present. 1: absent.
96. Scales above lateral line (SAL). 0: small, mode 9–13. 1: large, mode 5–8.
97. Scale shape in mature specimens. 0: circular or slightly ovoid (Fig. 17A–B) over entire body. 1: elongate in the rostrocaudal axis over most of body, their lengths 1.5–3.0 times their depths in first row above lateral line at midbody (Fig. 17C–D).
98. Pored scales in posterior lateral line (PLL). 0: mode 69–110 scales. 1: mode 110–131 scales.
99. Pored lateral line scales to anterior ventral lateral line ramus (PLR). 0: median 0–49. 1: 50–61. 2: 62–70.
100. Scales over anal-fin pterygiophores (APS) at anterior ventral lateral line ramus. 0: large, mode 5–7 rows. 1: moderate, mode 8–11 rows. 2: small, mode 12–16 rows.
101. Lateral line ventral rami (VLR). 0: none. 1: few, median 1–8 ventral rami in adults. 2: moderate number, median 9–18 ventral rami in adults. 3: many, median 19–51 ventral rami in adults, all very short.
102. Lateral line dorsal rami (DLR). 0: absent in majority of adults. 1: present in majority of adults.

Axial skeleton

103. Body cavity length (PCV). 0: mode = 17–22 PCV. 1: 23–29 PCV. 2: 30–35 PCV. 3: 36–39 PCV. 4: 40–51 PCV.
104. Rib 5 crest. 0: rib 5 approximately 3–5 times width of rib 6 at its midlength, its anterolateral surface produced into a small ridge (Fig. 18A). 1: rib 5 approximately 6–7 times width of rib 6 at its midlength, its anterolateral surface produced into a broad triangular crest (Fig. 18B).
105. Hemal spines. 0: present. 1: absent.
106. Displaced hemal spines. 0: absent (Albert, 2001, figs 35A–B). 1: present at posterior margin of body cavity (Albert, 2001, figs. 35C–E, 36A–D).
107. Anal-fin ray number (AFR). 0: mean 150–225 AFR. 1: mean 226–270 AFR.
108. Anal-fin ray branching. 0: few unbranched anterior anal-fin rays, all rays branched posterior to rays 10–17.

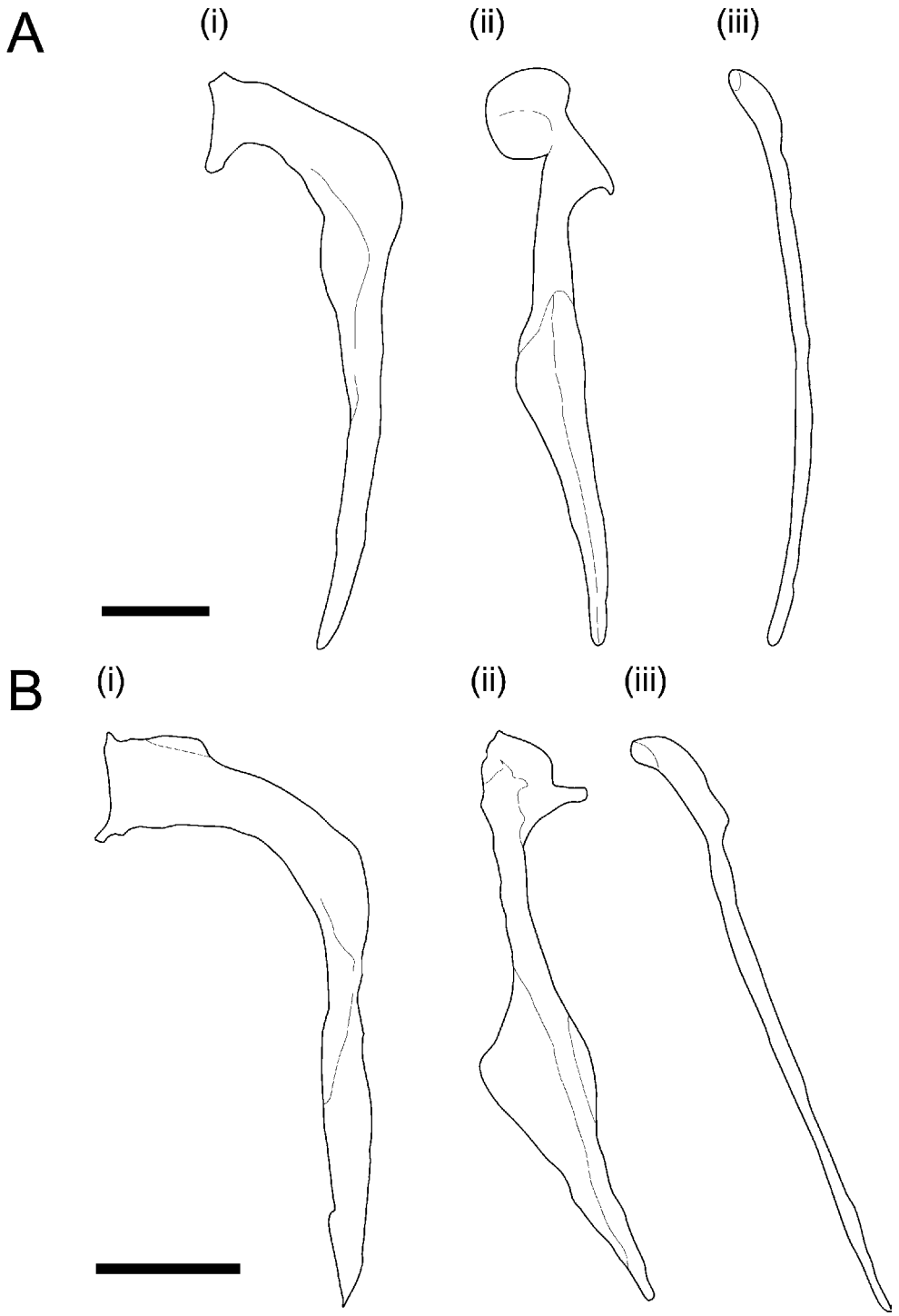

Figure 18 Frontal (i) and lateral (ii) views of 5th rib, and lateral (iii) view of 6th rib in two *Gymnotus* species. (A) *Gymnotus varzea* (MCP uncat. WGRC 01.030597), (B) *Gymnotus jonasi* (MCP uncat. WGRC 19.170597). Note broad anterior shelf on distal portion of 5th rib in (B) more than three times width of 6th rib. Scale bars = 1 mm.

1: many unbranched anterior anal-fin rays, all rays branched posterior to ray 18. 2: all fin rays unbranched.

109. Length anal-fin pterygiophores. 0: shorter than hemal spines at midbody. 1: equal to or longer than hemal spines at midbody.

Electric organ

110. Hypaxial electric organs. 0: single organ, anatomically undivided. 1: three anatomically discrete electric organs.
111. Electric organ depth, as number of rows of electroplates at caudal end of anal fin (CEP). 0: slender, mode

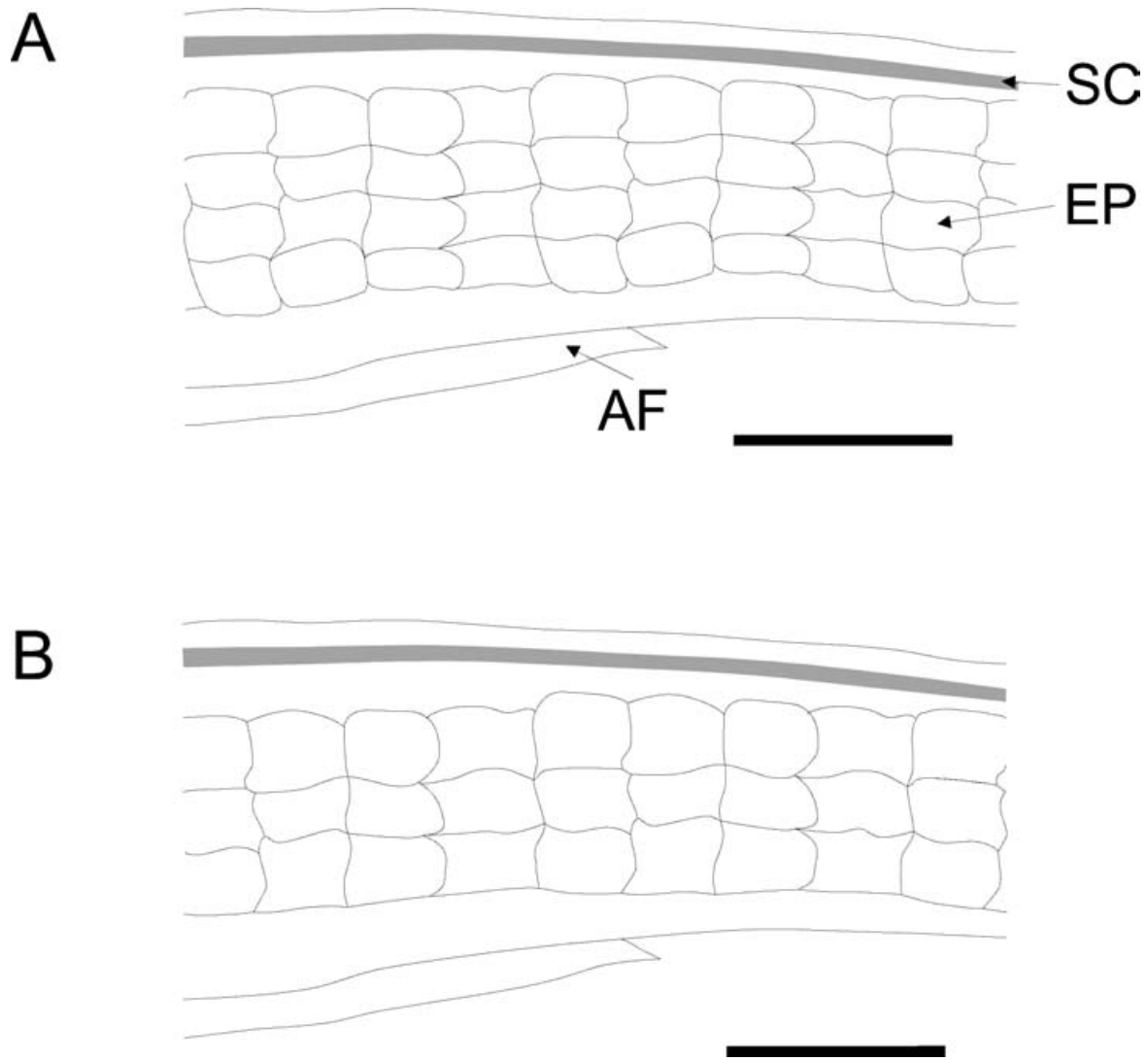

Figure 19 Portion of the electric organ of two *Gymnotus* species at the posterior end of anal fin. (A) *Gymnotus varzea* (MCP uncat. WGRC 10.030597) (B) *Gymnotus coropinae* WA (MCP uncat. WGRC 09.110300). Note four rows of electroplates (EP) above caudal end of anal fin (AF) in (A) and three rows in B. Spinal cord (SC) indicated in grey. Scale bars = 1 mm.

2–3 rows (Fig. 19B). 1: moderate depth, mode 4 rows (Fig. 19A). 2: deep, mode 5–6 rows. Ontogenetic changes in phenotypes of the caudal rows of electroplates, scales, and banding patterns in *G. tigre* is provided in Fig. 20.

112. EOD number of positive and negative phases away from baseline in adults. 0: 1 phase. 1: 2 phases. 2: 3 phases. 3: 4–5 phases.
113. EOD phase 2 amplitude (first head negative phase following first large head positive phase). 0: large, approximately equal to first large head positive phase. 1: small less than 25% first large head positive phase.

Interrelationships of *Gymnotus*

Interrelationships of *Gymnotus* inferred from this study are depicted in Fig. 21, with clade names and support indices listed for nodes indicated by Roman letters in Table 5. The topology of Fig. 21 is a strict consensus of 15 equally parsimonious trees, each of length 394 steps, derived from the data in Table 4 (CI = 0.35, RI = 0.70, RC = 0.24). This strict consensus topology is used in subsequent analyses of character evolution and biogeography. Diagnoses for 26 clades (A–AB) are provided in Appendix 2. The classification used in this study employs three hierarchically arranged taxa using the name of the type species *G. carapo*: the *G. carapo* group (Clade N) which includes 16 species, the *G. carapo* complex (Clade Z) which includes three species (*G. carapo*, *G. arapaima* and *G. ucamara*) and *G. carapo* which includes six allopatric populations (Albert & Crampton, 2003).

The main features of this working hypothesis of interrelationships confirm previous hypotheses of interrelationships among *Gymnotus* species (Albert & Miller, 1995; Albert, 2001; Albert & Crampton, 2003). These features are: 1, a basal division between *Gymnotus* clades endemic to Middle America (Clade C) and South America (Clade D); 2, a division of the

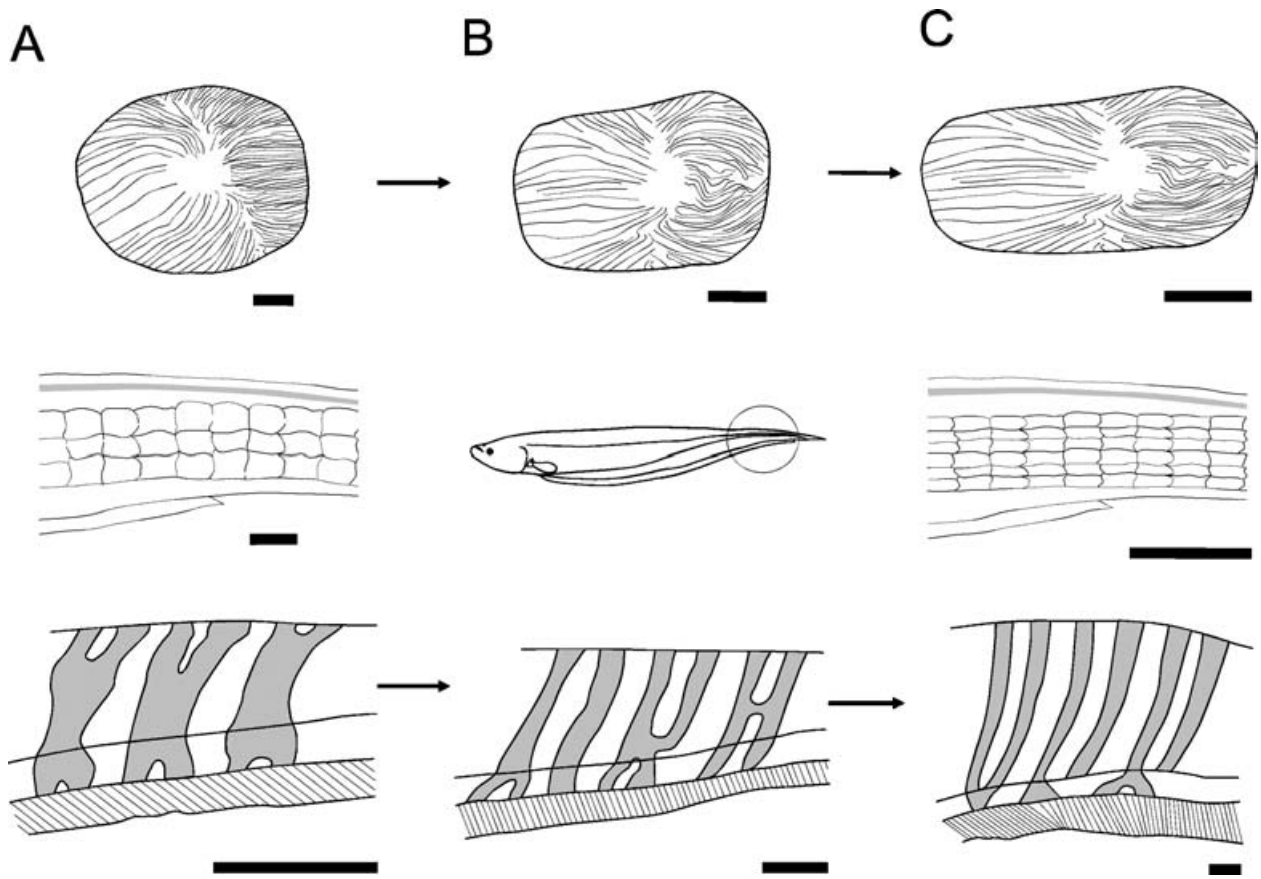

Figure 20 Ontogenetic changes in phenotype of scales, electroplates, and banding patterns of *Gymnotus tigre*. (A) UF 116553 (96 mm), (B) UF 117122 (173 mm), (C) UF 25552 (411 mm).

South American species into two monophyletic groups, the *G. pantherinus* group (Clade E) and *G. carapo* group (Clade N); and 3, the presence of species on the Pacific and Atlantic slopes of the Andes within both the *G. pantherinus* group (Clade F) and *G. carapo* group (Clades T and Z). Preliminary results from a MP analysis of molecular data including about 1216 bp of the nuclear RAG2 gene from 10 ingroup taxa are consistent with the division of *Gymnotus* into these three species groups (Albert *et al*., 2003).

Several nodes in the phylogenetic hypothesis of Fig. 21 are poorly supported from MP of the morphological data. Clades E, O, W, and Z have moderate BL support but little or no BD support (E: 8 and 0; O: 3 and 0; W: 4 and 1; Z: 4 and 2). The biogeographic inferences drawn upon these statements of relationship are largely insensitive to resolution of these four nodes. The main nodes of interest to biogeographic inferences are clades B, C, D, E, M, and N. Clade E is of concern in that the support for this taxon by the BL and BD indices are weak. There are however seven characters that strongly support the monophyly of this clade (16, 32, 51, 88, 99, 104, 111) of which one (104) is unique and unreversed on the tree topology of Fig. 21. In this regard it is important to note that preliminary data from analysis of the RAG2 gene (Albert *et al*., 2003; Lovejoy *et al*., in prep.) strongly support the monophyly of Clade E.

Rates of character state evolution

Rates of character evolution were evaluated from patterns of character-state change optimized unambiguously on a fully resolved tree topology (Fig. 22). Qualitative results of the analysis of phylogenetic plasticity were similar for all four equally parsimonious topologies resulting after a single round of reweighting on the RC. Characters of external morphology as a group are more phylogenetically plastic than characters of internal morphology as a group, as assessed by a lower ensemble RC (0.18 vs. 0.30). The 43 characters of external morphology include those of pigmentation, body proportions, squamation, fin ray meristics, and electric organ discharge (characters 1–30, 86, 95–102, 107–108, 112–113), and the 70 characters of internal morphology include those of osteology, myology and neurology (characters 31–85, 87–94, 103–106, 109–111). Although there are 1.6 times as many internal as external characters, the external characters provide the majority of phylogenetically informative state changes in the more recent branches (Fig. 22, nodes 1–7). Internal characters provide the majority of state changes at the deepest branches (Fig. 22, nodes 8–10). The consistency of this result is expressed in a strong correlation ($r^2 = 0.78$) in the ratio of external to internal character states changes over the entire range of clade-rank horizons. Despite these overall differences in rates of state change, both external and internal

1–10	11–20	21–30	31–40	41–50	51–60
61–70	71–80	81–90	91–100	101–110	111–113
Hypopomus artedi					
0000000000	0000000122	1000?00000	000000000-	0---0-0000	0000000100
1000000000	000000??00	0000100?10	0000000000	0000010000	010
Sternopygus macrurus					
0000000000	0000002001	1000000000	0000000200	0000210100	0000000000
1000000000	001000?001	0100000010	0000000000	0010011200	010
Electrophorus electricus					
0000000000	0000111101	1010101100	0000102200	0100210100	0110000000
0011101110	1000100000	010000-?11	20001??10?	0040100211	20?
G. cylindricus (MA)					
0000000000	0000001022	1200100111	1010010101	0100100000	0000000000
1100000001	1010110110	1201101101	0000000000	1120000010	10?
G. maculosus (MA)					
0000000000	0000001022	1200101111	1010010101	0100100000	0000000000
1100000001	1010110110	1201101011	0000010000	1120000010	20?
G. curupira (WA)					
1110110000	1000011111	2200001111	1010011010	0002101001	0000001010
0100010011	1000120110	0201110011	0110010110	2020001010	021
G. mamiraua (WA)					
1120210000	1000001211	1101001111	1010011000	0002101001	0001101010
1100010111	1010120010	0201110011	0020010000	2020000010	130
G. obscurus (WA)					
1120210000	1000001112	1101000111	1010011011	0001101001	0001101010
0100010111	1010120010	0201100011	0110010110	3120001010	101
G. varzea (WA)					
1110110000	1000001011	1101000111	1010011011	0001001001	0001101010
0100010111	1000120010	0201100011	0110010110	3130001010	121
G. sylvius (SE)					
1111310100	1000002111	1101000111	1010011010	0002201001	0001101011
0100010011	1011110010	0201110?1	1111010000	2020000010	130
G. inaequilabiatus (PA)					
1111110100	1000101001	1201000111	1010011010	0002201001	0001101011
0100010011	1011110010	0201110001	1121010000	1020000010	1?0
G. diamantinensis (EA)					
1111?10100	1000001011	0201000111	1010011010	0002201001	0001101011
0100010011	1011110010	0201110001	1121010000	1020000010	??0
G. bahianus (NE)					
011??00100	1000001111	1101000111	1010011000	0002101001	0001101011
000001?011	1011110010	0201110001	0011010001	2020000010	1?0
G. carapo (EA)					
1111110100	1000002222	1101001111	1110011000	0002201101	00?11?1011
000001?110	10?1?11110	0?0111?001	0?10010001	1020001010	1?0
G. carapo (PI)					
1111110100	1000002111	1101000111	1110011010	0002201100	0001101011
0000010111	1011111110	0201110011	0110010001	1020001010	1?0
G. carapo (GU)					
1111110100	1000002111	1101000111	1110011010	0002201100	0001101011
0000010111	1011111110	0211110011	0110010001	2020001010	130
G. carapo (RO)					
1111110100	1000002222	0101001111	1110011010	0002201100	0001101011
0000010111	1011111110	021111?011	0110010001	1030001010	1?0

Table 4 Matrix of 113 characters for 38 gymnotid and two outgroup taxa. '?' indicates missing data; '-' character state not pertinent. Character descriptions are provided by number in Results.

1–10	11–20	21–30	31–40	41–50	51–60
61–70	71–80	81–90	91–100	101–110	111–113
G. carapo (MD)					
1111110000	1000002112	1101000111	1110011010	0002201100	0001101011
0000010111	1011111110	0201110011	0110010001	2020001010	1?0
G. carapo (WA)					
1111110000	1100002211	0001100111	1111011000	0003201100	0001101011
0000010111	1011111110	0211110111	0110010101	2020001010	130
G. arapaima (WA)					
1111110000	1100002221	0001100111	1111011000	0003201100	0001101011
0000010111	1011111110	0211110111	0110010012	2020001010	130
G. ucamara (WA)					
1110110000	1000002211	1101000111	1110011010	0002201100	0001101011
0000011111	1011111110	0201110011	0110010001	2020001010	130
G. choco (PS)					
1110110000	1000002211	0001001111	1110011010	0002201100	0001101011
0000011111	1011111110	0201110011	0110010001	1020001010	0??
G. paraguensis (PA)					
1110110000	0010002211	1001100111	??10??????	??????????	???1??????
??????????	10????????	?????0???1	?1??001101	30200?1010	1??
G. tigre (WA)					
1110311000	0010002212	1211001111	??1001???1	100111???0	0?011??011
0?????????	10????????	?????0????	????001122	3040001010	221
G. henni (PS)					
1110301000	0010011212	2210001111	??1001???1	100111???0	0?01???010
0?????????	10????????	?????0????	????001122	214?001010	2??
G. esmeraldas (PS)					
11???00000	0010011212	1210000111	1010011011	1001111000	1101101010
0100011111	1010120010	0201100011	0110001112	214?001010	2??
G. pantherinus (SE)					
0000000000	0000010111	1100101111	1110011200	0100111000	1000101010
0000010101	1000110011	1201100111	1100010010	2031001010	021
G. panamensis (MA)					
11???00000	0000010002	21?1001111	??10??????	??????????	???0??????
??????????	1000??????	?????1???1	????010010	2031001010	0??
G. anguillaris (GO)					
1110210000	0000010102	2200001111	1110011110	0100211?0	1000101010
0000010101	1000110011	1201110111	1100010110	2031001010	0??
G. pantanensis (PA)					
1110210000	0000010001	2101001111	??10?11???	??????????	???0??????
??????????	1000??????	?????0????	?100010011	2031001010	0??
G. cataniapo (GO)					
1110110001	0000010112	1200101111	1?10011???	??10??????	??????????
??????????	1?00??????	?20112???1	?100010120	204?001110	0??
G. stenoleucus (GO)					
1220210001	0001011220	1001110111	??10??????	?????1????	??????????
??????????	10?0?100??	?????21111	1???000010	2041000110	0??
G. javari (WA)					
1220200001	0000011210	1110100111	1110011100	0110211000	1000100010
0100011101	1000110010	1201111111	2100010011	2041000110	030
G. pedanopterus (GO)					
1220110001	0000011221	0001100111	1110011010	0110211000	1000110000
0100011101	1000110010	120112???1	1100000010	2021001110	030

Table 4 *continued.*

1–10	11–20	21–30	31–40	41–50	51–60
61–70	71–80	81–90	91–100	101–110	111–113
G. coatesi (EA)					
1220100001	0000011221	0101001111	1110011001	0110211000	1000100011
0100011101	1000110010	1201111111	110001002?	3041000110	030
G. coropinae (GO)					
1220200000	0001011211	1210000111	1?10011100	0110211101?	000?100010
0100010171	1100??????	?201111??1	2100010010	2041000110	030
G. coropinae (WA)					
0220200000	0001010110	1210100111	1010011100	0110211011	0000100010
0100010101	1100110011	1201121111	2100010000	3041000110	030
G. melanopleura (WA)					
1220100011	0001002010	1111010111	1?10011??1	?0?00?????	?????0????
??????????	??????????	?????1???1	?1??010000	303?000110	0?0
G. jonasi (WA)					
1220100011	0001011010	0111010111	1010011001	1010011011	1000100110
0100001101	1100120111	1201121111	2100010000	3031000110	030
G. onca (WA)					
020??00011	0001010010	1111110111	1?10011??1	?0?00?????	?????0????
??????????	??????????	?????2???1	?1??010000	302?000110	0?0

Table 4 *continued.*

Species for which no specimens were cleared and stained due to unavailability of materials: *G. paraguensis* (PA), *G. henni* (PS), *G. panamensis* (MA), *G. pantanensis* (PA), *G. cataniapo* (GO), *G. stenoleucus* (GO), *G. melanopleura* (WA), *G. onca* (WA). Band (pair) width at midbody *G. carapo*: specimens 140–230 mm. Head colour pattern large irregular white blotches behind eyes and on chin. White cheek patch in specimens 140–260 mm. Anal-fin colour in *G. carapo* 140–230 mm. Mouth position in specimens with mean adult body size greater than 105 mm. Maxilla-palatine position in adult specimens greater than 150 mm. Dentary ventral posterior process (LaMonte, 1935) paedomorphic in adults of *G. pantherinus* group. Interopercle ascending process in specimens more than 200 mm. Frontal shape allometrically larger is specimens less than 140 mm. *Sternopygus:* dentary tooth rows brush-like; mesocoracoid distal portions of *S. xingu* = 1; postcleithrae for *S. aequilabiatus* = 0; cleithrum dorsoposterior facet of *S. xingu* = 1. *Electrophorus electricus*: hyomandibular posterior lateral line canal cartilaginous in juveniles *c*. 100 mm. *G. inaequilabiatus* (PA): postcleithrae of MCP 7155 (Rio Maquiné) = 1; cleithrum shape of MCP 7155 (Rio Maquiné) = 1. *G. diamantinensis* (EA): spots arranged in oblique lines; band pigment density bands entirely broken into spots; mouth width of MUSM 20268 (202 mm) = 1, MW of MZUSP 45320 (PT, 104 mm) = 2; body shape (BW/BD) of MUSM 20268 (202 mm) = 0; premaxillary tooth rows of MZUSP 45320 (100 mm), 9 on left 11 on right, of MUSM 20268 (202 mm) = 0; dentary teeth arrowhead-shaped of MUSM 20268 (202 mm) = 0, of MZUSP 45320 (PT, 104 mm) = 1; dentary teeth outer row of MUSM 20268 (202 mm) = 0, of MZUSP 45320 (PT, 104 mm) = 1; dentary tooth rows of MUSM 20268 (202 mm) = 2, of MZUSP 45320 (PT, 104 mm) = 0; dentary ventral posterior process of MUSM 20268 (202 mm) = 0, of MZUSP 45320 (PT, 104 mm) = 1; preopercle shelf margin of MUSM 20268 (202 mm) = 1, of MZUSP 45320 (PT, 104 mm) = 0; metapterygoid superior portion of MUSM 20268 (202 mm) = 1, of MZUSP 45320 (PT, 104 mm) = 0; hyomandibular trigeminal canals of MUSM 20268 (202 mm); frontal shape of MUSM 20268 (202 mm); parasphenoid shape of MUSM 20268 (202 mm); parasphenoid posterior processes of MUSM 20268 (202 mm) = 1, of MZUSP 45320 (PT, 104 mm) = 2; adductor mandibula intermusculars of MUSM 20268 (202 mm) = 0, of MZUSP 45320 (PT, 104 mm) = 1; number of electroplate caudal rows (CEP) in type series are from juveniles (= 0); condition in adults not known. *G. bahianus* (NE): band (or pigment patch) margins at tip of tail in non-type lots body squamation for HT = 0. *G. esmeraldas* (PS): pigment bands present at caudal tip in HT series band (or pigment patch) margins in MCZ 58729 (type lot) at tip of tail. *G. panamensis* (MA): dark pigment bands highly mottled. *G. cataniapo* (GU): anal fin posterior clear patch present in some juveniles to *c*. 180 mm. *G. stenoleucus* (GU): anal fin posterior clear patch present in some juveniles to *c*. 180 mm. *G. coatesi* (EA): mesocoracoid proximal portion in MCP uncat. *n* = 3, Tefé; lateral line ventral rami (VLR)WGRC uncat. Tefé, *n* = 3; EOD P2 small MCP uncat. Tefé, *n* = 3. *G. coropinae* (GO): band pigment density at caudal end AF. *G. coropinae* (WA): band pigment density at caudal end AF. *G. jonasi* (WA): white cheek patch in majority of specimens.

characters are phylogenetically informative over the range of nodes depths.

Geographic and ecological distributions

Gymnotus species are present in all nine Neotropical hydrogeographic regions circumscribed in Fig. 23. At least four *Gymnotus* clades are present on both slopes of the Andes and/or Middle America, including members in each of the three basal clades (Clades A, E and N). *Gymnotus* species diversity is highest in the Western Amazon, where 15 species are currently known. Ten of these species inhabit sediment rich, high conductivity, perennially hypoxic whitewater floodplains or *várzeas* (Henderson *et al*., 1998; Crampton, 1999; Petry *et al*., 2003). Like other components of *várzea* ichthyofaunas, many *Gymnotus* species exhibit widespread geographic distributions within this habitat (Albert & Crampton, 2003; Crampton *et al*., unpubl. obs.). *Gymnotus* species diversity is poor in the Paraguay–Paraná Basin (Fig. 23B; Albert *et al*., 1999; Silva *et al*., 2003). Species of the *G. pantherinus* group (Clade E) are entirely absent from the Brazilian shield and the Pacific Slopes of Colombia and Ecuador.

Clade	Name	BL	BD	BS
A	Gymnotidae	9	NA	87
B	*Gymnotus*	12	9	100
C	*G. cylindricus* group	8	4	98
D	'South American' clade	14	6	100
E	*G. pantherinus* group	8	0	–
F	*G. anguillaris* clade	4	2	–
G	unnamed clade	3	2	–
H	*G. pedanopterus* clade	3	1	–
I	*G. coatesi* clade	12	0	78
J	*G. coropinae* clade	3	0	–
K	unnamed clade	5	2	–
L	*G. coropinae*	4	0	–
M	*G. jonasi* clade	8	5	94
N	*G. carapo* group	9	3	81
O	*G. mamiraua* clade	3	0	–
P	unnamed clade	3	0	–
Q	unnamed clade	4	2	–
R	*G. varzea* clade	1	2	–
S	'elongate scales' clade	6	1	–
T	*G. tigre* clade	6	4	99
U	*G. esmeraldas* clade	5	2	70
V	'broken-bands' clade	5	2	–
W	*G. inaequilabiatus* clade	4	1	–
X	unnamed clade	2	1	75
Y	unnamed clade	4	4	95
Z	*G. carapo* complex	4	2	–
AA	*G. arapaima* clade	9	4	94
AB	*G. carapo* EA + RO clade	5	2	–

Table 5 Clade names and support indices for 26 internal branches of Fig. 21. Steps calculated for polytomies assuming hard-polytomy option. BL, Branch length; BD, Bremer decay value; BS, Bootstrap consensus value (– indicates < 70%).

Using the classification of habitats in Table 2, 19 of 31 (61%) *Gymnotus* species are found to inhabit *terra firme* streams and rivers, 7 (23%) blackwater floodplains, 14 (45%) whitewater floodplains. From these data it can be seen that 22 (71%) *Gymnotus* species are stenotopic, inhabiting a single habitat, and two species (*G. carapo* and *G. arapaima*) are cosmopolitan, being found in all three habitats within their geographic ranges. In the coastal rivers of the Pacific region of Colombia, *Gymnotus* species inhabit tropical forest streams without abundant aquatic macrophytes, with a low sediment load, low conductivity and low water flow (Maldonado, pers. comm.).

Discussion

Gymnotus carapo is paraphyletic

Gymnotus carapo is widely distributed in northern South America, throughout the Amazon and Orinoco Basins, the Island of Trinidad, and the coastal drainages of the Guianas and northeastern Brazil. Within this extensive area six allopatric populations of *G. carapo* are recognized from differences in the mean, modal or median values of morphometric and meristic traits, although none of these traits are diagnostic (Albert & Crampton, 2003). The mosaic distribution of these features among adjacent populations of *G. carapo* suggests that these six populations are members of a single widespread species connected by contemporary or recent gene flow. Nevertheless, populations of *G. carapo* from the western Amazon also share nine derived features with *G. arapaima* from the Rio Madeira, constituting a monophyletic group recognized here as the *G. arapaima* clade (Clade AA). Although largely distributed in allopatry, *G. carapo* and *G. arapaima* exhibit a zone of sympatry in the central Amazon in the region of Tefé, where *G. carapo* is a rare species and may be a vagrant from regions further upriver (Crampton, unpubl. obs.). We interpret these intraspecific and interspecific patterns as evidence that *G. carapo* is paraphyletic, having given rise to *G. arapaima*, perhaps from populations in the Central Amazon including the lower portions of Rio Negro and Madeira Basins.

The inferred paraphyly of *G. carapo* is consistent with the expectations of Neodarwinian theory that species give rise to species, and that geographically widespread species often seed the new species from populations within their range (Hafner *et al*., 1987; Templeton, 1989; Omland, 1997; Hubbell, 2001). The hypothesis that *G. carapo* is paraphyletic to *G. arapaima* is being tested with nuclear and mitochondrial genetic data by the authors (Lovejoy *et al*., in prep.).

Rates of character state evolution

Systematic ichthyologists have long observed that features of external morphology, including colour pattern and relative body proportions, tend to be more useful in differentiating closely related than distantly related species, and that features of internal anatomy, especially those of bones, muscles and nerves, are more conservative, usually proving informative about relationships among more distantly related taxa (e.g. genera, families; Cuvier, 1828; Starks, 1913; Hubbs & Lagler, 1958). These expectations are also observed in *Gymnotus* in which closely related species often differ by subtle differences in colour pattern, the mean or modal value of certain body proportions, scale counts, number of precaudal vertebrae and laterosensory canal pore patterns, and EOD peak power frequency. The deepest nodes of Figure 21 (including species groups) are characterized by discrete differences in body proportions and colour pattern as well as by characters of osteology, electric organ morphology and the number of phases of the EOD.

In these regards patterns of character state diversity in *Gymnotus* conform to several widely appreciated perceptions of phenotypic evolution in fishes: 1, characters of external morphology exhibit more phylogenetically plasticity than characters of internal morphology, 2, external characters provide the majority of phylogenetically informative state changes in less inclusive (more recent) nodes, 3, internal characters provide the majority of state changes more inclusive (less recent) nodes, and 4, both external and internal

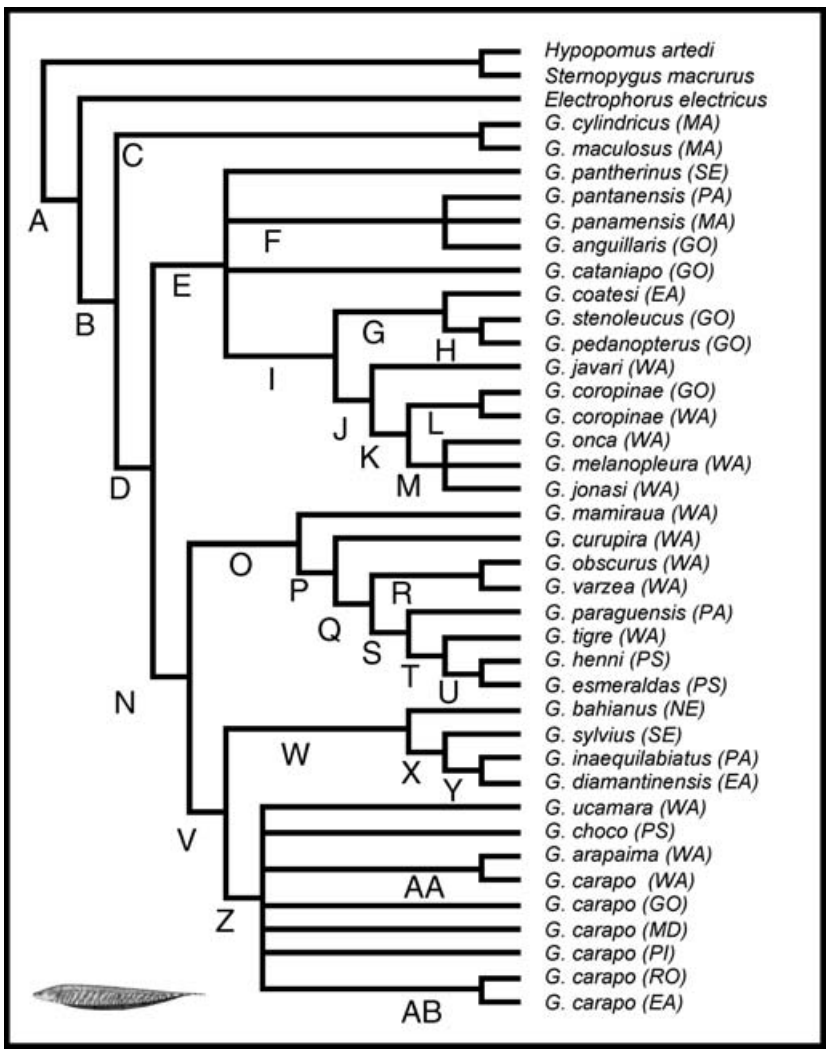

Figure 21 Interrelationships of *Gymnotus* species inferred from MP analysis of phenotypic data. Terminal taxa include 31 *Gymnotus* species, two allopatric populations of *G. coropinae*, six allopatric populations of *G. carapo*, and three gymnotiform outgroups. Terminal taxa followed in parentheses with hydrogeographic region of type locality (abbreviations as in Fig. 23). Strict consensus topology of 15 equally parsimonious trees, each of length 394 steps, from data in Table 4 (40 taxa, 113 characters, CI = 0.35, RI = 0.70, RC = 0.24). Clade names and support indices listed by Roman letter in Table 5.

characters are phylogenetically informative over the entire range of clade-rank horizons.

General perceptions of rate heterogeneity in systematics and character evolution are not necessarily observed in all cases. In molluscs, for example, characters of soft anatomy are generally thought to change less frequently than hard shell characters, although this was not found to be true for lophospiroid gastropods (Wagner, 2001). In stifftail diving ducks osteological characters associated with foraging ecology were found to be phylogenetically labile and obscured attempts to recover phylogeny (McCracken *et al*., 1999). An inverse relationship was found between timing of diversification and morphological disparity in iguanian lizards (Harmon *et al*., 2003). On the other hand, certain aspects in the diversity of electrical behaviours in *Gymnotus* are phylogenetically informative, an observation which is consistent with the emerging perception that behavioural characters are often useful in systematic studies (De Queiroz & Wimberger, 1993).

Band function and evolution

The appearance of the pigment bands is perhaps the most striking feature of interspecific diversity and geographic variation in *Gymnotus*. The plesiomorphic condition is to possess 18–23 oblique dark pigment bands with wavy margins that become pale in their middle during growth resulting in the appearance of band pairs in adults. The retention of regularly arranged, unbroken, pigment bands with high contrast, sharp band-interband margins is derived in Clade I (Fig. 21). The ecological role of pigment bands in *Gymnotus* or other gymnotiforms has not been examined directly. Pigment bands presumably function as cryptic coloration to avoid predation. Like other gymnotiform fishes *Gymnotus* species are nocturnally active, have poor eyesight and presumably do not rely on visual cues for mate recognition or other forms of social communication. During post-juvenile growth pigment bands undergo phenotypic changes depending in part on the phylogenetic position of the species within the genus. In all members

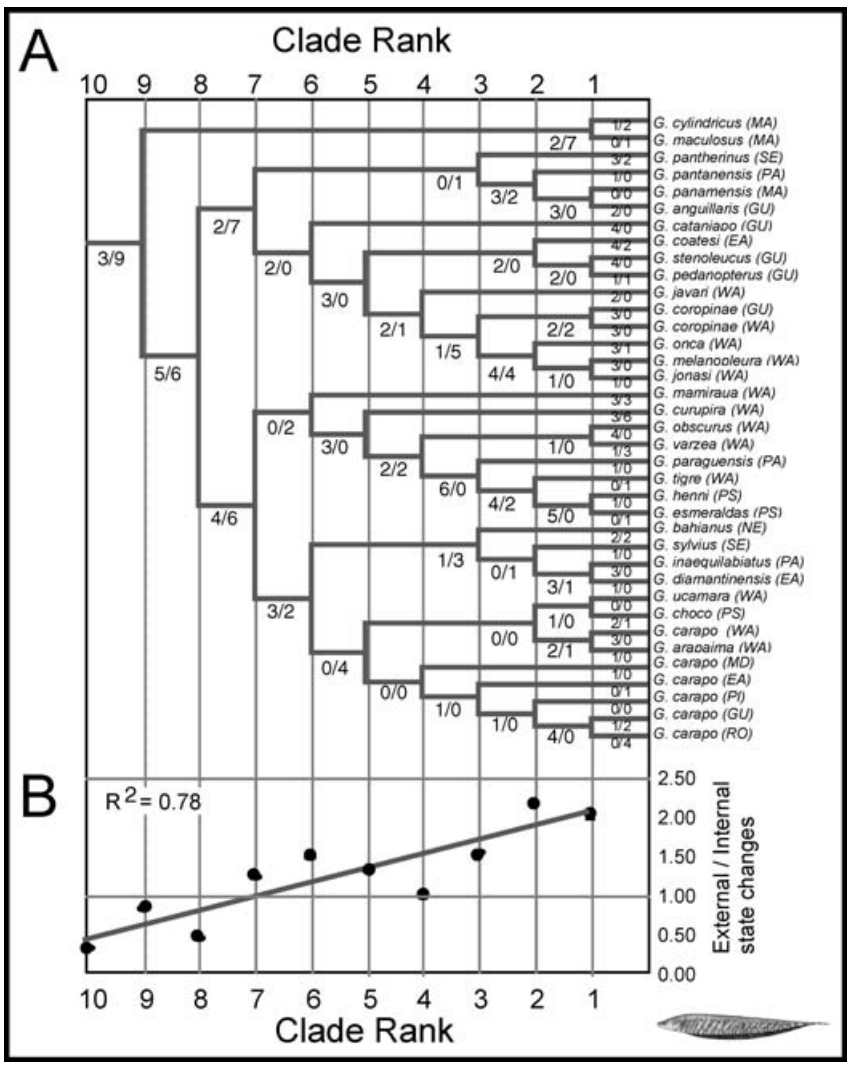

Figure 22 Relative rates of evolution in characters of external and internal morphology in *Gymnotus*. (A) States changes of external (above) and internal (below) characters optimized unambiguously at each internal node of a fully resolved phylogeny of *Gymnotus*. See Results for characters of external and internal morphology, and method of obtaining resolved topology. Clade Ranks were calculated assuming rates of diversification proportional to number of extant species. Descriptions of character state changes in Appendix 2. (B) Ratio of external to internal characters at each internal node of (A). Note that both external and internal characters are informative at all 10 internal clade rank horizons, and that external characters more phylogenetically plastic than internal characters (i.e. exhibit a higher overall RC). Note also that external characters provide the majority of phylogenetically informative state changes in more recent branches (ratio of external to internal state changes more than 1.00 at nodes 1–7, less than 1.00 at nodes 8–10).

of the *G. carapo* group the dark bands become paired during growth. In most members of Clade V, bands become broken into irregular patches or spots during growth. This phenotype is extreme in populations of *G. carapo* inhabiting open habitats, such as savannahs and in xeric areas of coastal Brazil, in which there is little forest canopy cover.

Species diversity and sampling efforts

Differences in the known diversity of Neotropical freshwater regions may reflect real differences in the evolutionary histories of these regions, and may also reflect disproportionate sampling efforts due to differential access of researchers to these regions. Although the full range of most gymnotiform species remains incompletely understood several observations suggest that known patterns of diversity in *Gymnotus* are not the result of differential sampling effort alone. Principal among these observations is that, although the total number of *Gymnotus* species among the hydrogeographic regions of Fig. 23 ranges from 1–15, the density of *Gymnotus* species is less diverse, ranging from 0.00–0.02 species per 1000 km^2 (densities calculated from the species and area data used to make Fig. 23B).

The high species diversity of *Gymnotus* in the Western Amazon is similar to that of the gymnotiform fauna as whole; whereas 15 of 32 (47%) *Gymnotus* species are represented in the Western Amazon, 93 of 174 (53%) of all known gymnotiform species are represented in the Western Amazon (Albert &

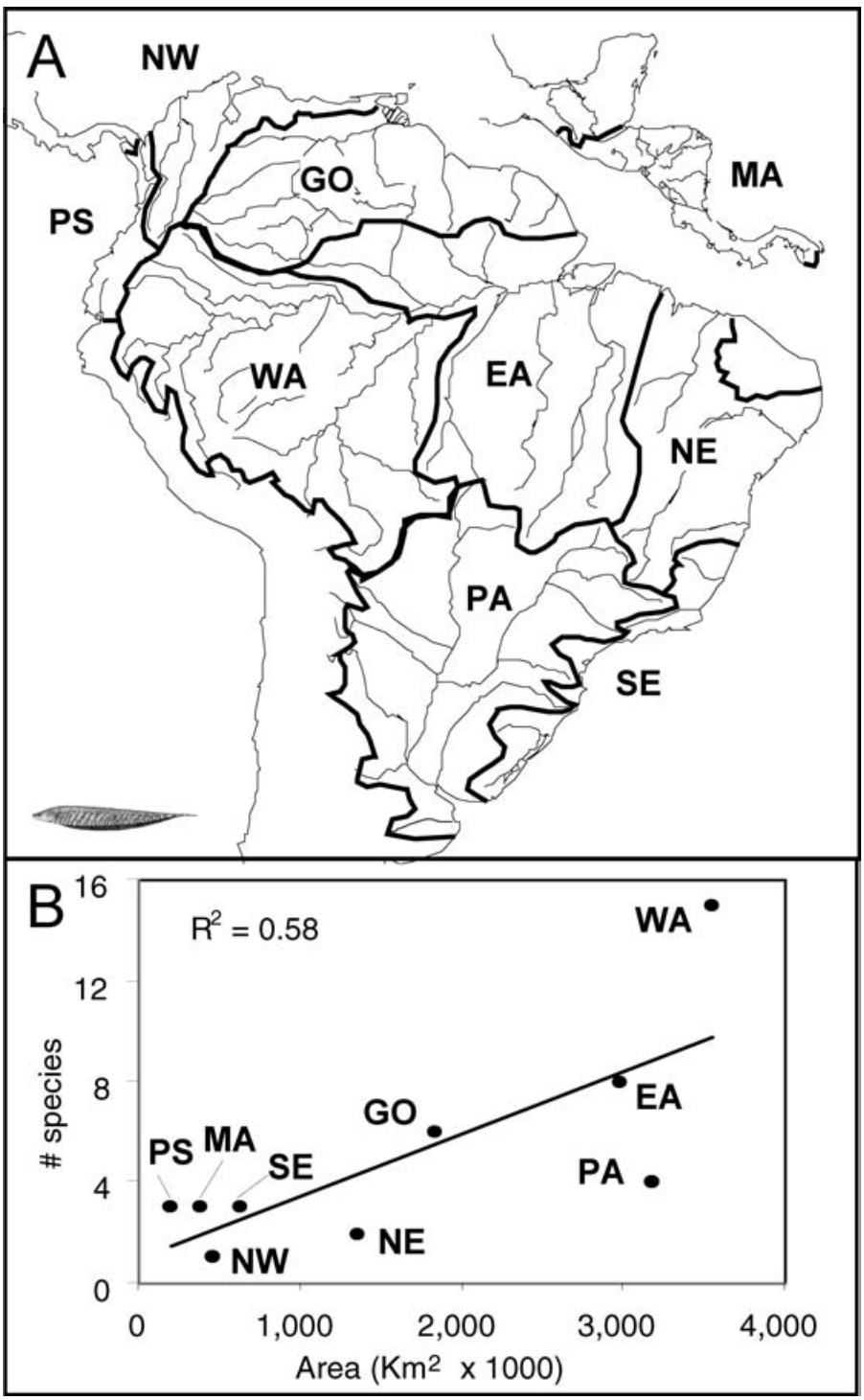

Figure 23 Descriptive biogeography of *Gymnotus*. (A) Neotropical hydrogeographic regions used in biogeographic analysis. Regions modified from Albert (2001). Abbreviations: EA, Amazon Basin east of Purus Arch and all tributaries below fall-line of Guyana Shield (2 985 000 km^2). GO, Guyanas – Orinoco Basin, including island of Trinidad and Upper Negro drainages above fall line (1 843 000 km^2). MA, Atlantic and Pacific slopes of Middle America from the Motagua to Tuyra Basins (393 000 km^2). NE, coastal drainages of northeast Brazil including Parnaíba, Piaui, São Francisco and Jequitinhonha Basins (1 357 000 km^2). NW, Northwestern South America including the Magdalena and Maracaibo Basins, and the north slope of Venezuela (471 000 km^2). PA, Paraguay-Paraná Basin including Dulce-Salí and Salado Basins of Argentina (3 185 000 km^2). PS, Pacific Slope of Colombia and Ecuador, from Baudó to Guayaquil Basins, including the Atrato (Caribbean) Basin (200 000 km^2). SE, coastal drainages of southeast Brazil and Uruguay from the Docé to Lagoa Mirim Basins (628 000 km^2). WA, Amazon Basin west of Purus Arch, below about 500 m elevation (3 556 000 km^2). (B) Species-area relationship in *Gymnotus*. Note species totals of two regions (WA and PA) deviate significantly from the regression ($R^2 = 0.59$, $P < 0.05$).

Crampton, 2005). This disproportionate representation of *Gymnotus* species in a single region may in part be a sampling bias resulting from the extensive work of one of us (WGRC) in the Tefé area of Brazil (Crampton, 1996, 1998a, 1998b), and by the authors in the Río Pacaya of Peru (Albert, 2002; Crampton *et al*., 2003). We anticipate the diversity of *Gymnotus* species from the Eastern Amazon will increase substantially with further field investigations.

The absence of *Gymnotus* from the Maracaibo Basin is not readily understood by current ecological conditions. Appropriate habitats in this basin has been extensively explored by professional ichthyologists (Royero, pers. comm.; Maldonado, pers. comm.), and the environmental conditions known to influence the distributions of electric fishes (i.e. water flow, temperature, dissolved oxygen, conductivity and vegetation [Crampton, 1998b]) are similar to coastal rivers and swamps of Middle America and the Chocó on the Pacific Slope of Colombia where *Gymnotus* does occur. Several other gymnotiform taxa (i.e. *Brachyhypopomus* spp., *Sternopygus* spp.) with habitat preferences similar to that of *Gymnotus* are present in the Maracaibo Basin.

The absence of the *G. pantherinus* group from the Brazilian Shield and the Pacific Slopes of Colombia and Ecuador also does not appear to be a sampling artifact, and is consistent with several observations suggesting an evolutionary history including extinction or lack of colonization. Materials for this study were examined from 33 museums representing collections made by numerous investigators over the course of more than a century. In addition, species of the *G. pantherinus* group have not been collected in several intensive ichthyofaunal surveys of rivers in the Brazilian Shield (Roux, 1973; Santos & Carvalho, 1982; Ferreira, 1984, 1986; Castro *et al*., 2003; Silvano *et al*. 2001). The presence of numerous lots of *G. pantherinus* in museum collections from the southeast of Brazil indicates that species of the *G. pantherinus* group are readily sampled using conventional collecting methods.

Similarly, the relative paucity of *Gymnotus* species in the Paraguay–Paraná Basin does not appear to be a consequence of sampling bias. This region is readily accessible from the large ichthyological communities in southern Brazil, Uruguay and Argentina. Nevertheless, the electric fish fauna of this region remains incompletely described; a new *Gymnotus* species is now being described from the Pantanal (Fernandes *et al*., in press), and one or two undescribed species from southeastern Brazil (Crampton, pers. obs.).

Historical biogeography

Background

The Cenozoic history of northwestern South America and southern Middle America is complex and incompletely understood. There is however a consensus that until the Middle Miocene (*c*. 16 Ma) most of the area of the modern Western Amazon drained northward to a delta located in the area of the modern Maracaibo Basin, and southern Middle America was separated from northwestern South America by more than 200 km of open ocean (Fig. 24; Galvis *et al*., 1979; Shagam *et al*., 1984; Kohn *et al*., 1984; Hoorn *et al*., 1995; Diaz de Gamero, 1996; Coates & Obando, 1996; Guerrero, 1997; Gregory-Wodzicki, 2000; Costa *et al*., 2001). Miocene tectonism in the northeastern Andes was responsible for the origins of the modern drainages of northwestern South America, including the Western Amazon, Orinoco, Maracaibo, Magdalena and Atrato Basins. Also during the Middle Miocene the Choco Block underlying the modern San Juan and Atrato Basins was accreted to the northwest corner of South America (Duque-Caro, 1990). The Isthmus of Panama emerged in the Late Pliocene (*c*. 3 Ma.) forming the only fully terrestrial connection between Middle and South America during the Cenozoic (Coney, 1982; Iturralde-Vincent & MacPhee, 1999).

The three main biogeographic models for the origins of the semi-insular ichthyofaunas of Middle America and trans-Andean northwestern South America are vicariance (Rosen, 1975; 1985; Vari, 1988; Vari & Weitzman, 1990), dispersal over water barriers (Darlington, 1938; Iturralde-Vincent & MacPhee, 1999), and dispersal over short-lived landbridges or landspans (Miller, 1966; Myers, 1966; Bermingham *et al*., 1997). The phylogenetic and geographic data reported here implicate instances of each of these models in the formation of modern *Gymnotus* species assemblages (Bussing, 1976).

The main observations constraining interpretations of historical biogeography in *Gymnotus* are the basal division of the genus into Middle American (Clade C) and South American (Clade D) Clades, and the presence of multiple cis and trans Andean sister taxa (Clades F, T, Z) nested well within Clade D. If these cis and trans Andean sister taxa are inferred to have diverged before, or in association with, the late Middle Miocene Andean uplift, the more basal division between Clades C and D occurred well before *c*. 12 Ma. This interpretation agrees with the conception of *Gymnotus* as a member of the 'paleoichthyofauna' of nuclear Middle America with origins predating the Pliocene rise of the Isthmus of Panama (Miller, 1966; Myers, 1966; Bussing, 1985).

Middle America

The split between Clades C and D before the late Middle Miocene may have occurred by vicariance within an ancestral species (Clade B) distributed throughout Middle and South America, or within South America with subsequent dispersal to Middle America in the Miocene or Plio-Pleistocene (Fig. 24). The principal difference between these two scenarios is the timing of the dispersal event to Middle America, either before or after the speciation of Clades C and D. The vicariant model constrains the timing of the divergence to after the physical dispersal of *Gymnotus* into Middle America.

The pre-Pleistocene palaeogeography of northwestern South America favoured emplacement (i.e. origins by speciation or dispersal) of fresh water animals to Middle America over water, and not land (Hoorn *et al*., 1995; Lundberg *et al*., 1998; Iturralde-Vincent & MacPhee, 1999). In this regard it is interesting to compare the hydrological and biotic influences of the modern Amazon freshwater discharge into the Atlantic with that of the Miocene palaeo-Amazon into the

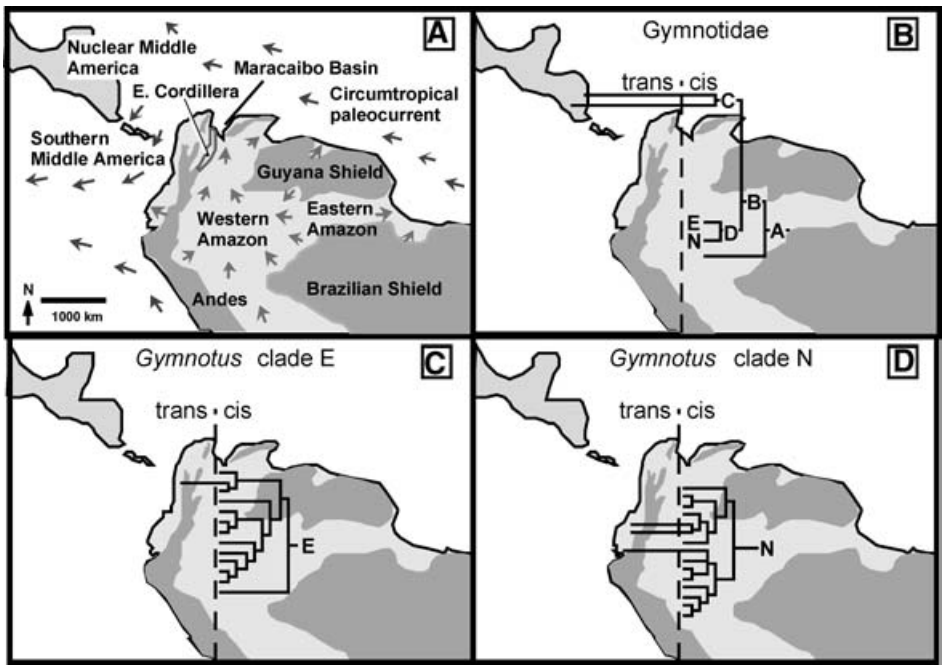

Figure 24 Historical biogeography of *Gymnotus*. (A) Palaeogeographic reconstruction of northern South America and Middle America immediately before the uplift of the Eastern Cordillera in the late Middle Miocene (*c*. 12 Ma). Map redrawn from Hoorn *et al.* (1995) and Ituralde-Vincent & MacPhee (1999). Long arrows indicate prevailing directions of marine palaeocurrents; short arrows direction continental sediment palaeotransport. Dark shading indicates highlands, light shading lowlands. Note mouth of palaeo-Amazon in area of modern Maracaibo Basin. (B) Basal four nodes of Gymnotidae (Clade A) superimposed on palaeogeographic reconstruction. Note basal split in *Gymnotus* (Clade B) between clades endemic to Middle America (Clade C) and South America (Clade D). The emplacement of Clade C in Middle America necessarily predates *c*. 12 Ma (see text). Under a vicariance model Clade C dispersed to Middle America before the speciation of Clades C and D; under a dispersal model Clade C dispersed to Middle America after speciation of Clades C and D within South America. (C) Phylogenetic relationships of *Gymnotus* Clade E. (D) Phylogenetic relationships of *Gymnotus* Clade N. Note the two cis-trans Andean taxa nested at terminal positions. Note the single cis-trans Andean species pair nested at a terminal position in the phylogeny. Physical position of terminals on maps only informative with respect to locations in Middle America and South America, or cis- and trans-Andean watersheds.

Caribbean. The fresh water plume of the modern Amazon is about 6700 km^3 per year, or 214 million litres per second averaged over the annual cycle (Goulding *et al*., 2003). This fresh water is distributed by the Southern Equatorial Current northwest along the coast of the Brazilian state of Amapá and French Guyana a distance of *c*. 600–800 km depending on the season. Not coincidentally the freshwater fish fauna of these regions is strongly Amazonian in species composition in comparison with other parts of the Guyanas or northeastern Brazil (Planquette *et al*., 1996; Jégu & Keith, 1999; Albert, 2001; Hardman *et al*., 2002; M. Goulding, pers. comm.).

There is no direct evidence bearing on the extent of the fresh-water plume emerging from the Miocene palaeo-Amazon. Comparison of the sediment fans of the modern and palaeo-Amazon rivers indicates similar total discharge volumes from these basins. The modern Amazon Fan, accumulated over the past 10–12 million years, extends over an area of *c*. 200 000 km^2 (Piper *et al*., 1997). As with the freshwater plume, much of the Amazon sediment load is distributed along the coast of the Guyanas *c*. 1500 km. Evidence for a wide geographic influence of the palaeo-Amazon is provided by the Middle Miocene Napipi Formation of hemipelagic mudstones in the Atrato Basin (Duque-Caro, 1990). An important source of these mudstones was sediment from the paleo-Amazon emerging from the area of the modern Maracaibo Basin, and carried westward *c*. 800 km by the prevailing Circumtropical Paleocurrent (Mullins *et al*., 1987). The northern coast of Colombia in the Middle Miocene may therefore be inferred to have been predominantly fresh water or brackish. The several marine transgressions and regression in the Middle to Upper Miocene (Rasänen *et al*., 1995; Paxton *et al*., 1996; Lovejoy *et al*., 1998) would have substantially altered the coastline, episodically isolating and uniting the mouths of coastal rivers, altering the distance between fresh waters of Middle and South America, and strongly effecting opportunities for transoceanic dispersal during this time interval.

Analysis of branching order and branch lengths in molecular studies of three other groups of freshwater fishes also indicate pre-Pleistocene emplacements in Middle America; the gymnotiform *Brachyhypopomus* (Bermingham & Martin, 1998); Middle American heroine cichlids (Martin & Bermingham, 2000); and the catfish *Rhamdia* (Perdices, 2002). In contrast molecular data for the characin *Roeboides* suggest a Pleistocene emplacement in Middle America (Bermingham & Martin, 1998). Molecular sequence data are not yet available for either of the two species of the *G. cylindricus* group.

Northwestern South America

According to a vicariance model both the *G. pantherinus* group (Clade E) and *G. carapo* group (Clade N) may be inferred to predate the Late Middle Miocene uplift of the northern Andes (Eastern Cordillera *c*. 11.8–12.2 Ma; Mérida Andes *c*. 11 Ma; Dengo & Covy, 1993; Diaz de Gamero, 1996; Lundberg *et al*., 1998). Before this time Clades E and N would have been distributed throughout the lowland regions of northwestern South America including the Pacific Slope. With the uplift of the Andean Eastern Cordillera the Maracaibo, Magdalena, Atrato and Pacific Slope regions became isolated (Hoorn *et al*., 1995) allowing the separation of at least three cis-trans Andean sister taxa (Clades F, T, Z). The absence of species from the modern Maracaibo and Magdalena Basins is presumably a result of subsequent extinction. A single *Gymnotus* species in Clade E persists in Panama, and four species in Clade N persist in trans-Andean drainages of Colombia and Ecuador.

The patterns of this vicariance model are consistent with observations on other groups of Neotropical fishes with cis-trans Andean distributions (Eigenmann, 1920; Vari, 1988; Vari & Weitzman, 1990; Vari, 1995; Lovejoy, 1996, 1997; Retzer & Page, 1997; Reis, 1998; Lovejoy & Araújo, 2000; Albert, 2001; Sivasundar *et al*., 2001; Montoya-Burgos, 2003). The widespread extinction of the lowland Amazonian ichthyofauna in the Magdalena Basin followed substantial environmental changes associated with the uplift of the Andean Eastern Cordillera (Guerrero, 1997). The Urumaco Formation (*c*. 10–5 Ma) in the modern Falcon Basin of Venezuela, and the La Venta Formation (*c*. 13 Ma) in the modern upper Magdalena Basin, contain fossil fish assemblages of taxa currently restricted to lowland tropical Orinoco-Amazon waters (Diaz de Gamero, 1996; Lundberg, 1997). There are no fossil gymnotiforms known from these formations.

Species assemblages

The most species-rich local assemblage of *Gymnotus* is the area of Tefé in the Western Amazon where 11 species occur in sympatry (Crampton *et al*., 1998a, 1998b; Albert & Crampton, 2001; Crampton & Albert, 2003; Crampton *et al*., 2005). Species in this assemblage are members of at least four distinct clades (Clades G, K, O and AA), each with a sister taxon in another part of South America. The reasons underlying the capacity of this region to permit the co-existence of so many *Gymnotus* species in sympatry (although not necessarily in syntopy) are poorly understood. The results of this study suggest the role of both ecological and historical factors, as well as the species-specific nature of their electric signals (Crampton & Albert, unpubl. obs.).

As with the Western Amazon, the *Gymnotus* species assemblages in all nine hydrogeographic regions of Table 2 are not monophyletic (Fig. 23A). In other words, the species present in each of these regions do not represent the results of local or regional radiations, but rather were assembled incrementally over a lengthy history by means of a combination of processes, including *in situ* speciation, extinction, immigration and ecological factors allowing coexistence in sympatry. Understanding the forces governing the number and identity of *Gymnotus* species in a regional assemblage therefore requires phylogenetic, biogeographic and ecological data as well as information about electric signals.

These phylogenetic and biogeographic patterns suggest that evolution in *Gymnotus* is a continental, not basin-wide, phenomenon. In this regard Amazonian species richness is not strictly a consequence of local or regional processes (Vitt *et al*., 1999; Schulte *et al*., 2000; Vitt *et al*., 2003). These patterns are representative of other highly diverse groups of Neotropical fishes, and not to resemble those of monophyletic, rapidly generated species flocks in isolated aquatic systems (e.g., Eschelle & Kornfield, 1984; Turner *et al*., 2001).

Historical ecology

Sediment provenance and palaeotransport directions indicate that from 25–12 Ma the regions between the Brazilian and Guyana cratonic Shields were dominated by low sinuosity, northwest directed fluvial systems, and mineral contents indicating the Guyana Shield as the main sediment source. Palynological data indicate the vegetation at this time was dominated by palm swamps and lowland riverine and non-floodplain (*terra firme*) tropical forests (Hoorn, 1994). The presence of mangrove palynomorphs and foraminiferan and dinoflagellate cysts suggests occasional marine incursions from the north, extending as far south as the modern Rio Putumayo (Hoorn, 1994; Paxton *et al*., 1996; Lovejoy *et al*., 1998; Vonhof *et al*., 1998, 2003). The palaeoenviromental profile of Western Amazonia changed dramatically to that of a modern *várzea* landscape in the late Middle Miocene (*c*. 12 Ma). Sediments indicate a fluvio-lacustrine system with an eastward transport direction, an Andean mineralogy with high sediment load, and a palaeovegetation composed largely of palm swamps, riverine forests, and a relative abundance of aquatic macrophytes forming floating meadows (Hoorn *et al*., 1995).

Among the *Gymnotus* species of the Tefé area, eight species live synoptically on the sediment-rich and high-conductivity *várzea* whitewater floodplain. Conductivity is a metric of overall dissolved salt concentrations and is correlated with habitat partitioning in some although not all electric fishes (Crampton, 1998a). Maximum parsimony optimization of habitat preference on the phylogenetic hypothesis of Fig. 21 suggests the presence of *Gymnotus* in *várzeas* has at least two independent origins derived from the ancestral condition of inhabiting low conductivity *terra firme* (non-floodplain) black and clearwater rivers and streams (Fig. 25). In this aspect of historical ecology *Gymnotus* is similar to that of the cyprinodontiform fish *Rivulus* (Hrbek & Larson, 1999).

The origination of the *Gymnotus* specialized to *várzea* habitats may have taken the form of *in situ* differentiation from a eurytopic ancestor, or by colonization from taxa previously restricted to *terra firme* streams and rivers. At least in the case of Clade N, habitat specialization in the *várzea* predates the split of *G. tigre* and *G. ucamara* from their Trans-Andean sister taxa, which occurred at or before *c*. 12 Ma (Hoorn *et al*., 1995). The origin of *várzea* specialization in Clade N therefore predates the formation of the modern eastwardly oriented flow of the Amazon Basin and the first known extensive areas of

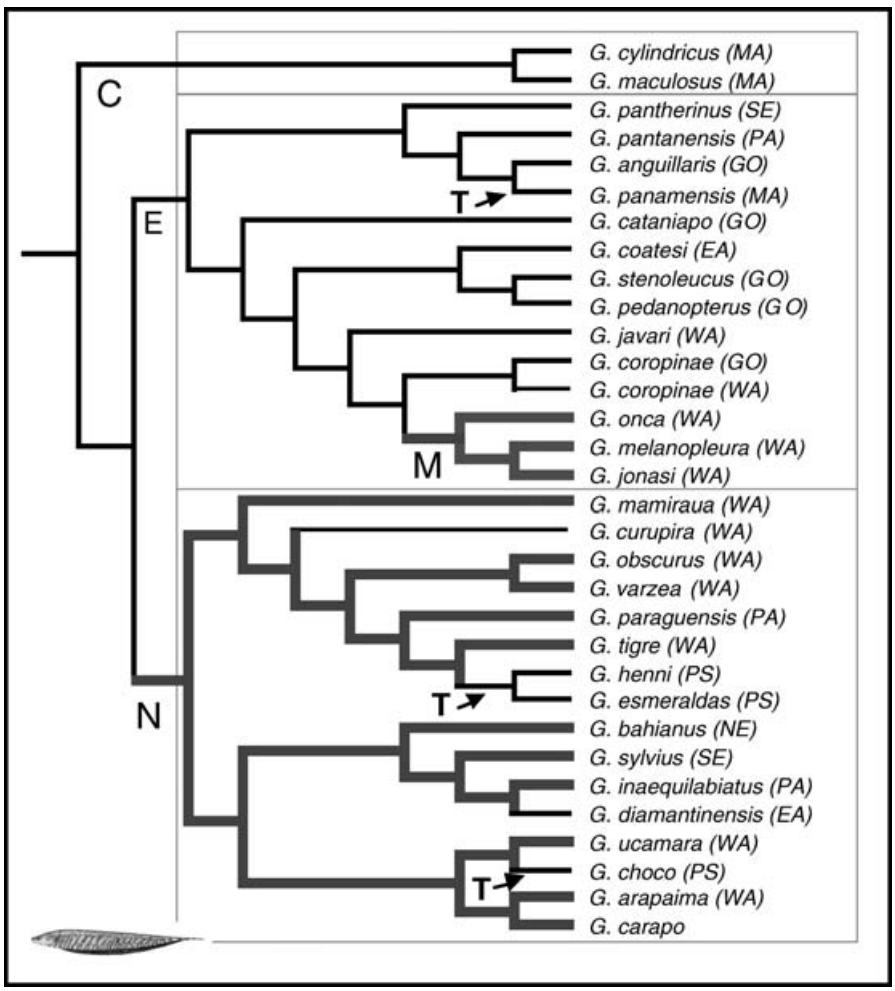

Figure 25 Habitat evolution in *Gymnotus*. Unambiguous optimization of habitat preference (9 steps, RC = 0.26) on a simplified topology of Fig. 24A with terminals limited to species-level taxa. Habitat data from Table 2. Three species groups (Clades C, E, and N) delimited in boxes. Branches in thin black lines represent taxa restricted to non-floodplain (*terra firme*) streams and low conductivity (black and clear water) rivers and their seasonally flooded lower reaches. Branches in thick grey lines represent taxa which commonly or exclusively inhabit whitewater floodplains (várzea). *Gymnotus carapo* and *G. arapaima* are eurytopic (coded polymorphic). Note this tree topology is consistent with at least two transitions to *várzea* habitats (clades M and N). T = Trans-Andean.

aquatic macrophytes in the Western Amazon (Hoorn, 1994; Hoorn *et al*., 1995).

Conclusions

Gymnotus is the most diverse and widespread genus of South American electric fishes. Patterns of diversity in *Gymnotus* represent some of the major themes in Neotropical aquatic biodiversity in general. *Gymnotus* is ancient with multiple trans-Andean clades, diverse with numerous species living in sympatric non-monophyletic assemblages, and widespread with phenotypes differentiating in adjacent drainages across the landscape. In these regards, patterns of diversity in *Gymnotus* are more typical of other diverse tropical taxa, than are the widely cited monophyletic species blooms of the African lake cichlids or other rapidly evolved species flocks. Unlike the celebrated cases of explosive evolutionary radiations, *Gymnotus* is a relatively ancient group that evolved over tens of millions of years, and over a continental arena. *Gymnotus* therefore represents an attractive target for future studies on the origins and maintenance of Neotropical diversity. In light of current rates of species descriptions in the Neotropics the phylogenetic results of this study must be regarded as a first-order estimate. Future work will require more complete geographical sampling of populations from across South America and analysis using molecular data.

Acknowledgements

We acknowledge the following people for access to specimens, information and ideas; B. Brown, X. Freilich, S. Schaefer (AMNH); J. Lundberg, M. Sabaj (ANSP); J. Armbruster (AUM); O. Crimmen, D. Siebert (BMNH); D. Catania, W. Eschmeyer (CAS); P. Stoddard (FIU); L. Page, R. Robins, G. Sheehy (FLMNH); C. Buti (FML); B. Chernoff, M. Rogers (FMNH); R. Royero-Léon (FUDECI); F. Kirschbaum (IGB); C. Aadland, J. Alves-Gomes, E. Ferreira, L. Rapp Y Daniel, J. Zuanon (INPA); R. Reis (MCP); K. Hartel (MCZ); M. Azpelicueta (MLP); P. Buckup, R. Campos-da-Paz (MNRJ); H. Britski, M. de Pinna, J. Lima De Figueiredo, O. Oyakawa, (MZUSP); E. Ahlander, S. Kullander, A. Silvergrip (NRM);

R. Winterbottom (ROM); W. Bussing (UCR); W. Fink, D. Nelson (UMMZ); J. Maldonado (UNC); H. Ortega (MUSM); M. Hagedorn (USNM); S. Jewett, L. Parenti, R. Vari (USNM); L. Almeido-Toledo, F. Campos de Matioli (USP); H. Mejlon (UUZM); I. Isbrücker (ZMA). We appreciate additional exchanges of data and ideas with R. Barriga, E. Bermingham, T. Berra, A. Caputi, T. DiBenedetto, M. Goulding, C. Hopkins, K. Lester, D. Taphorn, M. Triques, and L. Verdi. Special thanks to W. Bentes Monteiro and J. Alves de Oliveira for field assistance, and K. Aviles and J. Hill for laboratory assistance. We acknowledge the Neodat project (NSF/AID DEB grant 90-24797) for collection information. Aspects of this research were supported by grants to WGRC from the Fisheries Society (UK), CNPq (Brazil), and to JSA from the U.S. National Science Foundation (NSF-DEB 0215388, 0317278, 0138633).

References

AGUILERA, P.A., CASTELLO, M.E. & CAPUTI, A.A. 2001. Electroreception in *Gymnotus carapo*: differences between self-generated and conspecific-generated signal carriers. *Journal of Experimental Biology* **204**, 185–198.

ALBERT, J.S. 2001. Species diversity and phylogenetic systematics of American knifefishes (Gymnotiformes, Teleostei). *Miscellaneous Publications Museum Zoology*, University of Michigan **190**, 1–129.

ALBERT, J.S. 2002. Eternal vigilance on an Amazon floodplain. *Current Biology* **12**, R442–R443.

ALBERT, J.S. & CAMPOS-DA-PAZ, R. 1998. Phylogenetic systematics of American knifefishes: a review of the available data. In: MALABARBA, L., REIS, R.E., VARI, R.P., DE LUCENA, C.A.S. & DE LUCENA, Z.M.S. Eds., *Phylogeny and Classification of Neotropical Fishes*. Museu de Ciências e Tecnologia, Porto Alegre, pp. 409–438.

ALBERT, J.S. & CRAMPTON, W.G.R. 2001. Five new species of *Gymnotus* (Teleostei: Gymnotiformes) from an Upper Amazonian floodplain, with descriptions of electric organ discharges and ecology. *Ichthyological Exploration of Freshwaters* **12**(**3**), 241–226.

ALBERT, J.S. & CRAMPTON, W.G.R. 2003. Seven new species of the Neotropical electric fish *Gymnotus* (Teleostei, Gymnotiformes) with a redescription of *G. carapo* (Linnaeus). *Zootaxa* **287**, 1–54.

ALBERT, J.S. & CRAMPTON, W.G.R. 2005. Diversity and phylogeny of Neotropical electric fishes. In: BULLOCK, H., HOPKINS, C.D., POPPER, A.N. & FAY, R.R. Eds., *Electric Fishes*, In press.

ALBERT J.S., CRAMPTON, W.G.R., THORSEN, D.H., LESTER, K.L. & LOVEJOY, N.R. 2003. Species diversity and phylogenetic systematics of the Neotropical electric fish *Gymnotus* (Gymnotidae: Teleostei). *Abstracts Annual Meetings of the American Society of Ichthyologists and Herpetologists*, Manaus, Brazil, p. 7.

ALBERT, J.S., FERNANDES-MATIOLI, F.M. & DE ALMEIDA-TOLEDO, L.F. 1999. A new species of *Gymnotus* (Gymnotiformes, Teleostei) from Southeastern Brazil: Towards the deconstruction of *Gymnotus carapo*. *Copeia* **1999**, 410–421.

ALBERT, J.S. & FINK, W.L. 1996. *Sternopygus xingu*, a new species of electric fish (Gymnotoidei, Teleostei), from South America, with comments on the phylogenetic position of *Sternopygus*. *Copeia* **1996**, 85–102.

ALBERT, J.S., LANNOO, M.J. & YURI, T. 1998. Testing hypotheses of neural evolution in gymnotiform electric fishes using phylogenetic character data. *Evolution* **52**, 1760–1780.

ALBERT, J.S. & MILLER, R.R. 1995. *Gymnotus maculosus*: a new species of electric fish from Middle America (Teleostei: Gymnotoidei), with a key to the species of *Gymnotus*. *Proceedings Biological Society Washington* **108**, 662–678.

ALVES-GOMES, J.A., ORTÍ, G., HAYGOOD, M., MEYER, A. & HEILIGENBERG, W. 1995. Phylogenetic analysis of the South American electric fishes (Order Gymnotiformes) and the evolution of their electrogenic system: A synthesis based on morphology, electrophysiology, and mitochondrial sequence data. *Molecular Biology and Evolution* **12**, 298–318.

ARDANAZ, J.L., SILVA, A. & MACADAR, O. 2001. Temperature sensitivity of the electric organ discharge waveform in *Gymnotus carapo*. *Journal of Comparative Physiology A-Sensory Neural and Behavioral Physiology* **187**, 853–864.

BALIRWA, J.S., CHAPMAN, C.A., CHAPMAN, L.J., COWX, I.G., GEHEB, K., KAUFMAN, L., LOWE-MCCONNELL, R.H., SEEHAUSEN, O., WANINK, J.H., WELCOMME, R.L. & WITTE, F. 2003. Biodiversity and fishery sustainability in the Lake Victoria Basin: an unexpected marriage? *Bioscience* **53**, 703–715.

BENNETT, M.V.L. 1971. Electric organs. In: HOAR, W.S. & RANDAL, D.J. Eds., *Fish Physiology*. Academic Press, New York, pp. 346–491.

BERMINGHAM, E., MCCAFFERTY, S.S. & MARTIN, A.P. 1997. Fish biogeography and molecular clocks: Perspectives from the Panamanian Isthmus. In: KOCHER, T.D. & STEPIEN, C.A. Eds., *Molecular Systematic of Fishes*. Academic Press, San Diego, pp. 113–128.

BERMINGHAM, E. & MARTIN, A.P. 1998. Comparative mtDNA phylogeography of neotropical freshwater fishes: testing shared history to infer the evolutionary landscape of lower Central America. *Molecular Ecology* **7**, 499–517.

BLACK-CLEWORTH, P. 1970. The role of electrical discharges in the non-reproductive social behavior of *Gymnotus carapo* (Gymnotidae, Pisces). *Animal Behavior Monographs* **3**, 1–77.

BREMER, K. 1994. Branch support and tree stability. *Cladistics – the International Journal of the Willi Hennig Society* **10**, 295–304.

BUSSING, W.A. 1976. Geographic distribution of the San Juan ichthyofauna of Central America with remarks on its origin and ecology. In: THORSON, T.B. Ed., *Investigations of the Ichthyofauna of Nicaraguan Lakes*, University of Nebraska Press, Lincoln, pp. 157–175.

BUSSING, W.A. 1985. Patterns of distribution of the Central American ichthyofauna. In: STEHLI, F.G. & WEBB, S.D., Eds., *The Great American Biotic Interchange*. Plenum, New York, pp. 453–473.

CAMPOS-DA-PAZ, R. 1996. Redescription of the Central American electric fish *Gymnotus cylindricus* (Ostariophysi: Gymnotidae), with comments on character ambiguity within the ostariophysan clade. *Journal Zoology London* **240**, 371–382.

CAMPOS-DA-PAZ, R. 2000. Taxonomic status of *Rhamphichthys cingulatus* Brind and a more precise assignment of the type-locality of *Gymnotus coatesi* LaMonte (Ostariophysi: Gymnotiformes). *Copeia* **2000**, 1114–1117.

CAMPOS-DA-PAZ, R. 2002. *Gymnotus diamantinensis*, a new species of electric knifefish from upper rio Arinos basin, Brazil (Ostariophysi: Gymnotidae). *Ichthyological Exploration of Freshwaters* **13**,185–192.

CAMPOS-DA-PAZ, R. & COSTA, W.J.E.M. 1996. *Gymnotus bahianus* sp. nov., a new gymnotid fish from Eastern Brazil (Teleostei: Ostariophysi: Gymnotiforms), with evidence for the monophyly of the genus. *Copeia* **1996**, 937–944.

CAPUTI, A.A. 1999. The electric organ discharge of pulse gymnotiforms: the transformation of a simple impulse into a complex spatiotemporal electromotor pattern. *Journal of Experimental Biology* **202**, 229–1241.

CAPUTI, A.A., AGUILERA, P.A. & CASTELLO, M.E. 2003. Probability and amplitude of novelty responses as a function of the change in contrast of the reafferent image in *G. carapo*. *Journal of Experimental Biology* **206**, 999–1010.

CASTRO, R.M.C., CASATTI, L., SANTOS, H.F., FERREIRA, K.M., RIBEIRO, A.C., BENINE, R.C., DARDIS, G.Z.P., MELO, A.A., SOPIGLIA, R., ABREU1, T., BOCKMANN, F.A., CARVALHO, M., GIBRAN, F.Z. & LIMA, F.C.T. 2003. Estrutura e composição da ictiofauna de riachos do rio Paranapanema, sudeste e sul do Brasil, *Biota Neotropica* **3**, in press.

COATES, A.G. & OBANDO, J.A. 1996. The geological evolution of the Central American isthmus. In: JACKSON, J., BUDD, A.F. & COATES, A.G. Eds., *Evolution and Environment in Tropical America*. University of Chicago Press, Chicago, pp. 21–56.

CONEY, P.J. 1982. Plate tectonic constraints on the biogeography of Middle America and the Caribbean region. *Annals Missouri Botanical Garden* **69**, 432–443.

CORREA, S.A.L., CORREA, F.M.A. & HOFFMANN, A. 1998. Stereotaxic atlas of the telencephalon of the weakly electric fish *Gymnotus carapo*. *Journal of Neuroscience Methods* **84**, 93–100.

COSTA, J.B.S., BEMERGUY, R.L., HASUI, Y. & BORGES, M.D. 2001. Tectonics and paleogeography along the Amazon river. *Journal of South American Earth Sciences* **14**, 335–347.

CRAMPTON, W.G.R. 1996. Gymnotiform fish: an important component of Amazonian flood plain communities. *Journal of Fish Biology* **48**, 298–301.

CRAMPTON, W.G.R. 1998a. Electric signal design and habitat preferences in a species rich assemblage of gymnotiform fishes from the Upper Amazon Basin. *Anais da Academia Brasileira de Ciências* **70**, 805–847.

CRAMPTON, W.G.R. 1998b. Effects of anoxia on the distribution, respiratory strategies and electric signal diversity of gymnotiform fishes. *Journal Fish Biology* **53**, 502–520.

CRAMPTON, W.G.R. 1999. Os peixes da Reserva Mamiraua: diversidade e historia natural na planicie alagavel da Amazonia. In: QUEIROZ, H.L. & CRAMPTON, W.G.R. Eds., *Estrategias para Manejo de Recursos Pesqueiros em Mamiraua*. Sociedade Civil Mamiraua/CNPq, Brasilia, pp. 10–36.

CRAMPTON, W.G.R. & ALBERT, J.S. 2003a. A redescription of *Gymnotus coropinae*, an often misidentified species of gymnotid fish, with notes on ecology and electric organ discharge. *Zootaxa* **348**, 1–20.

CRAMPTON, W.G.R. & ALBERT, J.S. 2003b. Redescription of *Gymnotus coatesi* (Gymnotiformes, Gymnotidae), a rare species of electric fish from the lowland Amazon basin, with descriptions of osteology, electric signals and ecology. *Copeia* **2003**, 525–533.

CRAMPTON, W.G.R., LOVEJOY, N.R. & ALBERT, J.S. 2003. *Gymnotus ucamara*: a new species of Neotropical electric fish from the Peruvian Amazon (Ostariophysi: Gymnotidae). *Zootaxa* **277**, 1–18.

CRAMPTON, W.G.R., THORSEN, D.H. & ALBERT, J.S. 2005. Three new species from a diverse and sympatric assemblage of the electric fish *Gymnotus* (Ostariophysi: Gymnotidae) in the lowland Amazon Basin, with notes on ecology. *Copeia* 2005.

CUVIER, G. 1828. *Historical Portrait of the Progress of Ichthyology, from Its Origins to Our Own Time*. In: PIETCH, T.W. Ed., A.J. Simpson (translator), Histoire Naturelle des Poissons, vol. 1. by G. Cuvier. Reprinted 1995 by Johns Hopkins University Press, Baltimore.

DARLINGTON, P.J. 1938. The origin of the fauna of the Greater Antilles, with discussion of dispersal of animals over water and through air. *Quarterly Review Biology* **13**, 274–300.

DENGO, C.A. & COVEY, M.C. 1993. Structure of the Eastern Cordillera of Colombia: Implications for trap styles and regional tectonics. *AAPG Bulletin* **77**, 1315–1337.

DE QUEIROZ, A. & WIMBERGER, P.H. 1993. The usefulness of behavior for phylogeny estimation: levels of homoplasy in behavioral and morphological characters. *Evolution* **47**, 46–60.

DE VISSER, J., HERMISSON, J., WAGNER, G.P., MEYERS, L.A., BAGHERI-CHAICHIAN, H., BLANCHARD, J.L., CHAO, L., CHEVERUD, J.M., ELENA, S.F., FONTANA, W., GIBSON, G., HANSEN, T.F., KRAKAUER, D., LEWONTIN, R.C., OFRIA, C., RICE, S.H., VON DASSOW, G., WAGNER, A. & WHITLOCK, M.C. 2003. Perspective: Evolution and detection of genetic robustness. *Evolution* **57**, 1959–1972.

DIAZ DE GAMERO, M.L. 1996. The changing course of the Orinoco River during the Neogene: A review. *Palaeogeography, Palaeoclimatology, Palaeoecology* **123**, 385–402.

DUQUE-CARO, H. 1990. Major Neogene events in Panamaic South America. In: TSUCHI, R. Ed., *Pacific Neogene Events, their Timing, Nature and Interrelationships*. Tokyo University Press, Tokyo, pp. 101–114.

EERNISSE, D.J. & KLUGE, A.G. 1993. Taxonomic congruence versus total evidence, and amniote phylogeny inferred from fossils, molecules, and morphology. *Molecular Biology and Evolution* **10**, 1170–1195.

EIGENMANN, C.H. 1920. The Magdalena basin and the horizontal and vertical distribution of its fishes. *Indiana University Studies* **7**, 21–34.

EIGENMANN, C.H. & ALLEN, W.R. 1942. *Fishes of Western South America*. University of Kentucky, Lexington, 494 pp.

EIGENMANN, C.H. & FISHER, H.G. 1914. The Gymnotidae of Trans-Andean Colombia and Ecuador. *Contributions Zoological Laboratory Indiana University* **141**, 235–237.

ELLIS, M.M. 1913. The gymnotid eels of tropical America. Memoirs Carnegie Museum **6**, 109–195.

ESCHELLE, A.A. & KORNFIELD, I. 1984. *Evolution of Fish Species Flocks*. University of Maine at Orono Press. 257 pp.

EVANS, M. 1929. Some notes on the anatomy of the electric eel, *Gymnotus electrophorus*, with special reference to a mouth breathing organ and the swim-bladder. *Proceedings Zoological Society London* **2**, 17–22.

FARRIS, J.S. 1989. The Retention Index and the Rescaled Consistency Index. *Cladistics, The International Journal of the Willi Hennig Society* **5**, 417–419.

FARRIS, J.S., KLUGE, A. & ECKARDT, M.J. 1970. A numerical approach to phylogenetic systematics. *Systematic Zoology* **19**, 130–135.

FERREIRA, E.J.G. 1984. A ictiofauna da represa hidreletrica de Curua-Una Santarem, Para. I. Lista e Distribuicao das especies. *Amazoniana* **7**, 351–363.

FERREIRA, E.J.G. 1986. Estudos e levantamento do impacto ambiental da UHE de UHE de Cachoeira Porteira. Relatorio do Subprojeto 'Identificacao e descricao das principais especies de peixes existentes'. Convenio-Engerio/CNPq-INPA, Manaus.

FERNANDES-MATIOLI, F.M.C. & ALMEIDA-TOLEDO, L.F. 2001. A molecular phylogenetic analysis in *Gymnotus* species (Pisces: Gymnotiformes) with inferences on chromosome evolution. *Caryologia* **54**, 23–30.

FERNANDES-MATIOLI, F.M.C., ALMEIDA-TOLEDO, L.F. & TOLEDO-FILHO, S.A. 1998. Natural triploidy in the Neotropical species *Gymnotus carapo* (Pisces: Gymnotiformes). *Caryologia* **51**, 319–322.

FERNANDES-MATIOLI, F.M.C., MARCHETTO, M.C.N., ALMEIDA-TOLEDO, L.F. & TOLEDO-FILHO, S.A. 1998. High intraspecific karyological conservation in four species of *Gymnotus* (Pisces: Gymnotiformes) from southeastern Brazilian basins. *Caryologia* **51**, 221–234.

FERNANDES-MATIOLI, F.M.C., MATIOLI, S.R. & ALMEIDA-TOLEDO, L.F. 2000. Species diversity and geographic distribution of *Gymnotus* (Pisces: Gymnotiformes) by nuclear (GGAC)(n) microsatellite analysis. *Genetics and Molecular Biology* **23**, 803–807.

FERNANDES, F.M.C., ALBERT, J.S., DE FATIMA Z.M., SILVA, D., LOPES, C.E., CRAMPTON, W.G.R. & ALMEIDA-TOLEDO, L.F. In press. A new species of *Gymnotus* (Teleostei: Gymnotidae) from the Pantanal Matogrossense and adjacent drainages, with descriptions of chromosomal structure and inter-microsatellite DNA sequences, *Zootaxa*, in press.

GALVIS, J.V., HUGUETT, A. & ROUG, P. 1979. Geología de la Amazonia Colombiana. *Boletín Geológico Ingeominas* **22**, 1–86.

GAYET, M. & MEUNIER, F.J. 1991. Première découverte de Gymnotiformes fossiles (Pisces, Ostariophysi) dans le Miocène supérieur de Bolivie, *Comptes Rendus de l'Academie des Sciences Paris* **313**, 471–476.

GAYET, M., MEUNIER, F.J. & KIRSCHBAUM, F. 1994. *Ellisella kirschbaumi* Gayet & Meunier, 1991. gymnotiform e fossile de Bolivie et ses relations phylogénétiques au sein des formes actuelles. *Cybium* **18**, 273–306.

GOULDING, M.J., BARTHAM, R. & FERREIRA, E. 2003. *The Smithsonian Atlas of the Amazon*. Smithsonian Books, Washington. 253 pp.

GREGORY-WODZICKI, K.M. 2000. Uplift history of the Central and Northern Andes: a review. *Geological Society of America Bulletin* **112**, 1091–1105.

GUERRERO, J. 1997. Stratigraphy, sedimentary environments, and the Miocene uplift of the Colombian Andes. In: KAY, R.F., HADDEN, R.H., CIFELLI, R.L. & FLYNN, J.J. Eds., *Vertebrate Paleonotology in the Neotropics: The Miocene Fauna of La Venta, Colombia*. Smithsonian Press, Washington, DC, pp. 15–43.

HAFNER, M., HAFNER, J.C., PATTON, J.L. & SMITH, M.F. 1987. Macrogeographic patterns of genetic differentiation in the pocket gopher *Thomemys umbrinus*. *Systematic Zoology* **36**, 18–34.

HARDMAN, M., PAGE, L.M., SABAJ, M., ARMBRUSTER, J.W. & KNOUFT, J.H. 2002. A comparison of fish surveys made in 19008 and 1998 of the Potaro, Essequibo, and Demerara, and coastal river drainages of Guyana. *Ichthyological Exploration Freshwaters* **13**, 225–238.

HARMON, L.J., SCHULTE, J.A., LARSON, A. & LOSOS, J.B. 2003. Tempo and mode of evolutionary radiation in iguanian lizards. *Science* **301**, 961–964.

HEILIGENBERG, W.F. 1980. Species specificity of electric organ discharges in sympatric gymnotoid fish of the Rio Negro. *Acta Biológica Venezolana* **10**, 187–203.

HEILIGENBERG, W.F. & BASTIAN, A. 1986. Jamming avoidance responses. Model systems for neuroethology. In: BULLOCK, T.H. & HEILIGENBERG, W.F. Eds., *Electroreception*. John Wiley & Sons, New York, pp. 613–649.

HENDERSON, P.A., HAMILTON, W.D. & CRAMPTON, W.G.R. 1998. Evolution and diversity in Amazonian floodplain communities. In: NEWBURY, D.M., PRINS, H.H.T. & BROWN, N.D. Eds., *Dynamics of Tropical Communities*. Blackwell Science, Oxford, pp. 385–419.

HOEDEMAN, J.J. 1962. Notes on the ichthyology of Surinam and other Guianas, 11. New gymnotiform fishes from Surinam and French Guiana, with additional records and a key to the groups and species from Guiana. *Bulletin Aquatic Biology*, Amsterdam **3**, 97–107.

HOORN, C. 1994. An environmental reconstruction of the palaeo-Amazon river system (Middle to Late Miocene, NW Amazonia). *Palaeogeography, Palaeoclimatology, Palaeoecology* **112**, 187–238.

HOORN, C. 1996. Miocene deposits in the Amazonian foreland basin. *Science* **273**, 122–123.

HOORN, C., GUERRERO, J., SARMIENTO, G.A. & LORENTE, M.A. 1995. Andean tectonics as a cause for changing drainage patterns in Miocene Northern South-America. *Geology* **23**, 237–240.

HOPKINS, C.D. 1999. Design features for electric communication. *Journal of Experimental Biology* **202**, 1217–1228.

HOPKINS, C.D., COMFORT, N.C., BASTIAN, J. & BASS, A. 1990. Functional analysis of sexual dimorphism in an electric fish, *Hypopomus pinnicaudatus*, order Gymnotiformes. *Brain Behavior Research* **35**, 350–367.

HOPKINS, C.D. & HEILIGENBERG, W.F. 1978. Evolutionary designs for electric signals and electroreceptors in gymnotiform fishes of Surinam. *Behavior Ecology Sociobiology* **3**, 113–134.

HRBEK, T. & LARSON, A. 1999. The evolution of diapause in the killifish family Rivulidae (Atherinomorpha, Cyprinodontiformes): a molecular phylogenetic and biogeographic perspective. *Evolution* **53**,1200–1216.

HUBBELL, S.P. 2001. *The Unified Neutral Theory of Biodiversity and Biogeography*. Princeton University Press, Princeton, 375 pp.

HUBBS, C.L. & LAGLER, K.F. 1958. *Fishes of the Great Lakes Region*. cranbrook Institute of Science, Bulletin 26, 186 pp.

ITURALDE-VINCENT, M.A. & MACPHEE, R.D.E. 1999. Paleogeography of the Caribbean region: implications for Cenozoic biogeography. *Bulletin American Museum Natural History*. **238**, 1–95.

JÉGU, M. & KEITH, P. 1999. Le bas Oyapock limite septentrionale ou simple étape dans la progression de la faune des poissons d'Amazonie occidentale. *Acadèmie de Sciences/èditions scientifiques et médicales* **322**, 1133–1143.

KIRSCHBAUM, F. & WIECZOREK, L. 2002. Entdeckung einer neuen Fortpflanzungs-strategie bei südamerikainischen Messerfischen (Teleostei: Gymnotiformes: Gymnotidae): Maulbrüten bei *Gymnotus carapo*. *Verhalten der Aquarienfische* **2**, 99–107.

KOHN, B.P., SHAGAM, R., BANKS, P.O. & BURKLEY, L.A. 1984. Mesozoic-Pliocene fission track ages on rocks of the Venezuelan Andes and their tectonic implications. In: BONINI, W.E., HARGRAVES, R.B. & SHAGAM, R. Eds., *The Caribbean-South America Plate Boundary and Regional Tectonics*, pp. 365–384.

LEVITON, A.E., GIBBS, R.H., HEAL, E. & DAWSON, C.E. 1985. Standards in herpetology and ichthyology: Part I. Standard symbolic codes for institutional resource collections in herpetology and ichthyology. *Copeia* **1985**, 802–832.

LIEM, K.F., ECLANCHER, B. & FINK, W.L. 1984. Aerial respiration in the banded knife fish *Gymnotus carapo* (Teleostei: Gymnotoidei). *Physiological Zoology* **57**, 185–195.

LINNAEUS, C. 1766. *Systema Naturae*, Ed. XII, Holmiae, 532 pp.

LISSMANN, H.W. 1958. On the function and evolution of electric organs in fish. *Journal of Experimental Biology* **35**, 156–191.

LORENZO, D., VELLUTI, J.C. & MACADAR, O. 1988. Electrophysiological properties of abdominal electrocytes in the weakly electric fish *Gymnotus carapo*. *Journal Comparative Physiology A* **162**, 141–144.

LOVEJOY, N.R. 1996. Systematics of Myliobatoid elasmobranchs: with emphasis on the phylogeny and historical biogeography of Neotropical freshwater stingrays (Potamotrygonidae: Rajiformes). *Zoological Journal of the Linnean Society* **117**, 207–257.

LOVEJOY, N.R. 1997. Stingrays, parasites, and historical biogeography: a closer look at Brooks et al's hypotheses for the origins of Neotropical freshwater rays: Potamotrygonidae. *Systematic Biology* **46**, 218–230.

LOVEJOY, N.R., BERMINGHAM, R.E. & MARTIN, A.P. 1998. Marine incursions into South America. *Nature* **396**, 421–422.

LOVEJOY, N.R. & D. ARAÚJO, M.L.G. 2000. Molecular systematics, biogeography, and population structure of Neotropical freshwater needlefishes of the genus *Potamorrhaphis*. *Molecular Ecology* **9**, 259–268.

LUNDBERG, J.G. 1993. African-South American freshwater fish clades and continental drift: problems with a paradigm. In: GOLDBLATT, P. Ed., *Biological relationships between Africa and South America*, Yale University Press, New Haven, pp. 156–199.

LUNDBERG, J.G. 1997. Freshwater fishes and their paleobiotic implications. In: KAY, R.F., HADDEN, R.H., CIFELLI, R.L. & FLYNN, J.J. Eds., *Vertebrate Paleonotology in the Neotropics*: *The Miocene Fauna of La Venta, Colombia*. Smithsonian Press, Washington, DC, pp. 67–92.

LUNDBERG, J.G. 1998. The temporal context for the diversification of Neotropical fishes. In: MALABARBA, L., REIS, R.E., VARI, R.P., DE LUCENA, C.A.S. & DE LUCENA, Z.M.S. Eds., *Phylogeny and Classification of Neotropical Fishes*. Museu de Ciências e Tecnologia, Porto Alegre, pp. 49–68.

LUNDBERG, J.G., KOTTELAT, M., SMITH, G.R., STIASSNY, M.L.J. & GILL, A.C. 2000. So many fishes, so little time: An overview of recent ichthyological discovery in continental waters. *Annals Missouri Botanical Garden* **87**, 26–62.

LUNDBERG, J.G., MARSHALL, L.C., GUERRERO, J., HORTON, B., MALABARBA, M.C.S.L. & WESSELINGH, F. 1998. The stage for Neotropical fish diversification: A history of tropical South American Rivers. In: MALABARBA, L., REIS, R.E., VARI, R.P., DE LUCENA, C.A.S. & DE LUCENA, Z.M.S. Eds., *Phylogeny and Classification of Neotropical Fishes*. Museu de Ciências e Tecnologia, Porto Alegre, pp. 13–48.

MADDISON, W.P. & MADDISON, D.R. 2000. *MacClade, Analysis of Phylogeny and Character Evolution*, version 3.03, Sunderland, Sunderland Associates, Inc. Massachusetts.

MAGO-LECCIA, F. 1994. *Electric Fishes of the Continental Waters of America*. Biblioteca de la Academia de Ciencias Fisicas, Matematicas, y Naturales, Caracas, Venezuela, **29**, 1–206.

MARTIN, A.P. & BERMINGHAM, E. 2000. Regional endemism and cryptic species revealed by molecular and morphological analysis of a widespread species of Neotropical catfish. *Proceedings Royal Society London Series B-Biological Sciences* **267**, 1135–1141.

MCCRACKEN, K.G., HARSHMAN, J., MCCLELLAN, D.A. & AFTON, A.D. 1999. Data set incongruence and correlated character evolution: An example of functional convergence in the hind-limbs of stifftail diving ducks. *Systematic Biology* **48**, 683–714.

MEYER, A., KOCHER, T.D., BASASIBWAKI, P. & WILSON, A.C. 1990. Monophyletic origin of Lake Victoria cichlid fishes suggested by mitochondrial-DNA sequences. *Nature* **347**, 550–553.

MONTOYA-BURGOS, J.I. 2003. Historical biogeography of the catfish genus *Hypostomus* (Siluriformes: Loricariidae), with implications on the diversification of Neotropical ichthyofauna. *Molecular Ecology* **12**, 1855–1867.

MORITZ, C., PATTON, J.L., SCHNEIDER, C.J. & SMITH, T.B. 2000. Diversification of rainforest faunas: An integrated molecular approach. *Annual Review of Ecology and Systematics* **31**, 533–563.

MULLINS, H.T., GARDULSKI, A.F., WISE, S.W. & APPLEGATE, J. 1987. Middle Miocene oceanographic event in the eastern Gulf of Mexico: implications for seismic stratigraphic succession and Loop Current/Gulf Stream circulation. *Geological Society America Bulletin* **98**, 702–713.

NORRELL, M.A. & NOVACEK, M.J. 1992. Congruence between superpositional and phylogenetic patterns: comparing cladistic patterns with fossil records. *Cladistics* **8**, 319–337.

NORTHCUTT, R.G., HOLMES, P.H. & ALBERT, J.S. (2000). Distribution and innervation of lateral line organs of the Channel Catfish. *Journal of Comparative Neurology* **421**, 570–592.

OMLAND, K.E. 1997. Examining two standard assumptions of ancestral reconstructions: Repeated loss of dichromatism in dabbling ducks (Anatini). *Evolution* **51**, 1636–1646.

OMLAND, K.E. 1999. The assumptions and challenges of ancestral state reconstructions. *Systematic Biology* **48**, 604–611.

PARADIS, E. 1998. Detecting shifts in diversification rates without fossils. *American Naturalist* **152**, 176–187.

PATTERSON, C. 1982. Morphological characters and homolog In: JOYSEY, K.A. & FRIDAY, A.B. Eds., *Problems of Phylogenetic Reconstruction*. Academic Press, London, pp. 21–74.

PAXTON, C.G.M., CRAMPTON, W.G.R. & BURGESS, P. 1996. Miocene deposits in the Amazonian foreland basin. *Science* **273**, 123.

PIPER, D.J.W., PIRMEZ, C., MANLEY, P.L., LONG, D., FLOOD, R.D., NORMARK, W.R. & SHOWERS,W. 1997. Mass transport deposits of Amazon Fan. In: FLOOD, R.D., PIPER, D.J.W., KLAUS, A. & PETERSON, L.C. Eds., *Proceedings Ocean Drilling Program Scientific Results,* College Station, pp. 109–146.

PETRY, P., BAYLEY, P.B. & MARKLE, D.F. 2003. Relationships between fish assemblages, macrophytes and environmental gradients in the Amazon River floodplain. *Journal of Fish Biology* **63**, 547–579.

PLANQUETTE, P., KEITH, P., & LE BAIL, P.-Y. 1996. *Atlas des Poissons D'Eau Douce de Guyane*, *Tome 1*. Muséum Nacional d'Histoire Naturelle, Paris, 429 pp.

PLOTKIN, J.B., POTTS, M.D., YU, D.W., BUNYAVEJCHEWIN, S., CONDIT, R., FOSTER, R., HUBBELL, S.P., LAFRANKIE, J., MANOKARAN, N., SENG, L.H., SUKUMAR, R., NOWAK, M.A. & ASHTON, P.S. 2000. Predicting species diversity in tropical forests. *Proceedings of the National Academy of Sciences of the United States of America* **97**, 10850–10854.

RASÄNEN, M.E., LINNA, A.M., SANTOS, J.C.R. & NEGRI, F.R. 1995. Late Miocene Tidal Deposits in the Amazonian Foreland Basin. *Science* **269**, 386–390.

REIS, R.E. 1998. Systematics, biogeography, and the fossil record of the Callichthyidae: A review of available data. In: MALABARBA, L., REIS, R.E., VARI, R.P., DE LUCENA, C.A.S. & DE LUCENA, Z.M.S. Eds., *Phylogeny and Classification of Neotropical Fishes*. Museu de Ciências e Tecnologia, Porto Alegre, pp. 351–362.

REIS, R.E., KULLANDER, S.O. & FERRARIS, C.J. 2003. Introduction. In: REIS, R.E., KULLANDER, S.O. & FERRARIS, C.J., Jr. Eds., *Checklist of the Freshwater Fishes of South and Central America*. Edipucrs, Porto Alegre, pp. 1–3.

RETZER, M.E. & PAGE, L.M. 1997. Systematics of the stick catfishes, *Farlowella* (Pisces, Loricariidae). *Proceedings of the Academy of Natural Sciences of Philadelphia*, **147**, 33–88.

ROSEN, D.E. 1975. A vicariant model of Caribbean biogeography. *Systematic Zoology* **24**, 431–464.

ROSEN, D.E. 1985. Geological hierarchies and biogeographic congruence in the Caribbean. *Annals Missouri Botanical Garden* **72**, 636–659.

ROUX, C. 1973. Poissons teleosteens du plateau continental Bresliien. Unpublished Thesis, University D'aix Marseille.

RUTHERFORD, S.L. 2003. Between genotype and phenotype: protein chaperones and evolvability. *Nature Reviews Genetics* **4**, 263–274.

SANTOS, G.M. & CARVALHO, F.M. 1982. Levantamento preliminar, pesca e aspectos biologicos da ictiofauna do rio Araguiaia. Relatorio Tecnico. Projeto Santa Izabel. Convenio ELN/CNPq/INPA, Manaus.

SCHULTE, J.A., MACEY, J.R., ESPINOZA, R.E. & LARSON, A. 2000. Phylogenetic relationships in the iguanid lizard genus *Liolaemus*: multiple origins of viviparous reproduction and evidence for recurring Andean vicariance and dispersal. *Biological Journal of the Linnean Society* **69**, 75–102.

SCHUSTER, S. 2000. Changes in the electric organ discharge after pausing the electromotor system of *Gymnotus carapo*. *Journal of Experimental Biology* **203**, 1433–1446.

SEEHAUSEN, O. 2000. Explosive speciation rates and unusual species richness in haplochromine cichlid fishes: effects of sexual selection. *Advances in Ecological Research* **31**, 237–274.

SEEHAUSEN, O. 2002. Patterns in fish radiation are compatible with Pleistocene desiccation of Lake Victoria and 14 600 year history for its cichlid species flock. *Proceedings of the Royal Society of London Series B-Biological Sciences* **269**, 491–497.

SILVA, A., QUINTANA, L., GALEANO, M. & ERRANDONEA, P. 2003. Biogeography and breeding in Gymnotiformes from Uruguay. *Environmental Biology of Fishes* **66**, 329–338.

SILVANO, R.A.M., OYAKAWA, O.T., DO AMARAL, B.D. & BEGGOSI, A. 2001. Peixes do Alta Rio Juruá. EDUSP, Sao Paulo, 301 pp.

SHAGAM, R., KOHN, B.P., BANKS, P.O., DASCH, L.E., VARGAS, R., RODRIGUES, G.I. & PIMENTEL, N. 1984. Tectonic implications of Cetaceous-Pliocene fission-track ages from rocks of the circum Maracaibo basin region of western Venezuela and eastern Colombia. In: BONINI, W.E., HARGRAVES, R.B. & SHAGAM, R. Eds., *The Caribbean-South America Plate Boundary and Regional Tectonics*, pp. 385–412.

SIVASUNDAR, A., BERMINGHAM, E. & ORTÍ, G. 2001. Population structure and biogeography of migratory freshwater fishes (*Prochilodus*: Characiformes) in major South American rivers. *Molecular Ecology* **10**, 407–417.

SORENSON, M.D. 1999. *TreeRot*, version 2. Boston University, Boston, MA.

STARKS, E.C. 1913. The fishes of the Stanford Expedition to Brazil. *Stanford University Publication Series*, pp. 1–77.

STODDARD, P.K., RASNOW, B. & ASSAD, C. 1999. Electric organ discharges of the gymnotiform fishes: III. Brachyhypopomus. *Journal of Comparative Physiology* A-*Sensory Neural and Behavioral Physiology* **184**, 609–630.

STOPA, R.M. & HOSHINO, K. 1999. Electrolocation communication discharges of the fish *Gymnotus carapo* L. (Gymnotidae: Gymnotiformes) during behavioral sleep. *Brazilian Journal of Medical and Biological Research* **32**, 1223–1228.

SULLIVAN, J.P., LAVOUE, S. & HOPKINS, C.D. 2002. Discovery and phylogenetic analysis of a riverine species flock of African electric fishes (Mormyridae: Teleostei). *Evolution* **56**, 597–616.

SWOFFORD, D. 2003. *PAUP* Version 4.0 Phylogenetic Analysis Using Parsimony*, Sinauer Associates, Inc. Washington, DC.

TEMPLETON, A.R. 1989. The meaning of species and speciation: a genetic perspective. In: OTTE, D. & ENDLER, J.A. Eds., *Speciation and its Consequences*. Sinauer Associates, Sunderland, pp. 3–27.

TRIQUES, M.L. 1993. Filogenia dos gêneros de Gymnotiformes (Actinopterygii, Ostariophysi), com base em caracteres esqueléticos. *Comunicacão Museu Cienecias PURCS, sér. zool. Porto Alegre* **6**, 85–130.

TURNER, G.F., SEEHAUSEN, O., KNIGHT, M.E., ALLENDER, C.J. & ROBINSON, R.L. 2001. How many species of cichlid fishes are there in African lakes? *Molecular Ecology* **10**, 793–806.

VARI, R.P. 1988. The Curimatidae: a Lowland Neotropical fish family (Pisces: Characiformes); Distribution, Endemism, and Phylogenetic Biogeography. In: VANZOLINI, P. & HEYER, W.R. Eds., *Proceedings of a Workshop on Neotropical Distribution Patterns*. Academia Brasileira de Ciencias, Rio de Janeiro, pp. 343–377.

VARI, R.P. 1995. The Neotropical fish family Ctenoluciidae (Teleostei: Ostariophysi: Characiformes): Supra and interfamilial phylogenetic relationships, with a revisionary study. *Smithsonian Contributions to Zoology* **564**, 1–97.

VARI, R.P. & MALABARBA, L.R. 1998. Neotropical Ichthyology: An overview. In: MALABARBA, L., REIS, R.E., VARI, R.P., DE LUCENA, C.A.S. & DE LUCENA, Z.M.S. Eds., *Phylogeny and Classification of Neotropical Fishes*. Museu de Ciências e Tecnologia, Porto Alegre, pp. 1–11.

VARI, R.P. & WEITZMAN, S.H. 1990. A review of the phylogenetic biogeography of the freshwater fishes of South America. In: PETERS, G. & HUTTERER, R. Eds., *Vertebrates in the Tropics*. Museum Alexander Koenig, Bonn, pp. 381–393.

VERHEYEN, E., SALZBURGER, W., SNOEKS, J. & MEYER, A. 2003. Origin of the superflock of cichlid fishes from Lake Victoria, East Africa. *Science* **300**, 325–329.

VITT, L.J., PIANKA, E.R., COOPER, W.E. & SCHWENK, K. 2003. History and the global ecology of squamate reptiles. *American Naturalist* **162**, 44–60.

VITT, L.J., ZANI, P.A. & ESPOSITO, M.C. 1999. Historical ecology of Amazonian lizards: implications for community ecology. *Oikos* **87**, 286–294.

VOLKOV, I., BANAVAR, J.R., HUBBELL, S.P. & MARITAN, A. 2003. Neutral theory and relative species abundance in ecology. *Nature* **424**, 1035–1037.

VONHOF, H.B., WESSELINGH, F.P. & GANSSEN, G.M. 1998. Reconstruction of the Miocene western Amazonian aquatic system using molluscan isotopic signatures. *Palaeogeography Palaeoclimatology Palaeoecology* **141**, 85–93.

VONHOF, H.B., WESSELINGH, F.P., KAANDORP, R.J.G., DAVIES, G.R., VAN HINTE, J.E., GUERRERO, J., RASANEN, M., ROMERO-PITTMAN, L. & RANZI, A. 2003. Paleogeography of Miocene Western Amazonia: Isotopic composition of molluscan shells constrains the influence of marine incursions. *Geological Society of America Bulletin* **115**, 983–993.

WAGNER, P.J. 2001. Rate heterogeneity in shell character evolution among lophospiroid gastropods. *Paleobiology* **27**, 290–310.

WAGNER, P.J. & SIDOR, C.A. 2000. Age rank/clade rank metrics – Sampling, taxonomy, and the meaning of "stratigraphic consistency". *Systematic Biology* **49**, 463–479.

WEINS, J.J. 2000. Coding morphological variation within species and higher taxa for phylogenetic analysis. In: WIENS, J. Ed., *Phylogenetic Analysis of Morphological Data*. Smithsonian Institution Press, Washington, DC, pp. 115–145.

WESTBY, G.W.M. 1988. The ecology, discharge diversity, and predatory behavior of gymnotiforme electric fish in the coastal streams of French Guiana. *Behavioral Ecology Sociobiology* **11**, 341–354.

WESTNEAT, M.W. 1993. Phylogenetic relationships of the tribe Cheilinini (Labridae: Perciformes) *Bulletin Marine Science* **52**, 351–394.

WILKINSON, M. 1992. Ordered versus unordered characters. *Cladistics* **8**, 375–385.

WILKINSON, M., LAPOINTE, F.J. & GOWER, D.J. 2003. Branch lengths and support. *Systematic Biology* **52**, 127–130.

Appendix 1

Gymnotus specimens examined for osteological data. A total of 65 lots were examined with 95 specimens, including 8 paratype (PT) lots. For each of the 32 ingroup OTUs 2–10 specimens were cleared and stained (c&s) for alcian (cartilage) and alizarin (bone). Data are arranged alphabetically by species, and then by museum acronym and lot number. Outgroup and additional comparative specimens examined in Albert (2001). Locality data are presented in Materials Examined of Albert & Crampton (2003), Crampton *et al*. (2003) and Crampton & Albert (2003a, 2003b).

1. *G. anguillaris*: UMMZ 190413 (2 of 3 c&s) 131–289 mm.
2. *G. arapaima*: MCP uncat. WGRC 01.240699 (1 of 1 c&s) 215 mm. MCP uncat. WGRC 05.060899 (1 of 1 c&s) 220 mm. MCP uncat. WGRC 04.080696 (1 of 1 c&s) 187 mm. MCP uncat. WGRC 03.230698 (1 of 1 c&s) 191 mm.
3. *G. bahianus*: MCP 18110 (2 of 2 c&s) 90–92 mm. MNRJ 4346 PT (2 of 10 c&s) 133–240 mm.
4. *G. carapo* EA: UF 36597 (2 of 2 c&s) 155–180 mm.
5. *G. carapo* GU: UF 37030 (3 of 20 c&s) 101–176 mm. UF 80734 (10 of 47 c&s) 165–262 mm. USNM 225285 (2 of 12 c&s) 85–257 mm. UMMZ 190414 (3 of 6 c&s) 71–260 mm.
6. *G. carapo* MD: UF 82345 (2 of 2 c&s) 111–210 mm.
7. *G. carapo* PI: AUM 20624 (1 of 3 c&s) 179–225 mm.
8. *G. carapo* RO: MZUSP 30006 (2 of 10 c&s) 125–200 mm.
9. *G. carapo* WA: MZUSP 76064 (1 of 1 c&s) 253 mm. MZUSP 76068 (1 of 1 c&s) 104 mm.
10. *G. choco*: NRM 27734 PT (2 of 6 c&s) 165–260 mm.
11. *G. sp. indet*.: UF 117122 (2 of 3 c&s) 89–171 mm.
12. *G. coatesi*: MCP uncat. (2 of 3 c&s) 81–104 mm.
13. *G. coropinae* GU: UF 97641 (2 of 3 c&s) 131–132 mm.
14. *G. coropinae* WA: MZUSP 75180. WGRC 09.110300 (1 of 1 c&s) 120 mm. MZUSP 75186. WGRC 14.160300 (1 of 1 c&s) 102 mm.
15. *G. curupira*: MZUSP 75145 PT (1 of 1 c&s) 150 mm. MZUSP 75146 PT (1 of 1 c&s) 141 mm. MZUSP 75147. WGRC 03.040300 (1 of 1 c&s) 171 mm.
16. *G. cylindricus*: UMMZ 193986 (3 of 14 c&s) 26–183 mm.
17. *G. diamantinensis*: MZUSP 45320 PT (1 of 1 c&s) 104 mm.
18. *G. esmeraldas*: MCZ 162745 PT (2 of 4 c&s) 200–309 mm.
19. *G. inaequilabiatus*: UMMZ 207025 (3 of 17 c&s) 215–235 mm.
20. *G. javari*: UMMZ 224596 PT (2 of 10 c&s) 45–175 mm. UMMZ 224607a (2 of 5 c&s) 29–106 mm.
21. *G. jonasi*: MCP uncat. WGRC 17.020698 (1 of 1 c&s) 90 mm. MCP uncat. WGRC 19.170597 (1 of 1 c&s) 105 mm. MCP uncat. WGRC 05.040698 (1 of 1 c&s)

90 mm. MCP uncat. WGRC NR 01.050598 (1 of 1 c&s) 98 mm. MCP uncat. WGRC NR 03.070600 (1 of 1 c&s) 101 mm.

22. *G. maculosus*: UMMZ 190531 (1 of 7 c&s). UMMZ 197103 (2 of 17 c&s) 79–227 mm.
23. *G. mamiraua*: MCP uncat. WGRC 21.180699 (1 of 1 c&s) 200 mm. MCP uncat. WGRC 24.180699 (1 of 1 c&s) 205 mm. MCP uncat. WGRC 28.150597 (1 of 1 c&s) 210 mm. MCP uncat. WGRC 05.230608 (1 of 1 c&s) 206 mm. MCP uncat. WGRC 05.050598 (1 of 1 c&s) 215 mm.
24. *G.* MQ: MCP 7155 (1 of 1 c&s) 245 mm.
25. *G. obscurus*: BMNH 1998.3.12 PT (1 of 3 c&s) 94–161 mm. MZUSP 60605 WGRC 08.170597 (1 of 1 c&s) 140 mm. BMNH 1998.3.12.21. WGRC 16.070597 (1 of 1 c&s) 95 mm. MZUSP uncat. WGRC 06.300497 (1 of 1 c&s) 140 mm. UF 118836 WGRC 06.300497 (1 of 1 c&s) 144 mm.
26. *G. pantherinus*: LGP 932 (2 of 2 c&s) 236 mm.
27. *G. pedanopterus*: ANSP 162606 (1of 2 c&s) 86–129 mm. ANSP 141596 (2 of 14 c&s) 76–340 mm.
28. *G. sp. 2* MD: MUSM 20268b (2 of 2 c&s) 220–278 mm.
29. *G. sylvius*: LIUSP P2346 (1 of 1 c&s) 160 mm. LIUSP P2338 (1 of 1 c&s) 180 mm.
30. *G. ucamara*: MUSM 10184 (2 of 7 c&s) 118–156 mm.
31. *G. varzea*: UF 118834 WGRC NR08.070597 (1 of 1 c&s) 171 mm. MZUSP 60603 WGRC 12.170597 and WGRC 14.170597 (2 of 2 c&s) 156–145 mm.

Appendix 2

Diagnosis of Gymnotidae, *Gymnotus* and 24 included clades. Steps in parentheses are unambiguous character-state changes on the strict consensus tree topology of Fig. 21. Abbreviations: AFR, anal-fin rays; BD, body depth; BO, branchial opening; BW, body width; HD, head depth; HL, head length; HW, head width; IO, interorbital distance; P1, pectoral–fin length; PA, preanal distance; PCV, pre-caudal vertebrae; TL, total length. EOD, electric organ discharge; NC, character not included in phylogenetic analysis.

Clade A: Gymnotidae

Gymnotidae was diagnosed by 14 characters by Albert (2001); gape large, more than one third head length, extending to posterior nares; premaxilla large, elongate, articulation with maxilla oriented anteriorly; ventral margin of descending maxillary blade with a pronounced angle about two-thirds distance to its tip; *M. adductor mandibula* insertion on maxilla, undivided bundle at origin; mesethmoid tip concave; base of lateral ethmoid (bone or cartilage) narrow; cranial fontanels closed in adults; lateral valvula cerebellum large, exposed on lateral surface of brain; basihyal with dorsal groove anterior coracoid process absent; anal-fin pterygiophores equal or longer than hemal spines; body cavity very long, with 31 or more precaudal vertebrae; caudal appendage short, 0–16% total length.

An additional five characters are here added to this diagnosis: body shape cylindrical, BD 74–90% BW (27); lateral ethmoid unossified or absent (75); postcleithrae thin, discoid or sickle-shaped (90); displaced hemal spines absent (106); monophasic EOD with a single positive phases way from baseline (112, derived multiphasic discharge is present in South American species of *Gymnotus*).

Clade B: *Gymnotus* (steps: 12).

29. Gape superior, lower jaw prognathous, rictus decurved (CI: 1.00, RI: 1.00, RC: 1.00).
30. Eye position at horizontal with rictus (CI: 1.00, RI: 1.00, RC: 1.00).
31. Mesethmoid anterior margin concave with paired anteriolateral processes on either side of a shallow median notch (CI: 1.00, RI: 1.00, RC: 1.00).
33. Anterior narial pore pipe-shaped, partially or entirely in gape (CI: 1.00, RI: 1.00, RC: 1.00).
36. Maxilla orientation vertical (CI: 1.00, RI: 1.00, RC: 1.00).
38. Maxilla length short, approx. length of 7–9 teeth in dentary margin (CI: 0.33, RI: 0.43, RC: 0.14).
70. Hyomandibula PLL canal contacting posterior margin (CI: 0.50, RI: 0.67, RC: 0.33).
76. Parasphenoid narrow, its length more than 2.2 times its width (CI: 0.67, RI: 0.86, RC: 0.57).
79. Parietal shape rectangular, its length less than its width (CI: 1.00, RI: 1.00, RC: 1.00).
82. *M. adductor mandibula* undivided at insertion (CI: 1.00, RI: 1.00, RC: 1.00).
84. Basibranchials unossified (CI: 1.00, RI: 1.00, RC: 1.00).
101. Lateral line ventral rami (VLR) present in adults (CI: 0.27, RI: 0.60, RC: 0.16).

NC. Extrascapular fused with neurocranium.
NC. Capacity to regenerate postcoelomic neural and hemal spines.
NC. Cylindrical or barrel shaped electrocytes, without a stalk.

Clade C: *G. cylindricus* group clade (steps: 8).

18. Head depth (HD): very deep, mean adult HD 66–75%HL (CI: 0.13, RI: 0.41, RC: 0.05).
20. Snout length (PR): long, PR 37–40% HL (CI: 0.17, RI: 0.41, RC: 0.07).
40. Premaxillary teeth in outer row: few, 10 or less (CI: 0.25, RI: 0.70, RC: 0.18).
45. Dentary teeth outer row: mode 12–15 (CI: 0.29, RI: 0.62, RC: 0.18).
62. Metapterygoid superior portion reduced, ossifies to less than anterior margin of inferior portion (CI: 0.25, RI: 0.79, RC: 0.20).
78. Parasphenoid posterior processes gracile, elongate, posterior margin convex, deeply incised (CI: 0.25, RI: 0.75, RC: 0.19).
87. Pectoral fin, medial pectoral radial cartilage(s) very small or absent (CI: 0.50, RI: 0.86, RC: 0.43).
102. Lateral line dorsal rami (DLR) present in majority of adults (CI: 0.33, RI: 0.60, RC: 0.20).

Clade D: 'South American' clade (steps: 14).

1. Pigment bands present (oblique, unbroken or broken) (CI: 0.20, RI: 0.50, RC: 0.10).
2. Band (or pigment patch) margins irregular and wavy (CI: 0.67, RI: 0.92, RC: 0.62).
3. Band pigment density: dark bands paired, pale in middle (CI: 0.33, RI: 0.73, RC: 0.24).
5. Band (pair) width at midbody: dark bands 2–3 times broader than pale bands (CI: 0.30, RI: 0.50, RC: 0.15).
37. Maxilla rod- or paddle-shaped with straight ventral margin (CI: 1.00, RI: 1.00, RC: 1.00).
47. Dentary processes: dorsal abutting ventral (CI: 1.00, RI: 1.00, RC: 1.00).
55. Preopercle anterior notch present (CI: 0.50, RI: 0.80, RC: 0.40).
57. Preopercle median shelf large, more than half width of symplectic (CI: 0.50, RI: 0.90, RC: 0.45).
59. Mesopterygoid ascending process long, its base less than its length (CI: 0.50, RI: 0.80, RC: 0.40).
66. Angular ventrolateral lamellae expanded, extending over retroarticular (CI: 0.50, RI: 0.80, RC: 0.40).
86. Pectoral-fin rays (P1R): mode 14–16 (CI: 0.22, RI: 0.59, RC: 0.13).
92. Cleithrum length anterior limb: long, more than 1.8 times ascending (CI: 0.33, RI: 0.67, RC: 0.22).
101. Lateral line ventral rami (VLR): median: 9–18 ventral rami (CI: 0.27, RI: 0.60, RC: 0.16).
112. EOD phases from baseline in adults tetraphasic (CI: 0.60, RI: 0.71, RC: 0.43).

Clade E: *G. pantherinus* group clade (steps: 10).

16. Body profile (BD): slender, 6.1–9.0% TL (CI: 0.20, RI: 0.75, RC: 0.15).
17. Head length (HL): short, mean HL 8.4–9.4% TL (CI: 0.20, RI: 0.62, RC: 0.12).
32. Mesethmoid neck: broad, 3–4 times lateral process (CI: 0.33, RI: 0.85, RC: 0.28).
51. Dentary anterior hook present (CI: 0.33, RI: 0.67, RC: 0.22).
88. Mesocoracoid proximal portion broad (CI: 0.33, RI: 0.78, RC: 0.26).
91. Cleithrum narrow, its ventral margin straight (CI: 0.50, RI: 0.82, RC: 0.41).
99. Scales to first VLR (PLR): median 50–61 (CI: 0.20, RI: 0.47, RC: 0.09).
103. Body cavity long, 40–51 PCV (CI: 0.27, RI: 0.59, RC: 0.16).
104. Rib 5 with a broad medial triangular shelf, more than three times width of rib 6 (CI: 1.00, RI: 1.00, RC: 1.00).
111. Electric organ slender, mode 2–3 rows of electroplates at caudal end of anal fin (CI: 0.29, RI: 0.76, RC: 0.22).

Clade F: *G. anguillaris* clade (steps: 4).

5. Band (pair) width at midbody: dark bands 4–5 times broader than pale (CI: 0.30, RI: 0.50, RC: 0.15).
19. Head width (HW): wide, mean adult HW 68–70% HL (CI: 0.25, RI: 0.54, RC: 0.13).
21. Mouth width (MW): wide, 45–49% HL (CI: 0.20, RI: 0.27, RC: 0.05).
25. Pectoral fin length (P1): large, mean adult P1 45–54% HL (CI: 0.11, RI: 0.33, RC: 0.04).

Clade G: unnamed clade (steps: 3).

19. Head width (HW): narrow, HW 51–56% HL (CI: 0.25, RI: 0.54, RC: 0.13).
24. Preanal distance (PA): short, PA 56–89% HL (CI: 0.14, RI: 0.54, RC: 0.08).
38. Maxilla length: short, equal to extent of 4–6 teeth along dentary margin (CI: 0.33, RI: 0.43, RC: 0.14).

Clade H: *G. pedanopterus* clade (steps: 3).

22. Interorbital distance (IO): narrow, mean adult IO: 31–35% HL (CI: 0.17, RI: 0.47, RC: 0.08).
86. Pectoral-fin rays (P1R): few, mode 12–13 (CI: 0.22, RI: 0.59, RC: 0.13).
96. Scales above lateral line (SAL): small, mode 9–13 (CI: 0.25, RI: 0.63, RC: 0.16).

Clade I: *G. coatesi* clade (steps: 13).

2. Band (or pigment patch) margins: regular and straight (CI: 0.67, RI: 0.92, RC: 0.62).
3. Band pigment density: dark bands evenly pigmented (CI: 0.33, RI: 0.73, RC: 0.24).
10. Nape pale yellow patch: present (CI: 0.33, RI: 0.71, RC: 0.24).
17. Head length (HL): moderate, mean HL 9.5–11.0% TL (CI: 0.20, RI: 0.62, RC: 0.12).
18. Head depth (HD): slender, HD 53–59% HL (CI: 0.13, RI: 0.41, RC: 0.05).
43. Dentary teeth: five more needle-shaped (CI: 0.50, RI: 0.83, RC: 0.42).
57. Preopercle median shelf: small, less than half width of symplectic (CI: 0.50, RI: 0.90, RC: 0.45).
62. Metapterygoid superior portion: reduced, ossifies to less than anterior margin of inferior portion (CI: 0.25, RI: 0.79, RC: 0.20).
67. Anguloarticular. process: short, to ventral margin dentary (CI: 0.17, RI: 0.29, RC: 0.05).
87. Pectoral fin, medial pectoral radial cartilage(s) very small or absent (CI: 0.50, RI: 0.86, RC: 0.43).
103. Body cavity long: 40–51 PCV (CI: 0.27, RI: 0.59, RC: 0.16).
107. Anal-fin ray number (AFR): few, mean 150–225 AFR (CI: 0.17, RI: 0.69, RC: 0.11).
108. Anal-fin ray branching: multiple branches posterior to AFR 18 (CI: 0.50, RI: 0.80, RC: 0.40).

Clade J: *G. coropinae* clade (steps: 3).

20. Snout length (PR): short, PR 28–33% HL (CI: 0.17, RI: 0.41, RC: 0.07).
23. Branchial opening (BO): narrow, IO: 25–32% HL (CI: 0.33, RI: 0.78, RC: 0.26).
91. Cleithrum shape: very narrow, ventral margin straight (CI: 0.50, RI: 0.82, RC: 0.41).

Clade K: unnamed clade (steps: 5).

14. Body size small: small, grows to less than 160 mm max. TL (CI: 0.50, RI: 0.80, RC: 0.40).
32. Mesethmoid neck: narrow, approximately two times width of a single anterolateral mesethmoid process (CI: 0.33, RI: 0.85, RC: 0.28).
49. Dentary dorsoposterior process: broad distally (CI: 1.00, RI: 1.00, RC: 1.00).
50. Dentary ventral margin: lamella large, greater than depth of posterior process in lateral view (CI: 0.20, RI: 0.60, RC: 0.12).
72. Laterosensory canal associated with frontal wide, its anterior margin not confluent with lateral margin of adjacent frontal (CI: 1.00, RI: 1.00, RC: 1.00).

Clade L: *G. coropinae* (steps: 4).

10. Nape pale yellow patch: absent (CI: 0.33, RI: 0.71, RC: 0.24).
22. Interorbital distance (IO): very broad, IO: 41–50% HL (CI: 0.17, RI: 0.47, RC: 0.08).
51. Dentary anterior hook: absent in lateral view (CI: 0.33, RI: 0.67, RC: 0.22).
67. Anguloarticular. process long, beyond ventral margin of dentary (CI: 0.17, RI: 0.29, RC: 0.05).

Clade M: *G. jonasi* clade (steps: 8).

9. White cheek patch: present (CI: 1.00, RI: 1.00, RC: 1.00).
18. Head depth (HD): very deep, mean adult HD 66–75% HL (CI: 0.13, RI: 0.41, RC: 0.05).
24. Preanal distance (PA): short, PA 56–89% HL (CI: 0.14, RI: 0.54, RC: 0.08).
26. Anal-fin length (AF): short, 67–75% TL (CI: 0.50, RI: 0.67, RC: 0.33).
40. Premaxillary teeth in outer row: few, 10 or less (CI: 0.25, RI: 0.70, RC: 0.18).
42. Premaxillary tooth rows: one row on outer margin (CI: 0.33, RI: 0.78, RC: 0.26).
45. Dentary teeth outer row: few, mode 8–12 (CI: 0.29, RI: 0.62, RC: 0.18).
103. Body cavity short: 36–39 PCV (CI: 0.27, RI: 0.59, RC: 0.16).

Clade N: *G. carapo* group clade (steps: 9).

11. Anal fin posterior clear patch: present (CI: 0.50, RI: 0.94, RC: 0.47).
24. Preanal distance (PA): short, PA 56–89% HL (CI: 0.14, RI: 0.54, RC: 0.08).
25. Pectoral fin length (P1): large, mean adult P1 45–54% HL (CI: 0.11, RI: 0.33, RC: 0.04).
38. Maxilla length: short, equal in length to distance of 4–6 teeth on dentary margin (CI: 0.33, RI: 0.43, RC: 0.14).
42. Premaxillary tooth rows: one row on outer margin (CI: 0.33, RI: 0.78, RC: 0.26).
44. Dentary with 4–7 arrowhead-shaped teeth anteriorly, others conical posteriorly (CI: 1.00, RI: 1.00, RC: 1.00).
54. Preopercle laterosensory pore: doubled at dorsoposterior corner (CI: 0.50, RI: 0.93, RC: 0.46).
69. Hyomandibular. trigeminal canals: SO and IO divided (CI: 0.50, RI: 0.90, RC: 0.45).
93. Cleithrum anterior notch: present (CI: 0.67, RI: 0.94, RC: 0.63).

Clade O: *G. mamiraua* clade (steps: 3).

45. Dentary teeth outer row: few, mode 12–15 (CI: 0.29, RI: 0.62, RC: 0.18).
62. Metapterygoid superior portion: small, ossifies to less than anterior margin of inferior portion (CI: 0.25, RI: 0.79, RC: 0.20).
76. Parasphenoid broad, its length less than 2.2 times its width (CI: 0.67, RI: 0.86, RC: 0.57).

Clade P: *G. curupira* clade (steps: 3).

98. Posterior lateral line scales (PLL): many, mode 110 or more (CI: 0.20, RI: 0.60, RC: 0.12).
112. EOD phases from baseline in adults: triphasic (CI: 0.60, RI: 0.71, RC: 0.43).
113. EOD P2 small: less than 1% P1 (CI: 0.50, RI: 0.75, RC: 0.38).

Clade Q: unnamed clade (steps: 4).

40. Premaxillary teeth in outer row: few, 10 or less (CI: 0.25, RI: 0.70, RC: 0.18).
44. Dentary with 2–4 arrowhead-shaped teeth anteriorly, other s conical posteriorly (CI: 1.00, RI: 1.00, RC: 1.00).
86. Pectoral-fin rays (P1R): many, mode 17–21 (CI: 0.22, RI: 0.59, RC: 0.13).
101. Lateral line ventral rami (VLR): many, median 19–51 very short ventral rami (CI: 0.27, RI: 0.60, RC: 0.16).

Clade R: *G. varzea* clade (steps: 1).

102. Lateral line dorsal rami (DLR): present in majority of adults (CI: 0.33, RI: 0.60, RC: 0.20).

Clade S: 'elongate scales' clade (steps: 6).

11. Anal fin posterior clear patch: absent (CI: 0.50, RI: 0.94, RC: 0.47).
13. Anal fin posterior stripes: present in posterior region (CI: 1.00, RI: 1.00, RC: 1.00).
18. Head depth (HD): slender, HD 53–59% HL (CI: 0.13, RI: 0.41, RC: 0.05).
96. Scales above lateral line (SAL): small, mode 9–13 (CI: 0.25, RI: 0.63, RC: 0.16).
97. Scale shape in mature specimens: elongate, at least 1.5 longer than deep at midbody (CI: 1.00, RI: 1.00, RC: 1.00).
100. Scales over AF pterygiophores (APS): moderate size, mode 8–11 rows (CI: 0.29, RI: 0.72, RC: 0.21).

Clade T: *G. tigre* clade (steps: 6).

5. Band (pair) width at midbody: dark bands narrower than pale (CI: 0.30, RI: 0.50, RC: 0.15).
20. Snout length (PR): long, PR 37–40% HL (CI: 0.17, RI: 0.41, RC: 0.07).

23. Branchial opening (BO): narrow, IO: 25–32% HL (CI: 0.33, RI: 0.78, RC: 0.26).
100. Scales over AF pterygiophores (APS): small, mode 12–16 rows (CI: 0.29, RI: 0.72, RC: 0.21).
103. Body cavity long: 40–48 PCV (CI: 0.27, RI: 0.59, RC: 0.16).
111. Electric organ deep, mode 5–6 rows of electroplates at caudal end of anal fin (CI: 0.29, RI: 0.76, RC: 0.22).

Clade U: *G. esmeraldas* clade (steps: 5).

6. Band (pair) number (BND): few, median 0–16 (CI: 0.14, RI: 0.63, RC: 0.09).
16. Body profile (BD): slender, 6.1–9.0% TL (CI: 0.20, RI: 0.75, RC: 0.15).
24. Preanal distance (PA): long, mean adult PA 90–128% HL (CI: 0.14, RI: 0.54, RC: 0.08).
101. Lateral line ventral rami (VLR): median 9–18 ventral rami (CI: 0.27, RI: 0.60, RC: 0.16).
102. Lateral line dorsal rami (DLR): present in majority of adults (CI: 0.33, RI: 0.60, RC: 0.20).

Clade V: 'broken-bands' clade (steps: 5).

4. Dark bands above lateral line: most become broken into spots and blotches in specimens more than 150 mm TL (CI: 0.33, RI: 0.78, RC: 0.26).
17. Head length (HL): long, mean HL 9.5–13.5% TL (CI: 0.20, RI: 0.62, RC: 0.12).
27. Body shape (BW/BD): laterally compressed, 0.58–0.73 (CI: 0.10, RI: 0.36, RC: 0.04).
60. Mesopterygoid ascending process curved (CI: 0.33, RI: 0.86, RC: 0.29).
74. Frontal shape: narrow, its width less than its length at junction of supraorbital canal with neurocranium (CI: 1.00, RI: 1.00, RC: 1.00).

Clade W: *G. inaequilabiatus* clade (steps: 4).

8. Ground colour middorsum at midbody: light (CI: 0.25, RI: 0.57, RC: 0.14).
68. Mandible shape: short, compressed (CI: 0.25, RI: 0.63, RC: 0.16).
89. Mesocoracoid distal portion: ossified (CI: 0.33, RI: 0.50, RC: 0.17).
94. Cleithrum dorsoposterior facet: large (CI: 1.00, RI: 1.00, RC: 1.00).

Clade X: unnamed clade (steps: 2).

62. Metapterygoid superior portion: reduced, ossifies to less than anterior margin of inferior portion (CI: 0.25, RI: 0.79, RC: 0.20).
91. Cleithrum shape: narrow, ventral margin straight (CI: 0.50, RI: 0.82, RC: 0.41).

Clade Y: unnamed clade (steps: 4).

18. Head depth (HD): very deep, mean adult HD 66–75% HL (CI: 0.13, RI: 0.41, RC: 0.05).
22. Interorbital distance (IO): very broad, IO: 41–50% HL (CI: 0.17, RI: 0.47, RC: 0.08).
93. Cleithrum anterior notch: semi-lunar (CI: 0.67, RI: 0.94, RC: 0.63).
101. Lateral line ventral rami (VLR): few, median: 1–8 ventral rami in adults – long (CI: 0.27, RI: 0.60, RC: 0.16).

Clade Z: *G. carapo* complex (steps: 4).

32. Mesethmoid neck: broad, 3–4 times width of lateral mesethmoid process (CI: 0.33, RI: 0.85, RC: 0.28).
48. Dentary ventral posterior process: long, almost as long as dorsoposterior process (CI: 0.33, RI: 0.80, RC: 0.27).
77. Vomer: long, more half distance to parasphenoid lateral process (CI: 1.00, RI: 1.00, RC: 1.00).
78. Parasphenoid posterior processes: gracile, elongate, posterior margin convex, deeply incised (CI: 0.25, RI: 0.75, RC: 0.19).

Clade AA: *G. arapaima* clade (steps: 9).

12. Anal fin color: anterior half black (CI: 1.00, RI: 1.00, RC: 1.00).
21. Mouth width (MW): narrow, mean adult 27–35% HL (CI: 0.20, RI: 0.27, RC: 0.05).
22. Interorbital distance (IO): narrow, mean adult IO: 31–35% HL (CI: 0.17, RI: 0.47, RC: 0.08).
25. Pectoral fin length (P1): small, P1 34–44% HL (CI: 0.11, RI: 0.33, RC: 0.04).
34. Circumorbial series: tear-drop shaped (CI: 1.00, RI: 1.00, RC: 1.00).
39. Maxilla end shape: broad distally, paddle-shaped (CI: 0.14, RI: 0.57, RC: 0.08).
44. Dentary teeth arrowhead-shaped: 8–12 in anterior portion of dentary (CI: 1.00, RI: 1.00, RC: 1.00).
83. *M. adductor mandibula* intermuscular bones: ossified (CI: 0.33, RI: 0.33, RC: 0.11).
88. Mesocoracoid proximal portion: broad (CI: 0.33, RI: 0.78, RC: 0.26).

Clade AB: *G. carapo* EA + RO clade (steps: 5).

8. Ground colour middorsum at midbody: light (CI: 0.25, RI: 0.57, RC: 0.14).
19. Head width (HW): narrow, HW 51–56% HL (CI: 0.25, RI: 0.54, RC: 0.13).
20. Snout length (PR): long, PR 37–40% HL (CI: 0.17, RI: 0.41, RC: 0.07).
27. Body shape (BW/BD): cylindrical, 0.74–0.90 (CI: 0.10, RI: 0.36, RC: 0.04).
101. Lateral line ventral rami (VLR): few, median 1–8 ventral rami in adults (CI: 0.27, RI: 0.60, RC: 0.16).